Zeitschrift für angewandte Mathematik und Physik

ZAMP

Journal of Applied Mathematics and Physics

Journal de Mathématiques et de Physique appliquées

INHALT – CONTENTS – SOMMAIRE

ZAMP	Vol. VIII	Fasc. 6	Pag. 433—504	25. 11. 57

Birkhäuser Verlag · Basel und Stuttgart

Zeitschrift für angewandte Mathematik und Physik
Journal of Applied Mathematics and Physics
Journal de Mathématiques et de Physique appliquées
ZAMP

Redaktor/Editor/rédacteur: Prof. Dr. R. Sänger, Postfach Zürich 23 (Schweiz)

ZAMP erscheint regelmässig alle zwei Monate. *Redaktionsschluss:* spätestens 12 Wochen vor Erscheinungstermin. Manuskripte und alle die Redaktion betreffenden Zuschriften sind an den Redaktor zu richten. Manuskripte für *Kurze Mitteilungen* können, falls die Autoren auf Zustellung eines Korrekturabzuges verzichten, 8 Wochen vor Erscheinungstermin eingereicht werden. Die Beiträge werden in deutscher, englischer, französischer oder italienischer Sprache publiziert, doch soll jeder *Originalarbeit* und *Kurzen Mitteilung* eine kurze Zusammenfassung in einer andern als der Originalsprache beigegeben werden. *Abbildungsvorlagen* sollen reproduktionsfertig mit Reduktionsmaßstab versehen eingeliefert werden, hingegen soll die Beschriftung nur mit Bleistift, am besten auf einem lose vorgeklebten, durchsichtigen Papier, ausgeführt werden. Autoren von Originalarbeiten, welche einen Umfang von mehr als 16 Seiten aufweisen, haben einen *Satzbeitrag* zu entrichten. Dieser beträgt Fr. 20.– pro Seite von der 17. bis 24. Seite und Fr. 35.– pro Seite von der 25. Seite an. Beginnend mit Vol. IX, 1958, betragen die Satzbeiträge: Fr. 25.– pro Seite von der 17. bis 24. Seite, Fr. 40.– pro Seite von der 25. bis 32. Seite und Fr. 50.– pro Seite von der 33. Seite an. Die Verfasser von *Zusammenfassenden Berichten, Originalarbeiten* und *Kurzen Mitteilungen* erhalten 50 Gratisseparata ohne Umschlag.

ZAMP is published regularly every two months. All papers must be in the hands of the editor at least 12 weeks before publication of the issue. Manuscripts and all other correspondence concerning contributions to the periodical should be adressed *to the Editor*. Manuscripts of *Brief Reports* can be submitted 8 weeks before publication of the issue, if the authors dispense with proof-reading. The contributions will be published in English, German, French, or Italian; to each *Original Paper* and *Brief Report* should be added a brief summary in a language other than the original one. Drawings and photographs for *illustrations* should be sent ready for reproduction with indication of the proposed reduction; lettering on the illustrations should be entered in pencil, preferably on a loosely attached transparent sheet. Authors of Original Papers exceeding 16 pages are requested to pay a *contribution* of Sw.Frs. 20.– per page for pages 17–24, and of Sw.Frs. 35.– per page for pages 25 and over. From Vol. IX, 1958 on the *contributions* are fixed as follows: Sw.Frs. 25.– per page for pages 17–24, Sw.Frs. 40.– per page for pages 25–32 and Sw.Frs. 50.– per page for pages 33 and over. The authors of *Survey Articles, Original Papers,* and *Brief Reports* receive 50 free separata prints without cover.

ZAMP paraît régulièrement tous les deux mois. Derniers délais pour présenter les manuscrits: trois mois avant la parution de chaque numéro. Tous les manuscrits et toute correspondance relatifs à la rédaction sont à adresser au rédacteur. Les manuscrits pour des *communications brèves* peuvent être présentés huit semaines avant la parution, si les auteurs renoncent à contrôler les épreuves. Les articles seront publiés en langues française, anglaise, allemande ou italienne; cependant, chaque *article original* et toute *communication brève* devront être accompagnés d'un résumé en une autre langue. Les *illustrations* doivent être prêtes à la reproduction et il faudra y indiquer l'echelle de réduction. La légende devra être inscrite au crayon, de préférence sur papier transparent, légèrement collé à l'illustration. Pour articles originaux qui dépassent 16 pages, une *contribution* de frs.s. 20.– par page doit être payée pour les pages 17–24; à partir de page 25 la contribution est de frs.s. 35.– par page. Dès Vol. IX, 1958, les contributions seront fixés comme suit: frs.s. 25.– par page pour les pages 17–24 et frs.s. 40.– par page pour les pages 25–32; à partir de page 33 la contribution est de frs.s. 50.– par page. Les auteurs de *comptes rendus*, ainsi que ceux d'*articles originaux* et de *communications brèves* recevront 50 tirés à part sans couverture de leur article.

Jahresabonnement (6 Nummern): Inland sFr. 46.–, Ausland sFr. 58.– (DM 58.–), Einzelnummer sFr. 12.–
Annual subscription (6 issues): Switzerland Sw.Frs. 46.–, foreign Sw.Frs. 58.– (DM 58.–), single copy Sw.Frs. 12.–
Abonnement annuel (6 numéros): Suisse frs.s. 46.–, étranger frs.s. 58.– (DM 58.–), le numéro frs.s. 12.–
Postabonnement – Post-Office Subscription – Abonnement par office postal: Belgien, Dänemark, Finnland, Holland, Italien, Luxemburg, Marokko, Norwegen, Portugal, Schweden
Inserate/Advertisements/Annonces: 1/1 Seite/page: Fr./DM 165.–, ½ Seite/page: Fr./DM 88.–, ¼ Seite/page: Fr./DM 50.–

Theory of Oscillation Type Viscometers: The Oscillating Cup[1])

Part I

By Joseph Kestin and Gordon Frank Newell, Providence, R. I.[2])

Abstract

This is the first of a series of papers dealing with the theory of oscillation type viscometers with particular emphasis on those in which a finite right circular cylinder (cup or disk) oscillates in contact with a fluid. The purpose is to obtain formulae which relate the density and viscosity of the fluid to the frequency and logarithmic decrement of the oscillation and the various physical properties of the suspension system. The study is to include an accurate analysis of the fluid motion in the vicinity of the edges since this is the main source of error in most existing theories. The first paper gives a general formulation of the problem and an exact solution (including transients) for the oscillating cup viscometer with the fluid inside the cup.

List of Symbols

The following is a partial list of symbols including only those that are used repeatedly:

A surface of contact between fluid and cylinder;
$D(s)$ defined in equation (16);
$f(\tau)$ transient, equation (42);
h half height of cylinder or height of liquid in an open cup;
I moment of inertia of suspension system;
I' moment of inertia of fluid inside cup;
I_k modified Bessel function of order k;
J_k Bessel function of order k;
$M(\tau)$ frictional moment exerted by the fluid;
n normal to A outward from the fluid;
r radial coordinate in the fluid;

[1]) This work was supported by the United States Air Force through the Air Force Office of Scientific Research and Development Command under contract No. AF 18(600)1548. Part of the work was done while one of the authors (G. F. N.) was being supported by a grant from the Alfred P. Sloan Foundation.

[2]) Brown University.

R	radius of cylinder;
s_m	see equation (34);
s_μ	see equation (25);
s_{jm}	see equation (38);
S_k	roots of equation (39);
t	time;
T_0	natural period of oscillation;
w	dimensionless form of $\bar{\Omega}$, see equation (12);
z	vertical coordinate in fluid;
$\alpha(\tau)$	angular displacement of body;
α_0	initial angular displacement of body;
δ	boundary layer thickness $(\nu/\omega_0)^{1/2}$;
Δ	logarithmic decrement;
Δ_0	logarithmic decrement in vacuum;
η	dimensionless vertical coordinate z/δ;
η_0	dimensionless height h/δ;
μ_j	zeros of J_1, $J_1(\mu_j) = 0$;
ν	kinematic viscosity of fluid;
ξ	dimensionless radial coordinate r/δ;
ξ_0	dimensionless radius of cylinder R/δ;
ζ	density of fluid;
τ	dimensionless time $\omega_0 \tau$;
ω	circular frequency of oscillation;
ω_0	circular frequency in vacuum;
Ω	angular velocity of the fluid;
*	complex conjugate;

bar over symbol denotes the Laplace transform of the function.

1. Introduction

The use of oscillating systems for the measurement of the viscosity of fluids leads to great simplicity of design and a high accuracy of measurement. The only measurements required are those of length, mass, and time all of which can be made very accurately, the errors being reducible to 1 part per 1000.

The types of systems in most common use consist of the following arrangement: A cylindrically symmetric body is suspended by a torsion wire along its axis so as to have a certain observable natural period and logarithmic decrement in a vacuum. If the body is then placed in contact with a fluid, the oscillation of the body will also impart motion to the fluid with two principal consequences. (1) The fluid is viscous and some of the energy is dissipated in heat. This gives rise to an increased value of the logarithmic decrement of oscillation for the combined system. (2) The fluid has mass and an effective

moment of inertia which causes the system as a whole to have a longer period of oscillation.

The changes in frequency and decrement caused by the fluid depend only upon the density and viscosity of the fluid and measurable properties of the suspension system and, therefore, in principle, one could infer the viscosity and density of the fluid from measurements of the frequency and decrement. In most cases the density can be measured directly with greater accuracy so that only the viscosity is of interest.

The main difficulty that has prevented the use of this type of system for precision viscosity measurements is the absence of sufficiently accurate theoretical relations between the observed frequency and/or decrement of oscillation and the unknown viscosity. Typical applications using existing approximate formulae have resulted in errors ranging from a few percent to as much as 100% in the calculated viscosity.

The following is the first in a series of papers in which the theory of some of the more common types of oscillating systems will be extended so as to give, wherever possible, formulae that are as accurate as is necessary in order to make full use of the accuracy of existing data.

The specific types of oscillating systems that have been proposed or are in use are classified as follows:

(1) The solid body is a disk or circular cylinder of finite height suspended in a virtually infinite fluid [1–3][3]).

(2) An arrangement as in (1), except that the solid body is a sphere [1, 4, 5].

(3) The solid is a disk again but the disk oscillates in a plane parallel with two fixed plates placed above and below the disk so as to retard the motion of the fluid situated in the region between the plates [3].

(4) The body is a hollow cylinder or sphere and the fluid is contained inside the body. The region outside the body may be a vacuum or it may be a fluid. In the latter case the fluid motion outside can be treated separately and is equivalent to one of the above cases [5–7].

The literature dealing with either experimental or theoretical aspects of these problems is quite lengthy. The references noted above are some of the more recent publications most of which contain more extensive bibliographies of earlier work.

Of the cases listed above, only the spherical bodies lead to relatively simple exact formulae. These have already been treated elsewhere [5] and will not be considered here. Unfortunately there are some experimental difficulties involved in the design and manufacture of this type of viscometer and it has not been used as much as the others.

The remaining cases all have one principal difficulty in common. None of the existing theories except [6] accurately account for the peculiar behavior

[3]) Numbers in brackets refer to References, page 465.

of the fluid in the vicinity of the edges where the vertical and horizontal surfaces of the cylinder meet. Most of the following work will be directed toward the analysis of these edge effects which are the principal source of error in present theories.

The first case to be treated in this and in the second paper is the hollow cylinder with the fluid inside and a vacuum outside: the oscillating cup viscometer. This will be studied in considerable detail mainly because this is the only one of the cylindrical shaped bodies that has been treated exactly. The analysis of this serves a dual purpose of being an end in itself and also as a testing ground for various approximation methods. An exact solution for the cup has actually been obtained and used by Shvidkovskii *et al.* [6] but they give only one form of the solution which in some situations is very difficult to use.

The following sections also give a general formulation of the mathematical problems common to all the other viscometers to be studied later.

2. Formulation of the Problem

The formulation and notation used in this section follows closely that described in more detail in [8, 1, 3, 4].

The motion of the body is described by the equation

$$I\,\omega_0^2\left[\frac{d^2\,\alpha(\tau)}{d\tau^2}+2\,\Delta_0\,\frac{d\alpha(\tau)}{d\tau}+(1+\Delta_0^2)\,\alpha(\tau)\right]=M(\tau)\,, \tag{1}$$

in which $\alpha(\tau)$ is the angular displacement of the body from equilibrium, $\omega_0=2\pi/T_0$ is the natural angular frequency of oscillation in a vacuum, T_0 is the corresponding period of oscillation, $\tau=\omega_0\,t$ is a dimensionless unit of time t, I is the moment of inertia of the solid body, $I\,\omega_0^2$ is therefore the spring constant, $M(\tau)$ is the frictional moment exerted by the fluid, and Δ_0 denotes the logarithmic decrement in a vacuum [for $M(\tau)=0$].

The analysis of equation (1) is facilitated by the use of the Laplace transform. We assume that initially the system is displaced from its equilibrium and then released so that

$$\alpha(\tau)=\alpha_0 \quad \text{and} \quad \frac{d\alpha(\tau)}{d\tau}=0 \quad \text{for } \tau=0\,. \tag{2}$$

If we denote the Laplace transform of any function $f(\tau)$ by

$$\bar{f}(s)=\int_0^\infty e^{-s\tau}\,f(\tau)\,d\tau\,, \tag{3}$$

then $\bar{\alpha}(s)$ satisfies the equation

$$[(s+\Delta_0)^2+1]\,\bar{\alpha}(s)-\frac{\overline{M(s)}}{I\,\omega_0^2}=(s+2\,\Delta_0)\,\alpha_0\,. \tag{4}$$

In order to determine $M(\tau)$, or its transform $\overline{M(s)}$, we must investigate the motion of the fluid, and for this we make the usual assumption that no secondary motion is developed, i. e., we omit the non-linear terms in the Navier-Stokes equations. The present analysis is, strictly speaking, applicable to zero amplitude oscillations or to data extrapolated to zero amplitude. In practice, however, the amplitude is usually small enough so that no extrapolation is necessary.

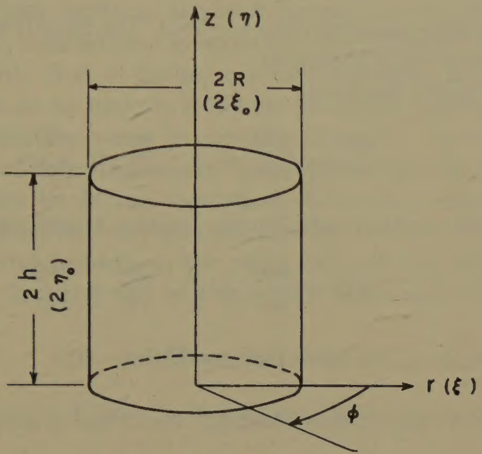

Figure 1
System of coordinates.

The fluid motion can be described in terms of its angular velocity Ω which in a polar-cylindrical system of coordinates r, φ, z (Figure 1), satisfies the differential equation [5],

$$\frac{\partial \Omega}{\partial \tau} = \nu \left\{ \frac{\partial^2 \Omega}{\partial r^2} + \frac{3}{r} \cdot \frac{\partial \Omega}{\partial r} + \frac{\partial^2 \Omega}{\partial z^2} \right\}, \tag{5}$$

where ν is the kinematic viscosity of the fluid. The boundary conditions to be satisfied by Ω are

$$\left.\begin{aligned} &\Omega(r, z, t) = \frac{d\alpha}{dt} \quad \text{at the boundary, } r = R,\ z = 0 \text{ and } z = 2\,h\,, \\ &\Omega(r, z, 0) = 0. \end{aligned}\right\} \tag{6}$$

The first condition implies that there is no slip at the boundary between the fluid and the oscillating body. The second condition implies that the fluid is initially at rest.

The torque $M(\tau)$ is related to the fluid motion through the equation

$$M(\tau) = -\varrho\,\nu \iint\limits_A r^2 \frac{\partial \Omega}{\partial n}\, d\sigma\,, \tag{7}$$

in which ϱ is the density of the fluid, A denotes the surface of contact between the fluid and the body, n is the normal to A from the fluid into the body and $d\sigma$ is an element of surface area.

It is convenient to introduce dimensionless space coordinates defined by

$$\xi = \frac{r}{\delta}, \quad \xi_0 = \frac{R}{\delta}, \quad \eta = \frac{z}{\delta}, \quad \eta_0 = \frac{h}{\delta} \quad \left(\delta = \sqrt{\frac{\nu}{\omega_0}}\right), \tag{8}$$

along with the dimensionless time $\tau = \omega_0 t$. The length δ is, in some sense, an average boundary layer thickness.

Equation (5) now becomes

$$\frac{\partial \Omega}{\partial \tau} = \frac{\partial^2 \Omega}{\partial \xi^2} + \frac{3}{\xi} \cdot \frac{\partial \Omega}{\partial \xi} + \frac{\partial^2 \Omega}{\partial \eta^2}. \tag{9}$$

If there is no fluid motion initially, the Laplace transform of equation (9) gives

$$s \overline{\Omega} = \frac{\partial^2 \overline{\Omega}}{\partial \xi^2} + \frac{3}{\xi} \cdot \frac{\partial \overline{\Omega}}{\partial \xi} + \frac{\partial^2 \overline{\Omega}}{\partial \eta^2} \tag{10}$$

and equation (6) gives the boundary condition

$$\overline{\Omega} = \omega_0 (s \overline{\alpha} - \alpha_0) \quad \text{on } A. \tag{11}$$

We can also make $\overline{\Omega}$ non-dimensional by choosing

$$w = \frac{\overline{\Omega}}{\omega_0 (s \overline{\alpha} - \alpha_0)}. \tag{12}$$

The fluid motion is then described by the completely dimensionless equation

$$s w = \frac{\partial^2 w}{\partial \xi^2} + \frac{3}{\xi} \cdot \frac{\partial w}{\partial \xi} + \frac{\partial^2 w}{\partial \eta^2}, \qquad w = w(\xi, \eta, s) \tag{13}$$

with the boundary condition

$$w(\xi, \eta, s) = 1 \quad \text{on } A. \tag{14}$$

$\overline{M}(s)$ can be expressed in terms of w and the result substituted in equation (4) to give

$$\frac{\overline{\alpha}(s)}{\alpha_0} = \frac{1}{s} - \frac{1 + \Delta_0^2}{s[(s + \Delta_0)^2 + 1 + D(s)]}, \tag{15}$$

with

$$D(s) = + \frac{\varrho \, \delta^5}{I} \, s \iint\limits_A \xi^2 \, \frac{\partial w}{\partial n} \, d\sigma, \tag{16}$$

in which n and $d\sigma$ are also measured in units of δ.

By inversion of the Laplace transform, $\alpha(\tau)$ can be written as the integral

$$\alpha(\tau) = \frac{\alpha_0}{2\pi i} \int\limits_C ds\, e^{s\tau} \left\{ \frac{1}{s} - \frac{1 + \Delta_0^2}{s\,[(s + \Delta_0)^2 + 1 + D(s)]} \right\} \tag{17}$$

along any vertical contour C in the right-hand half of the complex plane.

The mathematical problem is to solve equations (13) and (14) for w, or, strictly speaking, for just $\partial w/\partial n$ at the surface only, to determine $D(s)$ from equation (16) and then to substitute in equation (17) to find $\alpha(\tau)$.

The goal is primarily that of finding accurate formulae for $\alpha(\tau)$ which are not so cumbersome as to be useless. It should be kept in mind that the ultimate purpose is to infer the value of viscosity from the *observed* behavior of $\alpha(\tau)$. Unless $\alpha(\tau)$ is relatively simple or at least approximately so, the problem of finding the viscosity by fitting theoretical curves for various values of ν with experimentally observed curves is impractical.

Present experimental techniques for using such an instrument are based upon the assumption that $\alpha(\tau)$ will be very nearly a damped oscillation of the type

$$\alpha(\tau) \sim e^{-\Delta\omega\tau} \cos(\omega\,\tau + \psi) \tag{18}$$

and the values of viscosity are to be inferred from measurements of ω or Δ or both.

3. Exact Solution for the Cup

In treating the oscillating cup, there are two slightly different physical situations to be considered. In the first scheme the cup is closed at the top with the aid of a lid which remains in contact with the fluid (e. g., a gas). In the second, the fluid (e. g., a liquid) possesses a free surface. In the first case the boundary conditions are as given in equation (14), whereas in the second case we have

$$\frac{\partial w}{\partial \eta} = 0 \quad \text{at} \quad \eta = \eta_0\,, \tag{19}$$

where η_0 denotes the dimensionless height of the column of liquid, on condition that surface tension is neglected.

These two cases are mathematically identical, because in the first case (cup of height $2\,\eta_0$), the plane at $\eta = \eta_0$ is a plane of symmetry along which condition (19) is satisfied. It is, therefore, sufficient to solve the problem for the lower half of the cup only; the drag on the total surface will be just double that on the bottom half.

The simplest procedure for solving equations like equation (13) are to use separation of variables or to expand in some suitable complete set of orthogonal

functions. Actually these two basic procedures are quite similar because the most suitable set of functions in which to make expansions are those which naturally arise from the separation of variables. There are, however, several modifications of these basic schemes which lead to several different forms of the solution. Since the methods in question are fairly well known, we will simply outline the principal steps. Five different forms of the solution each of which will later be particularly useful in some special situations were obtained by the five methods described below.

(i) We notice that the function

$$w'(\xi, \eta, s) \equiv w(\xi, \eta, s) - 1$$

satisfies the inhomogeneous differential equation

$$\frac{\partial^2 w'}{\partial \xi^2} + \frac{3}{\xi} \cdot \frac{\partial w'}{\partial \xi} + \frac{\partial^2 w'}{\partial \eta^2} - s\, w' = s \tag{20}$$

with homogeneous boundary conditions

$$w' = 0 \quad \text{on } A\,. \tag{21}$$

The set of functions $\xi^{-1} J_1(\mu_j\, \xi/\xi_0)$, with J_1 denoting the Bessel function of first order, satisfy the differential equation

$$\left\{\frac{d^2}{d\xi^2} + \frac{3}{\xi} \cdot \frac{d}{d\xi} + \frac{\mu_j^2}{\xi_0^2}\right\} \frac{J_1(\mu_j\, \xi/\xi_0)}{\xi} = 0\,, \tag{22}$$

which arises from equation (20) with $s = 0$ by separation of variables. If we define the parameters μ_j so that these functions will vanish at $\xi = \xi_0$, then

$$J_1(\mu_j) = 0\,,$$

i. e., the μ_j's are the zeros of J_1. These functions form a complete orthogonal set and any function which is continuous in the interval $0 \leqq \xi \leqq \xi_0$ and vanishes at $\xi = \xi_0$ can be expanded in a convergent series of such functions. In particular we can write

$$w'(\xi, \eta, s) = \sum_{j=1}^{\infty} b_j'(\eta, s)\, \xi^{-1} J_1\left(\frac{\mu_j\, \xi}{\xi_0}\right). \tag{23}$$

If we substitute this into equation (20) and make a similar expansion of the right-hand side of equation (20), we obtain an equation which can be satisfied only if the b_j' are solutions of the ordinary differential equations

$$\left\{\frac{d^2}{d\eta^2} - s_\mu^2\right\} b_j'(\eta, s) = \frac{-2\, \xi_0\, s}{\mu_j\, J_0(\mu_j)} \tag{24}$$

with

$$s_\mu^2 = \frac{\mu_j^2}{\xi_0^2} + s\,. \tag{25}$$

Since w' vanishes on the boundary we must require that

$$b_j'(0, s) = b_j'(2\,\eta_0, s) = 0\,. \tag{26}$$

The solution of equations (24) and (26) is

$$b_j'(\eta, s) = \frac{-\,2\,\xi_0\,s}{\mu_j\,s_\mu^2\,J_0(\mu_j)}\left[\frac{\cosh s_\mu\,(\eta_0-\eta)}{\cosh s_\mu\,\eta_0} - 1\right]$$

and so from equation (23) we obtain

$$w(\xi, \eta, s) = 1 + 2\,s \sum_{j=1}^{\infty} \frac{-\,1}{\mu_j\,s_\mu^2}\left[\frac{\cosh s_\mu\,(\eta_0-\eta)}{\cosh s_\mu\,\eta_0} - 1\right]\frac{\xi_0\,J_1(\mu_j\,\xi/\xi_0)}{\xi\,J_0(\mu_j)}\,. \tag{27}$$

If this is substituted into equations (16) and integrated term by term, one obtains the final result,

$$D(s) = \frac{I'}{I}\,s^2 \sum_{j=1}^{\infty} \frac{8}{\mu_j^2}\left\{1 - \frac{s}{s_\mu^2}\left[1 - \frac{\tanh s_\mu\,\eta_0}{s_\mu\,\eta_0}\right]\right\}. \tag{28}$$

I' represents the moment of inertia of the fluid inside the cup;

$$I' = \frac{1}{2}\,\pi\,\varrho\,\eta_0\,\xi_0^4\,\delta^5 = \frac{1}{2}\,\pi\,\varrho\,h\,R^4 \tag{29a}$$

for a fluid with a free surface at $\eta = \eta_0$ and

$$I' = \pi\,\varrho\,\eta_0\,\xi_0^4\,\delta^5 = \pi\,\varrho\,h\,R^4 \tag{29b}$$

for a full cup with a lid at $\eta = 2\,\eta_0$.

It is also possible to obtain an alternative form of equation (29) by using the identity $8 \sum \mu_j^{-2} = 1$. This gives

$$D(s) = s^2\,\frac{I'}{I} - s^3\,\frac{I'}{I}\,8 \sum_j \frac{1}{\mu_j^2\,s^2}\left[1 - \frac{\tanh s_\mu\,\eta_0}{s_\mu\,\eta_0}\right]. \tag{28a}$$

(ii) If we had a very long cylinder, we know that, for most values of η, $w(\xi, \eta, s)$ is nearly independent of η. We would then have

$$\frac{\partial^2 w}{\partial \xi^2} + \frac{3}{\xi}\cdot\frac{\partial w}{\partial \xi} - s\,w \sim 0 \quad \text{with} \quad w(\xi_0, \eta, s) = 1\,.$$

The solution of this equation is

$$w \sim \frac{\xi_0\,I_1\,(\sqrt{s}\,\xi)}{\xi\,I_1\,(\sqrt{s}\,\xi_0)}\,,$$

in which I_1 is the modified Bessel function of order 1. This is, of course, the exact solution for a cylinder of infinite height.

These facts suggest that we try to find the difference function

$$w'' = w - \frac{\xi_0 \, I_1 (\sqrt{s}\, \xi)}{\xi \, I_1 (\sqrt{s}\, \xi_0)}$$

which satisfies the same differential equation as w but the boundary conditions

$$w''(\xi_0, \eta, s) = 0 \,, \quad w''(\xi, 0, s) = w''(\xi, 2\,\eta_0, s) = 1 - \frac{\xi_0 \, I_1 (\sqrt{s}\, \xi)}{\xi \, I_1 (\sqrt{s}\, \xi_0)} \,. \tag{30}$$

As in (i), we again seek to find an expansion of w'' of the type

$$w''(\xi, \eta, s) = \sum_{j=1}^{\infty} b_j''(\eta, s)\, \xi^{-1} \, J_1\left(\frac{\mu_j \, \xi}{\xi_0}\right). \tag{31}$$

Substitution of this into the differential equation gives a set of homogeneous equations for the b'', namely

$$\left\{\frac{d^2}{d\eta^2} - s_\mu^2\right\} b_j''(\eta, s) = 0 \,.$$

We require that $b_j''(0, s) = b_j''(2\,\eta_0, s)$ so that $b_j''(\eta, s)$ must be of the form

$$b_j''(\eta, s) = b_j''(0, s)\, \frac{\cosh s_\mu (\eta - \eta_0)}{\cosh s_\mu \, \eta_0} \,. \tag{32}$$

The values of the coefficients $b_j''(0, s)$ are finally determined by substituting equation (32) into equation (31) and forcing w'' to satisfy the conditions given in equation (30). Integration of the solution gives the result

$$D(s) = s^2 \, \frac{I'}{I} \left\{ \frac{4\, I_2 (\sqrt{s}\, \xi_0)}{\sqrt{s}\, \xi_0 \, I_1 (\sqrt{s}\, \xi_0)} + \frac{8\, s}{\eta_0} \sum_j \frac{\tanh (s_\mu \, \eta_0)}{\mu_j^2 \, s_\mu^3} \right\}. \tag{33}$$

This expression is exactly equivalent to equation (28) and could have been derived from equation (28) if one knew the appropriate expansion identities to transform from one to the other. The method and the result given by equation (33) are essentially the same as given in [6].

(iii) We can apply a procedure which differs from that given in (i) only in that the role of the ξ and η coordinates are interchanged. The set of functions $\sin[(2\,m + 1)\,\pi\,\eta/2\,\eta_0]$ bear the same relation to equation (20) as did the functions $\xi^{-1} \, J_1(\mu_j \, \xi/\xi_0)$. They are solutions of the equation

$$\left\{\frac{d^2}{d\eta^2} + \left[\frac{(2\,m + 1)\,\pi}{2\,\eta_0}\right]^2\right\} \sin \frac{(2\,m + 1)\,\pi\,\eta}{2\,\eta_0} = 0 \,,$$

which arises from equation (20) by separation of variables in the same way as did equation (22).

These functions vanish for $\eta = 0$ and have a vanishing derivative at $\eta = \eta_0$, provided m is an integer. They form a complete set and any continuous function satisfying the same boundary conditions can be expanded in a convergent series (Fourier series) of these functions.

Corresponding to equation (23) we seek a solution in the form

$$w'(\xi, \eta, s) = \sum_{m=0}^{\infty} a'_m(\xi, s) \sin\frac{(2\,m+1)\,\pi\,\eta}{2\,\eta_0}.$$

In analogy with equations (24), (25) we obtain

$$\left\{\frac{d^2}{d\xi^2} + \frac{3}{\xi}\cdot\frac{d}{d\xi} - s_m^2\right\} a'_m(\xi, s) = \frac{4\,s}{\pi\,(2\,m+1)}$$

with

$$s_m^2 = s + \left(\frac{(2\,m+1)\,\pi}{2\,\eta_0}\right)^2 \tag{34}$$

and the a'_m must satisfy the boundary conditions

$$a'_m(\xi_0, s) = 0\,, \quad a'_m(0, s) \text{ finite.}$$

The solutions of these equations finally lead to the result analogous to equation (28),

$$D(s) = +\,s^2\,\frac{8\,I'}{\pi^2\,I} \sum_{m=0}^{\infty} \frac{1}{(2\,m+1)^2} \left\{1 - \frac{s}{s_m^2}\cdot\frac{I_3(s_m\,\xi_0)}{I_1(s_m\,\xi_0)}\right\}, \tag{35}$$

and a summation of the leading terms gives the alternative form

$$D(s) = s^2\,\frac{I'}{I} - s^3\,\frac{8}{\pi^2}\cdot\frac{I'}{I} \sum_{m=0}^{\infty} \frac{I_3(s_m\,\xi_0)}{(2\,m+1)^2\,s_m^2\,I_1(s_m\,\xi_0)}\,. \tag{35a}$$

(iv) The following method bears the same relation to (ii) as (iii) did to (i). If we have a very squat cylinder, the ξ dependence of w is only slight for most values of ξ. We expect that

$$\frac{\partial^2 w}{\partial\eta^2} - s\,w \sim 0 \quad \text{with} \quad w(\xi, 0) = w(\xi, 2\,\eta_0) = 1\,,$$

i. e.,

$$w \sim \frac{\cosh\sqrt{s}\,(\eta_0 - \eta)}{\cosh\sqrt{s}\,\eta_0}\,,$$

the solution for two infinite plates.

This suggests that we try to evaluate

$$w''' = w - \frac{\cosh\sqrt{s}\,(\eta_0 - \eta)}{\cosh\sqrt{s}\,\eta_0}\,.$$

We expand this in a Fourier series and determine the coefficients in a manner analogous to that of (ii). The only difference is that the η and ξ coordinates exchange roles in the same manner as in (i) and (iii). The procedure is straightforward and gives the result,

$$D(s) = s^2 \frac{I'}{I} \left\{ \frac{\tanh(\sqrt{s}\,\eta_0)}{\sqrt{s}\,\eta_0} + \frac{32\,s}{\pi^2\,\xi_0} \sum_{m=0}^{\infty} \frac{1}{(2\,m+1)^2\,s_m^3} \cdot \frac{I_2(s_m\,\xi_0)}{I_1(s_m\,\xi_0)} \right\}. \tag{36}$$

(v) The final method is, in essence, a combination of (i) and (iii). The set of product functions $\xi^{-1} J_1(\mu_j\,\xi/\xi_0) \sin[(2\,m+1)\,\pi\,\eta/2\,\eta_0]$ form a complete orthogonal set for expansions of any function of the two variables ξ and η that vanishes on the boundary of the cup. The product functions are, of course, the 'elementary' solutions of the differential equation obtained by separation of variables.

If we make a double series expansion of w'

$$w'(\xi, \eta, s) = \sum_j \sum_m a_{j\,m}\,\xi^{-1} J_1\left(\frac{\mu_j\,\xi}{\xi_0}\right) \sin\frac{(2\,m+1)\,\pi\,\eta}{2\,\eta_0},$$

substitute this into equation (20) and make a similar expansion of the right-hand side of equation (20), we obtain immediately the coefficients $a_{j\,m}$ which define the solution. Actually one can proceed in a number of other ways to the same result, namely

$$D(s) = \frac{I'}{I}\,s^2 - \frac{I'\,64\,s^3}{I\,\pi^2} \sum_{j,m} \frac{1}{\mu_j^2\,(2\,m+1)^2\,(s - s_{j\,m})} \tag{37}$$

with

$$s_{j\,m} \equiv -\left(\frac{(2\,m+1)\,\pi}{2\,\eta_0}\right)^2 - \frac{\mu_j^2}{\xi_0^2}. \tag{38}$$

We now have at our disposal a sizeable collection of exact forms for $D(s)$, namely equations (28), (28a), (33), (35), (35a), (36), and (37), however, any comparison of usefulness of the various forms for $D(s)$ or any approximations must be considered in conjunction with the evaluation of the integral in equation (17) for the actual motion of the cup, $\alpha(\tau)$.

Formally, at least, $\alpha(\tau)$ can be evaluated by residue theory since the only singularities of the integrand are poles. This gives

$$\alpha(\tau) = -\alpha_0 \sum_k \frac{(1 + \Delta_0^2)\exp(S_k\,\tau)}{S_k\,[2\,S_k + 2\,\Delta_0 + D'(S_k)]}, \tag{39}$$

in which S_k are the roots of the equation

$$(S_k + \Delta_0)^2 + 1 + D(S_k) = 0, \tag{40}$$

i. e., the poles of the integrand. $D'(S_k)$ denotes the derivative of $D(s)$ at $s = S_k$

and the k-th term of the series represents the residue of the integrand at the point $s = S_k$.

If $I'/I = 0$, then $D(s) \equiv 0$ and equation (40) reduces to a simple quadratic with only two solutions;

$$(S_k + \Delta_0)^2 + 1 = 0 , \quad S_k = \pm i - \Delta_0 , \tag{41a}$$

and

$$\alpha(\tau) = e^{-\Delta_0 \tau} \alpha_0 (\cos \tau + \Delta_0 \sin \tau) . \tag{41b}$$

This, of course, represents the motion of the cup in the absence of any fluid.

If we now consider what happens for $0 < I'/I \ll 1$, we see that regardless of how small I'/I may be, $D(s)$ cannot be small for all values of s because it has infinitely many poles at the points s_{jm} [equations (37), (38)]. Near each of these poles which lie on the negative real axis there is one point where $D(s)$ will assume any given value of order 1 or larger and in particular there is one point S_k near each s_{jm} where $D(S_k)$ has a value that satisfies equation (40). Since all quantities in equation (40) are real for real values of S_k, it is easy to prove that each of the new roots S_k is also a negative real number.

Besides the infinitely many negative roots which lie near the s_{jm}, we still have two roots which for $I'/I \ll 1$ lie near the points $\pm i - \Delta_0$. Since the complex conjugate (denoted by *) of equation (40) gives

$$(S_k^* + \Delta_0)^2 + 1 + D(S_k^*) = 0 ,$$

it follows that if S_k is a root of equation (40), so also is S_k^*. Any root of equation (40) must, therefore, either be real or one of a complex conjugate pair and the two roots near $\pm i - \Delta_0$ must still form a complex conjugate pair even for $I'/I \neq 0$.

Despite the fact that $I' \to 0$ causes a singular behavior in the roots of equation (40), $\alpha(\tau)$ approaches equation (41b) continuously as $I' \to 0$. It is easy to see that the terms of equation (39) associated with the two complex roots vary continuously into those for $I' = 0$ and give equation (41b), so it is only necessary to see that as $I' \to 0$, the contribution from the infinitely many negative roots contribute nothing to $\alpha(\tau)$. This is true because at each negative root S_k, $D(S_k)$ is at least of order 1 and since S_k is very near a pole of $D(s)$, $D'(S_k)$ is very large, of order $I/I' \gg 1$ to be exact. $D'(S_k)$ dominates the denominator of equation (39) and causes each of the new terms to be of order I'/I. For $I'/I \ll 1$, $\alpha(\tau)$, therefore, is of the form

$$\alpha(\tau) = e^{-\Delta \omega \tau} \alpha_0 (A \cos \omega \tau + B \sin \omega \tau) + f(\tau) \tag{42}$$

with $f(\tau)$ of order I'/I and the various other parameters differing from those of equation (41b) by quantities of order I'/I.

The Δ and ω in equation (42) are obtained from the two complex roots S_k and S_k^* by writing them as

$$S_k = \omega\,(-\Delta \pm i)\,. \tag{43}$$

Since equation (40) is complex, one may choose to consider the two real equations obtained by taking the real and imaginary parts of equation (40), namely

$$\operatorname{Re} D\,[\omega\,(-\Delta \pm i)] = -1 + \omega^2 - (\Delta\omega - \Delta_0)^2 \tag{44a}$$

$$\operatorname{Im}\; D\,[\omega\,(-\Delta \pm i)] = \pm 2\,\omega\,(\Delta\omega - \Delta_0)\,. \tag{44b}$$

Many of the results obtained above for $I'/I \ll 1$ are modified only slightly for larger values of I'/I. The transcendental equation for the S_k is analytic in I'/I and the values of S_k will therefore also be analytic functions of I'/I. The roots must still be either real or form complex conjugate pairs and those which were real for $I'/I \ll 1$ will be real for all values of I'/I.

To investigate the real roots further, we consider the behavior of the function $D(s)/s^2$ along the real axis. We observe from equations (37) and (38) that: (a) $D(s)/s^2$ has poles at s_{jm} and the s_{jm} are independent of I'/I, (b) the residues at these poles are all positive, (c) the derivative of $D(s)/s^2$ is everywhere negative, and (d) $D(s)/s^2 \to 0$ for $s \to +\infty$. Condition (b) implies that $D(s)/s^2$ becomes positively infinite as one approaches any pole from the right and negatively infinite from the left. This along with (c) implies that between every two consecutive poles on the real line, $D(s)/s^2$ is monotone decreasing from $+\infty$ to $-\infty$ and (d) guarantees that $D(s)/s^2 > 0$ to the right of the largest s_{jm}.

The S_k are solutions of the equation

$$\frac{D(S_k)}{S_k^2} = -\frac{1}{S_k^2} - \left(1 + \frac{\Delta_0}{S_k}\right)^2$$

both sides of which are sketched in Figure 2 for real S_k. Figure 2 is not drawn to scale but serves only to illustrate the shape of the curves as described above. The desired values of S_k are at the intersections of the two curves.

It is apparent from the graph or the above description of its properties, that there is a value of S_k between every pair of consecutive poles of $D(s)$. As I'/I increases, the values of S_k move continuously to the left but always remain trapped between the values of s_{jm}.

The two roots which were at $\pm i - \Delta_0$ for $I'/I = 0$ also move continuously as I'/I increases and it is clear that $\alpha(\tau)$ can always be formally separated into two parts as in equation (42). The part $f(\tau)$ which we call the transient part consists of an infinite series of terms each of which has a time dependence given by the factor $\exp(S_k\,\tau)$ with $S_k < 0$. The magnitude of the largest S_k

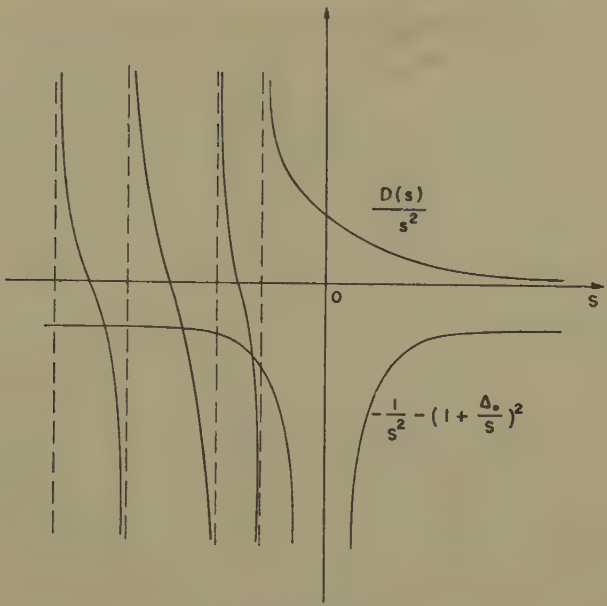

Figure 2
Graphical scheme for locating the roots S_k.

(smallest $|S_k|$), S_1, is a measure of the rate at which the slowest transient term decays. Figure 2 shows that S_1 is less than the largest s_{jm}, s_{01}, but larger than the second largest s_{jm}, which may be either s_{02} or s_{11}, thus,

$$\left.\begin{array}{l} -\left[\dfrac{\pi}{2\,\eta_0}\right]^2 - \dfrac{\mu_2^2}{\xi_0^2} = s_{02} \\ -\left[\dfrac{3\,\pi}{2\,\eta_0}\right]^2 - \dfrac{\mu_1^2}{\xi_0^2} = s_{11} \end{array}\right\} < S_1 < s_{01} = -\left[\frac{\pi}{2\,\eta_0}\right]^2 - \frac{\mu_1^2}{\xi_0^2}. \tag{45}$$

4. Survey of Practical Applications

The motion of the cup is described by equation (42) and to guarantee the possibility of accurate experimental measurements of ω and Δ and accurate calculation of ν and ϱ from them, we must insist that the following conditions be satisfied. (a) The transient $f(\tau)$ in equation (42) is either uniformly small compared with α_0, decays rapidly as compared with the decay of the main oscillation or varies so slowly compared with the main oscillation that it is essentially a constant. In other words, we want $f(\tau)$ to be such that its presence does not obstruct the observation of the main oscillation. (b) Δ must be small

enough so that one can observe at least a few oscillations before the amplitude becomes too small to measure. As a practical matter this means $\Delta < 1/10$ approximately. (c) We must have usable formulae from which ν and ϱ can be calculated from Δ and ω to an accuracy consistent with the accuracy of the experimental data. (d) Δ and ω must be sufficiently sensitive to the values of ν and ϱ so that small errors in the observation will not translate into large errors in the calculated values of ν. In addition to these, there are other practical limitations imposed by the availability of proper materials, instruments etc., but these problems will not be considered here.

All the above conditions relate in one way or another to the properties of the function $D(s)$ which is also a function of the parameters I'/I, η_0 and ξ_0. I'/I, equation (29), depends upon the density of the gas and on the suspension system but not on ν; η_0 and ξ_0, equation (8), depend upon ν and the geometry but not on ϱ; whereas $\eta_0/\xi_0 = h/R$ is independent of the fluid. A determination of I'/I and η_0 or ξ_0 from observed values of Δ and ω using equation (44) is thus equivalent to a determination of ϱ and ν, respectively. To test whether or not in any particular situation the above conditions are satisfied, one must have at least some preliminary estimate of ϱ and ν and thus also I'/I, ξ_0 and η_0.

$D(s)\, s^{-2}\, I/I'$ is a function only of $s\, \xi_0^2$ and $s\, \eta_0^2$ so that in essence I'/I scales the magnitude of $D(s)$, ξ_0^2 or η_0^2 scale its argument whereas $\eta_0/\xi_0 = h/R$ determine the functional form. All properties of the cup are therefore naturally classified according to the magnitude of I'/I, ξ_0 or η_0 and h/R, thus according to the inertia of the fluid, the size of the cup and its shape. Actually a more suitable measure of 'size' is the quantity $|s_{01}| = [\pi/2\,\eta_0]^2 + [\mu_1/\xi_0]^2$ and we shall designate a cup as 'large' or 'small' as this quantity is small or large compared with 1. A small cup is one for which the boundary layer thickness is large compared with either R or h and it gives rise to the physical situation in which the fluid moves with the cup almost as a rigid body. A large cup is one for which the boundary layer thickness is small compared with both R and h and gives rise to a situation in which only a small layer of fluid with a distance of order δ from the walls of the cup is set in motion.

The various consequences of having large, small or intermediate values of I'/I, h/R and 'size' will be considered individually in Part II where suitable approximate forms for $D(s)$ will be obtained for each case along with precise conditions under which the conditions above listed are satisfied, particularly (c) and (d). We can, however, make certain preliminary estimates here based upon the qualitative properties of $D(s)$.

If $I'/I \ll 1$, as would probably be true if the fluid were a gas, we see from the discussion of equation (42) that we have the generally favorable conditions that $f(\tau) = O(\alpha_0\, I'/I) \ll \alpha_0$, $\Delta - \Delta_0 = O(I'/I)$, and $\omega = 1 + O(I'/I)$. This, for sufficiently small I'/I, automatically guarantees that conditions (a) and (b) are satisfied regardless of the shape or size of the cup.

We see from equation (45) that the slowest transient is proportional to $\exp(S_k \tau) < \exp(s_{01} \tau)$ and decreases by a factor of order $\exp(-2\pi |s_{01}|)$ in a time corresponding to one natural period of oscillation. Since we describe a cup as small if $|s_{01}| \gg 1$, it follows that for the small cup the transient decays very rapidly, in a time much less than one natural period and this will guarantee that condition (a) is satisfied regardless of the size of I'/I or of h/R. Actually the condition $|s_{01}| \gg 1$ is much stronger than necessary because if condition (b) is satisfied, it would follow that the decay time of the main oscillation is longer than the actual period of oscillation which in turn is always larger than the natural period. For the transient to decay rapidly compared with the main oscillation, it would, as a practical matter, suffice if the transient decayed to $1/e$ of the value in one natural period or less. Thus we would consider condition (a) to be satisfied if $|s_{01}| \gtrsim 1/2\pi$.

By arguments similar to the above, we would conclude that for a large cup, the slowest transient decays very slowly, but this, in itself, is of little importance. One must consider all the transient terms together particularly those with a shorter decay time. The analysis of the large cup requires special treatment in almost all aspects and will be discussed in Part II. We will find, however, that condition (a) usually is satisfied for the large cup by virtue of having both a slowly decaying and small amplitude transient. The one situation in which condition (a) may give trouble is that in which I'/I is of order one or larger and the dimensions of the cup are such that the decay time of the transient is comparable with the natural period ($|s_{01}|$ equal to about 1/10). Actually in this situation where condition (a) is likely to be violated, we will find that most of the other conditions give trouble also.

Zusammenfassung

Diese Abhandlung ist der erste Bericht aus einer Veröffentlichungsreihe, die sich mit der Theorie schwingender Viskosimeter befasst. Dabei sind besonders die behandelt, bei denen ein endlicher Kreiszylinder (Becher oder Scheibe) von einem flüssigen Medium gefüllt oder umgeben schwingt. Die Aufgabe der Untersuchung ist es, die Abhängigkeit der Frequenz und des logarithmischen Dekrementes der Schwingung von der Dichte und der Viskosität der Flüssigkeit und von den verschiedenen physikalischen Grössen des Aufhängungssystems zu finden. Weiterhin ist eine genaue Analyse der Flüssigkeitsbewegung in den Randzonen eingeschlossen, da diese die Hauptursache der Fehler in den meisten der vorhandenen Theorien war. Die erste Abhandlung gibt die grundlegende Formulierung des Problemes und eine exakte Lösung (einschliesslich der Einschwingzeit) für das Viskosimeter, bei dem ein mit der zu messenden Flüssigkeit gefüllter schwingender Becher verwendet wird.

(Received: June 17, 1957.)

Theory of Oscillation Type Viscometers: The Oscillating Cup

Part II

By David Alan Beckwith[1]) and Gordon Frank Newell[2]), Providence, R. I.

Abstract

The following is a continuation of Part I. The emphasis in this part is on inquiring how the frequency and decrement of the oscillation are related to the viscosity and density of the fluid for cups of various shapes and sizes. In particular, estimates are made of the errors that would result from calculations of the viscosity and density from observed values of the frequency and decrement and known experimental uncertainties of the latter. Methods are also described which enable one to perform these calculations explicitly.

1. Introduction

In Part I[3]) an exact solution of the oscillating cup was obtained and some of the qualitative features of this solution, particularly the transient part, were discussed. The main objective now is to analyze in more detail the properties of the main oscillation and to determine, among other things, if conditions (b), (c) and (d) of section I,4. can be satisfied. Although exact solutions are available, they are difficult to use because ν and ϱ are related to Δ and ω through a pair of simultaneous transcendental equations, equation (I,44), involving $D[\omega(-\Delta \pm i)]$ which has been found only in the form of infinite series. The solution of these equations, therefore, requires special consideration.

The properties of the oscillating cup depend upon its size, shape, and the moment of inertia of the fluid. Because various limiting cases show quite different properties and require different mathematical treatments, it is most convenient to consider these limiting cases separately. We consider first various shapes of small cups for which $|s_{01}| \gg 1$, equation (I,45); then the large

---

[1]) Brown University, now at Bell Telephone Laboratories, Murray Hill, N. J.

[2]) Brown University.

[3]) This is a continuation of Part I, preceding paper, and will employ the same notation. Equation numbers, figures, etc. referring to Part I will be designated by a prefix I.

cups, $|s_{01}| \ll 1$; then the class of systems with $I'/I \ll 1$; and finally any remaining cases.

Much of the following analysis will center around the problem of finding accurate but manageable approximations for $D(s)$ when $s = \omega(\pm i - \Delta)$. In the absence of any fluid motion, $\omega = 1$ and $\Delta = \Delta_0$, we anticipate that under most conditions in which we will be interested, we can assume at least that $\Delta_0 \ll 1$, $\Delta \ll 1$, ω is of order 1 and $|s| = \omega|\pm i - \Delta|$ is therefore also of order 1. $D(s)\, s^{-2}\, I/I'$ is a function only of $s\,\xi_0^2$ and $s\,\eta_0^2$ and it will usually be implied without further comment that $|s\,\xi_0^2|$ and $|s\,\eta_0^2|$ are of the same order of magnitude as ξ_0^2 and η_0^2 respectively for $s = \omega(\pm i - \Delta)$.

2. The Small Cup

By 'small' cup, we mean

$$|s_{01}| = \left[\frac{\pi}{2\,\eta_0}\right]^2 + \left[\frac{\mu_1}{\xi_0}\right]^2 \gg 1 \tag{1}$$

which implies that either η_0 or ξ_0 or both are small compared with 1. We have already seen in section I,4. that this gives a rapidly decaying transient (even for $|s_{01}| \gtrsim 1/2\,\pi$) so that the transient needs no further comment and we turn our attention to finding convenient expressions for $D(s)$ for $|s| = 0(1)$.

We note that equation (1) implies also that $|s_{j\,m}| \geqq |s_{01}| \gg |s|$ for all j's and m's with $|s|$ of order 1. An expansion of equation (I,37) in powers of s would actually be a series in $s/s_{j\,m}$ for various values of j and m and should therefore converge rapidly. It is also a power series in ν^{-1} because

$$-s_{j\,m} = \left[\frac{(2\,m+1)\,\pi}{2\,\eta_0}\right]^2 + \left[\frac{\mu_j}{\xi_0}\right]^2 = \left\{\left[\frac{(2\,m+1)\,\pi}{2\,h}\right]^2 + \left[\frac{\mu_j}{R}\right]^2\right\}\frac{\nu}{\omega_0} \tag{2}$$

is proportional to ν for all values of j and m. This expansion of equation (I,37) gives

$$D(s) = s^2\,\frac{I'}{I}\left[1 + \sum_{l=1}^{\infty} a_l\left(\frac{-s\,\omega_0}{\nu}\right)^l\right] \tag{3}$$

with

$$a_l = \frac{64}{\pi^2}\sum_{j=1}^{\infty}\sum_{m=0}^{\infty}\mu_j^{-2}\,(2\,m+1)^{-2}\left\{\left[\frac{(2\,m+1)\,\pi}{2\,h}\right]^2 + \left[\frac{\mu_j}{R}\right]^2\right\}^{-l}. \tag{4}$$

Regardless of the values of R and h, the first term ($j = 1$, $m = 0$) of equation (4) gives at least the correct order of magnitude of a_l and therefore successive

terms in equation (3) differ approximately by a factor $s/s_{01} = O(1/s_{01})$. The fractional error in $|D(s)|$ resulting from terminating the series, equation (3), after l terms is roughly $|1/s_{01}|^{l+1}$. If we want this fractional error to be of order 10^{-3} or less, for example, and are willing to compute no more than five terms in equation (3), then we must require that

$$|s_{01}| \gtrsim 3 \tag{5}$$

which we accept as the practical limitation of usefulness of the small cup approximation replacing equation (1).

We have obtained a rapidly convergent series in equation (3) at the expense of creating a doubly infinite series representation of the coefficients a_l in equation (4). One should notice, however, that the a_l depend only upon h and R, in fact a_l can be written as h^l or R^l times a function of only h/R. This is of considerable practical importance because one would use the same cup to measure the viscosity of many fluids under various conditions of pressure, temperature, etc. The a_l do not depend upon the fluid and need be evaluated only once for any given cup.

If the given values of R and h are of comparable size, the series in equation (4) converges rapidly enough so that a numerical term by term evaluation presents no practical difficulty. Furthermore the rate of convergence increases rapidly with increasing l. If R/h is very large or very small, a term by term evaluation of equation (4) is rather tedious, however, and we shall seek better ways of evaluating the a_l. One could obtain suitable approximations directly from equation (4) but only by using considerable caution because one sees very soon that a convergent power series expansion of a_l in powers of R/h or h/R does not exist. A much better scheme of finding the a_l for $R/h \ll 1$ or $R/h \gg 1$ is to use one of the other forms of $D(s)$ derived in section I,3.

We consider first the case $R/h \ll 1$. One would expect that equation (I,28) or, preferably, equation (I,33) would be a good starting point as suggested partly by the manner in which these equations were derived. The expansion difficulties mentioned above can be attributed to the function $\tanh s_\mu \eta_0$ of equations (I,28) or (I,33). From the definition of s_μ, equation (I,25), we see that

$$s_\mu^2 \eta_0^2 = (s\,\xi_0^2 + \mu_j^2)\left(\frac{h}{R}\right)^2 \gg 1 \quad \text{for all } j\,, \tag{6}$$

and therefore

$$\tanh s_\mu \eta_0 = 1 - 2\exp(-2\,s_\mu \eta_0) + \cdots. \tag{7}$$

The term $2\exp(-2\,s_\mu \eta_0)$ has approximately the order of magnitude $\exp(-\mu_j\, h/R) \leqq \exp(-\mu_1\, h/R)$ and clearly does not have a power series

expansion in R/h but it is asymptotically smaller than any finite power of R/h. By treating separately these exponentially small terms, one can expand the remaining part of $D(s)$, equation (I,33) is powers of s and R/h thereby obtaining for a_l the expressions

$$\left.\begin{aligned}
a_1 &= +\frac{R^2}{3!\,2^4} - \left(\frac{R}{h}\right) R^2 \left(8 \sum_{j=1}^{\infty} \mu_j^{-5}\right) + \left(\frac{R}{h}\right) \frac{16\,R^2}{\mu_1^5} \exp \frac{-\mu_1 h}{R}, \\
a_2 &= +\frac{R^4}{4!\,2^4} - \left(\frac{R}{h}\right) R^4 \left(12 \sum_{j=1}^{\infty} \mu_j^{-7}\right), \\
a_3 &= +\frac{R^6}{5!\,3 \times 2^4} - \left(\frac{R}{h}\right) R^6 \left(15 \sum_{j=1}^{\infty} \mu_j^{-9}\right), \\
a_4 &= +\frac{13\,R^8}{6!\,3 \times 2^9} - \left(\frac{R}{h}\right) R^8 \left(\frac{35}{2} \sum_{j=1}^{\infty} \mu_j^{-11}\right), \\
a_5 &= +\frac{33\,R^{10}}{8!\,2^{13}} \left[1 + O\left(\frac{R}{h}\right)\right].
\end{aligned}\right\} \qquad (8)$$

The quantities of the type $\sum \mu_j^{-n}$ can be evaluated from tables of the μ_j. One finds that

$$\left.\begin{aligned}
8 \sum \mu_j^{-5} &= 1{\cdot}030 \times 10^{-2}, & 12 \sum \mu_j^{-7} &= 1{\cdot}01 \times 10^{-3}, \\
15 \sum \mu_j^{-9} &= 0{\cdot}85 \times 10^{-4}, & \frac{35}{2} \sum \mu_j^{-11} &= 0{\cdot}7 \times 10^{-5}.
\end{aligned}\right\} \qquad (8a)$$

The expressions for the a_l in equation (8) are not exact but the exponentially small term in a_1 is an approximation that gives at least the order of magnitude of the most important error term. The fractional error in evaluating ν will be essentially equal to the fractional error in a_1. If we neglect this exponential term, the relative error in a_1 will be approximately (R/h) $(0{\cdot}3) \exp(-3{\cdot}8\, h/R)$. This serves mainly to define the range of applicability of equation (8). Although we have assumed $R/h \ll 1$, we see that even for $R/h \leq 1/2$, the relative error in a_1 is less than 10^{-4} and for $R/h \leq 2/3$, the relative error is less than 10^{-3} which is about as accurate as presently needed for most measurements.

The other a_l, $l > 1$ in equation (8) also contain exponentially small errors of similar type but, except for these, the expected series expansions of the a_l in powers of R/h conveniently degenerate into just two terms.

To evaluate the a_l when $h/R \ll 1$, we use a scheme analogous to that described above for $R/h \ll 1$. This time we start with equation (I, 35) or (I,36) and note that $|s_m \xi_0| \gg 1$ for all m, equation (I,34). We must, therefore, use an asymptotic expansion of the modified Bessel functions as the analogue of

equation (7). This leads to an *asymptotic* expansion of the a_l, namely

$$\left.\begin{aligned}
a_1 &= +\frac{h^2}{3} - \frac{h}{R}\cdot\frac{(16)^2}{\pi^5} \\
&\quad\times h^2\left[\zeta_5 - \left(\frac{h}{R}\right)\frac{3}{\pi}\,\zeta_6 + \left(\frac{h}{R}\right)^2\frac{3}{2\,\pi^2}\,\zeta_7 + \left(\frac{h}{R}\right)^3\frac{3}{\pi^3}\,\zeta_8 + \cdots\right], \\
a_2 &= +\frac{2\,h^4}{15} - \frac{h}{R}\cdot\frac{6\,(16)^2\,h^4}{\pi^7}\left[\zeta_7 - \left(\frac{h}{R}\right)\frac{4}{\pi}\,\zeta_8 + \left(\frac{h}{R}\right)^2\frac{5}{2\,\pi^2}\,\zeta_9 + \cdots\right], \\
a_3 &= +\frac{17\,h^6}{315} - \frac{h}{R}\cdot\frac{30\,(16)^2\,h^6}{\pi^9}\left[\zeta_9 - \left(\frac{h}{R}\right)\frac{24}{5\,\pi}\,\zeta_{10} + \cdots\right], \\
a^4 &= +\frac{62\,h^8}{2835} + \cdots, \quad a_5 = +\frac{1382\,h^{10}}{155\,925},
\end{aligned}\right\} \tag{9}$$

in which

$$\zeta_j \equiv \sum_{m=0}^{\infty} (2\,m+1)^{-j}\,, \tag{9a}$$

$$\zeta_5 = 1{\cdot}0045\,,\quad \zeta_6 = 1{\cdot}0015\,,\quad \zeta_7 = 1{\cdot}0005\,,\quad \zeta_8 = 1{\cdot}0001\,.$$

The accuracy of equation (9) is inherently limited by the asymptotic nature of the expansions of the a_l but as a pıactical matter, it is more seriously limited by the use of only a few terms. If we want to compute a_1 to a relative accuracy of 10^{-3}, then we must require $h/R \lesssim 1/5$, a rather strong restriction on geometry.

Figure 3 shows the approximate regions of the ξ_0, η_0 plane in which the various formulae apply. The small cup region is where equation (3) applies and cases (a), (b) and (c) denote respectively the regions in which the a_l are most easily evaluated using equation (8), (9) and (4), respectively.

The physical significance of the first few terms of equation (3) is quite clear. For a small cup, the fluid moves with the cylinder almost as a rigid body and consequently the main effect of the fluid is to change the moment of inertia of the system from I to $I + I'$. If, indeed, we substitute only the first term of equation (3) into (I,40) or (I,44) and for simplicity neglect Δ_0^2 terms, we find, as expected, that

$$\omega \sim \left[\frac{I}{I+I'}\right]^{1/2} \quad (\Delta \sim \Delta_0\,\omega) \tag{10a}$$

and so

$$\frac{I'}{I} \sim \frac{1-\omega^2}{\omega^2}. \tag{10b}$$

The viscosity does not enter the picture unless we take at least two terms of equation (3). To the next approximation we find

$$\frac{\omega_0}{\nu} \sim \frac{2\,(I+I')\,(\Delta - \Delta_0\,\omega)}{I'\,a_1\,\omega} \tag{11a}$$

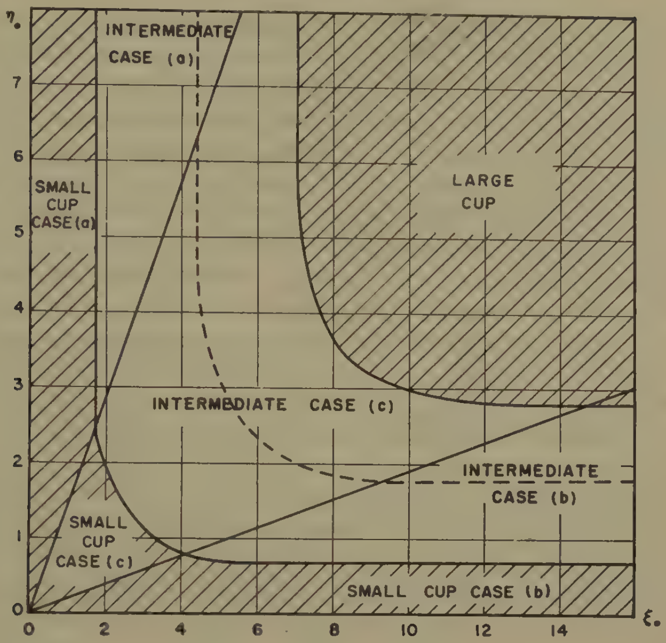

Figure 3

Separation of the η_0, ξ_c plane into regions in which various formulae of the text apply. Broken line, Δ_{max}, is the approximate location of the maximum of Δ with respect to ν.

or

$$\Delta \sim \left(\Delta_0 + \frac{1}{2} \cdot \frac{\omega_0}{\nu} a_1 \frac{I'}{I + I'}\right) \left(\frac{I}{I + I'}\right)^{1/2}. \tag{11b}$$

The second term of equation (3) has relatively little effect on the value of ω; the main effect of the viscosity is to produce an increase in the decrement due to the fact that the nearly periodic motion of the fluid is slightly out of phase with that of the cup.

Additional terms in equation (3) can be attributed to the fact that the effective moment of inertia of the fluid is slightly less than I' if there is a finite boundary layer thickness.

Equations (10) and (11) permit us to test whether or not the small cup satisfies conditions (b), (c) and (d) listed at the beginning of section I,4. Condition (b), that $\Delta \lesssim 1/10$, is easily satisfied because in equation (11b), $a_1(\omega_0/\nu)$ is of order $1/|s_{01}|$ which we already have assumed to be less than about 1/3, equation (5). The product $I' I^{1/2}/(I + I')^{3/2}$ has an absolute maximum value of $2/3\sqrt{3}$ and $I^{1/2}/(I + I')^{1/2} \leqq 1$, therefore $\Delta \lesssim \Delta_0 + 1/15$ for all values of I' and I. To guarantee that $\Delta \lesssim 1/10$, it is only necessary that Δ_0 be sufficiently small.

Whether or not conditions (c) and (d) can be satisfied depends to some extent on how we choose to calculate ν and ϱ from $\varDelta$ and ω. We anticipate the possibility that ϱ, and therefore also I', can be measured by other means and that ν is actually the only unknown. Potentially a measurement of either ω *or* $\varDelta$ would suffice to determine ν if ϱ is already known. A calculation of ν from ω and I' would, however, necessitate measuring the small viscosity dependent corrections to equation (10) and consequently the inferred value of ν would be very sensitive to the slightest errors in ω and I'. If, on the other hand, we should calculate ν from measured values of $\varDelta$ and I', we see from equations (10a) and (11a) that ν^{-1} is nearly proportional to $\varDelta - \varDelta_0\,\omega$ and, if $\varDelta_0\,\omega \ll \varDelta$, the fractional error in the computed value of ν would be about equal to the fractional error in $\varDelta$ (assuming that $\varDelta$ is the least accurate measurement). If we should choose to determine both $\varDelta$ and ω from measurements of both $\varDelta$ and ω then we expect the errors in ν and ϱ to be comparable with the errors in $\varDelta - \varDelta_0\,\omega$ and $\omega^2 - 1$ respectively. Since both decrements and changes in frequency can be measured quite accurately, the small cup is potentially a suitable instrument for determining both ν and ϱ.

The final problem now is to devise ways of actually calculating ν (and ϱ) from $\varDelta$ (and ω) using equations (I,44a), (I,44b) and (3). We will not give any more explicit formulas than these because such would only make the problem appear more difficult than it really is. One can, however, solve these equations explicitely for ν and I' in terms of $\varDelta$ and ω. I' is eliminated by taking the ratio of equations (I,44a) and (I,44b). The resulting transcendental equation for ν can then be solved in series. The fact that ν^{-1} is nearly proportional to $(\varDelta - \varDelta_0\,\omega)$ means that the series expansion for $D(s)$ in powers of ν^{-1} can be inverted to give ν^{-1} as a power series in $(\varDelta - \omega\,\varDelta_0)$. Having determined ν^{-1}, one then substitutes this into equation (I,44a) and evaluates I' as a similar series.

In view of the fact that such formulae will be rather awkward, it may be simpler to solve the original equations numerically by a method of successive approximations starting with a trial solution determined by equations (10b) and (11a).

If the value of I' is known from other sources more accurately than it can be computed from ω and $\varDelta$, one should either eliminate ω from equations (I,44a) and (I,44b) or solve them simultaneously for ω and ν instead of I' and ν. In any case the amount of work required depends strongly on the rate of convergence of equation (3), the accuracy desired, etc. Space does not permit a detailed discussion of the numerical solution for all possible situations.

3. The Large Cup

The large cup is defined by $|s_{01}| \ll 1$ which obtains only if both $\eta_0 \gg 1$ and $\xi_0 \gg 1$. This suggests that one should try to obtain a power series expansion of $D(s)$ in powers of η_0^{-1} and ξ_0^{-1}. Since $D(s)$ depends upon η_0 and ξ_0 only in the

combinations $s\,\eta_0^2 = s\,h^2\,\omega_0/\nu$ and $s\,\xi_0^2 = s\,R^2\,\omega_0/\nu$, such a power series would in effect be a power series in ν or s^{-1}. Unfortunately any attempt to make a Taylor series expansion of $D(s)$ in integer powers of s^{-1} fails almost immediately.

We will sketch two different ways of finding an asymptotic form for $D(s)$. The first method is based upon using the exact expression for $D(s)$ given by equation (I,36); the second method is based upon an asymptotic solution of the original differential equation for w, equation (I,13). In both cases we will compute only enough terms to indicate the procedure and simply quote the result obtained by extension of the same methods. For a more detailed account see [9].

Starting from equation (I,36), we make a large argument expansion of $\tanh(\sqrt{s}\,\eta_0)$ and $I_j(s_m\,\xi_0)$. The lowest approximation gives

$$D(s) \sim s^2\,\frac{I'}{I}\left\{\frac{1}{\sqrt{s}\,\eta_0} + \frac{32\,s}{\pi^2\,\xi_0}\sum_{m=0}^{\infty}\frac{1}{(2\,m+1)^2\,s_m^2}\right\}. \tag{12}$$

From equation (I,34), we see that $s_m^2 \sim s$ at least for $m \ll |\sqrt{s}\,\eta_0|$. By substituting, $s_m^{-3} = s^{-3/2} + (s_m^{-3} - s^{-3/2})$ and noting that $\sum (2\,m+1)^{-2} = \pi^2/8$, we obtain the equivalent expression

$$D(s) \sim s^2\,\frac{I'}{I}\left\{\frac{1}{\sqrt{s}\,\eta_0} + \frac{4}{\sqrt{s}\,\xi_0} + \frac{32}{\sqrt{s}\,\pi^2}\sum_{m=0}^{\infty}\frac{s_m^3 - s^{3/2}}{(2\,m+1)^2\,s_m^3}\right\}. \tag{12a}$$

The infinite series represents a small contribution as compared with the first two terms but the evaluation of it and similar types of terms in higher order approximations require special care. For $m \ll |\sqrt{s}\,\eta_0|$, the numerators in the series are small but also nearly proportional to $(2\,m+1)^2/\eta_0^2$. The $(2\,m+1)^2$ cancels the one in denominator giving terms that are nearly independent of m. For all m, the terms of the series are slowly varying functions of m and to sum the series we must use the Euler-MacLaurin summation formula which yields

$$\sum_{m=0}^{\infty}\frac{s_m^3 - s^{3/2}}{(2\,m+1)^2\,s_m^3} \sim \frac{\pi}{4\,\eta_0}\int_0^{\infty}\frac{dx\,[(s+x^2)^{3/2} - s^{3/2}]}{x^2\,(s+x^2)^{3/2}} = \frac{\pi}{2\sqrt{s}\,\eta_0}. \tag{13}$$

This is correct to any finite power of η_0^{-1} but there is an error proportional to a negative exponential in η_0.

Substitution of equation (13) into (12a) gives three terms of the asymptotic expansion. A similar treatment of the higher order terms gives the result

$$\begin{aligned} D(s) = s^2\,\frac{I'}{I}\Big\{ & \frac{4}{s^{1/2}\,\xi_0} - \frac{6}{s\,\xi_0^2} + \frac{3}{2\,s^{3/2}\,\xi_0^3} + \frac{3}{2\,s^2\,\xi_0^4} + \cdots \\ & + \frac{1}{s^{1/2}\,\eta_0} - \frac{16}{\pi\,s\,\xi_0\,\eta_0} + \frac{9}{s^{3/2}\,\xi_0^2\,\eta_0} - \frac{8}{\pi\,s^2\,\xi_0^3\,\eta_0} + \cdots \\ & - 2\,\eta_0^{-1}\,s^{-1/2}\exp(-2\,s^{1/2}\,\eta_0) + \cdots\Big\}. \end{aligned} \tag{14}$$

The first line is a series in powers of $(s^{1/2}\,\xi_0)^{-1}$ whereas the second line is $(s^{1/2}\,\eta_0)^{-1}$ times a similar series. There are no terms containing η_0^{-j}, $j \geqq 2$ but there are exponentially small terms the most important of which is contained in the third line. The 'large cup' region of Figure 3 shows the range of ξ_0 and η_0 where equation (14) gives $D(s)$ to within about 0·1% for $|s|$ of order 1.

The second method of deriving equation (14) shows the physical significance of the various terms. It is clear from the physical meaning of a 'boundary layer thickness' that for $\xi_0 \gg 1$ and $\eta_0 \gg 1$, only a relatively small layer of fluid (thickness of order $1 \ll \xi_0$, η_0 in units of δ) near the surfaces of the cup take part in the motion. Except within a distance of order 1 from the edge where the surfaces meet at right angles, the motion of the fluid near the verticle walls of the cup is only slightly influenced by the motion of the fluid near the bottom (or top) surfaces of the cup and vice versa. It is convenient, therefore, to consider the fluid motion as a linear superposition of three flows (*a*) the flow that would exist near the walls of a cylinder of infinite height (with no bottom), (*b*) the flow that would exist near a plane of infinite radius (with no cylinder walls), and (*c*) a flow localized near the intersection of the cylinder and the plane. Since $D(s)$ is a linear function of w, $D(s)$ is the sum of the contributions from each of these flows.

The solutions for (*a*) and (*b*) are contained in section I,3. and these contribute to $D(s)$ the two terms

$$D(s) \sim s^2\,\frac{I'}{I}\left\{\frac{4\,I_2\,(\sqrt{s}\,\xi_0)}{\sqrt{s}\,\xi_0\,I_1\,(\sqrt{s}\,\xi_0)} + \frac{\tanh(\sqrt{s}\,\eta_0)}{\sqrt{s}\,\eta_0}\right\}. \tag{15}$$

An asymptotic expansion of the first term yields all the terms in the first line of equation (14) which we can, therefore, interpret as due to the drag of the fluid on the vertical wall. The first of these terms differs from the leading term of the small cup expansion, equation (3), by a factor of order $4\,\xi_0^{-1}$ which one can explain by the fact that a moving layer of fluid of unit thickness near the wall has a moment of inertia equal to about $4\,\xi_0^{-1}\,I'$ as compared with the moment of inertia I' of the entire fluid which is set in motion when we have a small cup.

A large argument expansion of the second term of equation (15) gives the first term of the second line of equation (14) which we interpret as due to the drag of the fluid on the flat surfaces and it gives also the exponentially small term of the third line of equation (14) which one may think of as due to an interference between the flows near the top and bottom surfaces. The factor $\eta_0^{-1}\,I'$ that appears in these terms represents the moment of inertia of the fluid layer set in motion by the flat surfaces.

The remaining terms in the second line of equation (14) must be due to the edge correction. The largest of these terms indeed contains a factor $I'\,\xi_0^{-1}\,\eta_0^{-1}$

which has the same order of magnitude as the moment of inertia of the fluid within unit distance from the edge. These terms can be obtained by considering the fluid flow in the immediate vicinity of the edge. If one denotes by w_1 the difference (c) between the total flow w and the two flows (a) and (b) described above, then w satisfies the same differential equation as w but different boundary conditions. An asymptotic solution for w_1 can be derived directly from the differential equation by making use of the fact that w_1 is small except near the intersection of a plane and a cylinder of relatively small curvature. This procedure is straight-forward but too long to describe in detail here [9].

We now consider the various requirements listed in section I,4. for the cup to be suitable as a viscometer. We shall find it necessary, among other things, to postulate

$$\frac{I'}{I}\left(\frac{4}{\xi_0}+\frac{1}{\eta_0}\right)\ll 1\,. \tag{16}$$

The analysis is greatly simplified by anticipating this result and making use of it.

The arguments presented in section I,4. regarding the suitability of a viscometer when $I'/I \ll 1$ apply also here if only equation (16) is true. This arises because $D(s)$ is actually of order $(I'/I)\ (4\,\xi_0^{-1}+\eta_0^{-1})$ for a large cup instead of order I'/I as assumed in section I,4. or in other terms because $I'\ (4\,\xi_0^{-1}+\eta_0^{-1})$ is the 'effective' moment of inertia of the fluid rather than I'.

From this we conclude that the transient $f(\tau)$, equation (I,42), is of order $(I'/I)\ (4\,\xi_0^{-1}+\eta_0^{-1})$. It is also possible to find simple approximations for $f(\tau)$ using equation (16). One can do this by substituting the asymptotic form for $D(s)$ directly into equation (I, 17), and deforming the contour of integration to the left of the two complex roots that give the main oscillation so as to lie along both sides of the negative real axis. This can be done provided $\tau \ll \xi_0^2$ and η_0^2 despite the fact that the asymptotic approximation for $D(s)$ is incorrect on the negative real axis. A second method is to use equation (38) but to integrate over the densely distributed roots S_k on the negative real axis. The result of this procedure is [9]

$$f(\tau)\sim\frac{-\alpha_0\,I'}{I}\left(\frac{4}{\xi_0}+\frac{1}{\eta_0}\right)\frac{1}{\pi}\int\limits_0^\infty\frac{dy\,y^{1/2}\,e^{-y\tau}}{(y^2+1)^2}\quad\text{for }\tau\ll\xi_0^2\text{ and }\eta_0^2 \tag{17}$$

and from this

$$f(\tau)\sim-\frac{\alpha_0\,I'}{I}\left(\frac{4}{\xi_0}+\frac{1}{\eta_0}\right)\frac{1}{2\sqrt{\pi}\,\tau^{3/2}}\qquad\text{for }1\ll\tau\ll\xi_0^2\text{ and }\eta_0^2\,, \tag{17a}$$

provided equation (16) is valid.

This shows that the transient $f(\tau)$ is always negative (relative to α_0) and has a monotone decreasing amplitude. For later times, τ of order ξ_0^2 or η_0^2, τ is of the same order of magnitude as the decay time of the slowest transient. The

transient is then dominated by the exponential decay of the slowest transient just as was the case with the small cup on a much shorter time scale.

If equation (16) is not valid the transient will have a relatively large amplitude and such a complicated time dependence that it would be very difficult to observe the main oscillation. Equation (16) is therefore a necessary and sufficient condition for condition (a) of section I,4. to be satisfied.

If we use equation (16) again and the consequence of it that $s \sim i$ for the main oscillation, we find by substituting equation (14) into equation (I,44a and b) that to a lowest approximation

$$1 - \omega \sim \Delta - \Delta_0 \sim \frac{1}{2\sqrt{2}} \cdot \frac{I'}{I} \left(\frac{4}{\xi_0} + \frac{1}{\eta_0}\right) = \frac{1}{2\sqrt{2}} \cdot \frac{I'}{I} \left(\frac{4}{R} + \frac{1}{h}\right) \left(\frac{\nu}{\omega_0}\right)^{1/2}. \quad (18)$$

From this we see that equation (16) is also necessary and sufficient for condition (b) of section I,4. (namely $\Delta \ll 1$) to be satisfied provided that Δ_0 is also small. Equation (18) also indicates the accuracy with which various quantities can be calculated and the most important aspect to observe is that $1 - \omega$ and $\Delta - \Delta_0$ are nearly equal.

Unless one can measure both $1 - \omega$ and $\Delta - \Delta_0$ so accurately that their difference can be inferred with significant accuracy (an unlikely possibility), an observation of both $1 - \omega$ and $\Delta - \Delta_0$ is redundant. An observation of either would to a first approximation be a measure only of the product $I' \nu^{1/2}$. If, however, ϱ and thus I' can be measured by other means with sufficient accuracy, then the fractional error in the computed value of ν would be twice that of $\Delta - \Delta_0$ or of $1 - \omega$, whichever quantity is used by itself as a basis for computing ν. Potentially, both $1 - \omega$ and $\Delta - \Delta_0$ can be measured accurately, but in any particular situation one should use only that measurement which is the more accurate.

Again we shall not try to give explicit formulas for ν in terms of I' and $1 - \omega$ or ν in terms of I' and $\Delta - \Delta_0$ to an accuracy consistent with the accuracy of equation (14). The procedure for doing this and the results are awkward but elementary. The series expansion for $D(s)$, effectively in powers of $\nu^{1/2}$, can be inverted to give $\nu^{1/2}$ as a power series either in $\Delta - \Delta_0$ or in $1 - \omega$. If one is to measure Δ and I', one should eliminate ω from equations (44a, b) whereas if one measures Δ and I', one should eliminate Δ from equations (44a and b). Even though one may be able conveniently to measure both $\omega - 1$ and $\Delta - \Delta_0$, if $1 - \omega$ can be measured more accurately than $\Delta - \Delta_0$, the theory implies that $\Delta - \Delta_0$ can be computed from $1 - \omega$ and I' more accurately than it can be measured and conversely, if $\Delta - \Delta_0$ can be measured more accurately than $1 - \omega$.

4. Intermediate Size Cup

In the previous two sections, we have considered all cases except those for which the smaller of ξ_0 and η_0 is of order 1, the unshaded area of Figure 3.

The analysis of the remaining cases is complicated by the fact that there is no suitable power series expansion of $D(s)$ in powers of ν^{-1} or $\nu^{1/2}$. We shall find, however, that the behavior of the 'intermediate size' cup is very complicated unless

$$\frac{I'}{I} \ll 1 \tag{19}$$

and the analysis of this section will be based upon the consequences of this assumption. Some of the methods to be used here can also be used further to simplify the analysis of the small and large cups as well when equation (19) holds.

We have already seen in section 1,4. that if equation (19) is valid then $f(\tau)$, $1 - \omega$ and $\Delta - \Delta_0$ are all of order I'/I. The transient should give no serious trouble as a consequence of the fact that it has a small amplitude and will decay at a moderately fast rate for $|s_{01}| \gtrsim 1/2\,\pi$. We will be more concerned with how $1 - \omega$ and $\Delta - \Delta_0$ depend upon the properties of the fluid. Because of the greater complexity of the present problem, we shall not try to describe it in quite as much detail as the previous cases but will simply describe the qualitative properties and indicate how one would proceed to an accurate analysis.

The starting point of this discussion is the pair of equations (I,44a, b). For small I'/I, Δ and ω can be expanded in a Taylor series in powers of I'/I. The leading term of this expansion gives

$$\omega - 1 = \frac{1}{2}\,\mathrm{Re}\,D\,(\pm i) + O\left[\left(\frac{I'}{I}\right)^2\right], \tag{20a}$$

$$\Delta - \Delta_0 = \pm\frac{1}{2}\,\mathrm{Im}\,D\,(\pm i) + O\left[\left(\frac{I'}{I}\right)^2\right]. \tag{20b}$$

The complete series is easily obtained and will involve various powers of $D(\pm\, i)$, which is of order I'/I, and various derivatives of $D(s)$ at $s = \pm\, i$. The simplifying feature of equation (20) is that it involves $D(s)$ only at $s = \pm\, i$. $D(\pm\, i)$ is, however, still a function of ξ_0 and η_0 and thus of the unknown ν and the known values of h and R.

We obtain directly from equation (I,37), the expressions

$$\mathrm{Re}\,D\,(\pm i) = -\frac{I'}{I} + \frac{I'}{I}\,64\,\pi^{-2}\sum_{j,m}\mu_j^{-2}\,(2\,m+1)^{-2}\,(1+s_{jm}^2)^{-1} \tag{21a}$$

$$= -\frac{I'}{I}\,64\,\pi^{-2}\sum_{j,m}\mu_j^{-2}\,(2\,m+1)^{-2}\,s_{jm}^2\,(1+s_{jm}^2)^{-1} \tag{21b}$$

$$\pm\,\mathrm{Im}\,D\,(\pm i) = \frac{I'}{I}\,64\,\pi^{-2}\sum_{j,m}\mu_j^{-2}\,(2\,m+1)^{-2}\,(-s_{jm})\,(1+s_{jm}^2)^{-1} \tag{21c}$$

in which s_{jm} is proportional to ν, equation (2).

Each of the individual terms of equation (21b) is a monotone decreasing function of ν and so, therefore, is the sum. Thus to order $(I'/I)^2$ at least, $1 - \omega$ is a monotone decreasing function of ν with $1 - \omega \to 0$ for $\nu \to 0$ (limit of large cup) and $1 - \omega \to (I'/I)/2$ for $\nu \to \infty$ (limit of small cup). For any given values of h and R, $1 - \omega$ is simply I'/I times a function of ν only. There is nothing very unusual about this function and if the given values of R and h are of comparable size, it could be tabulated as a function of ν quite easily from a term by term evaluation of the series.

Each of the terms of equation (21c) vanishes for $\nu \to 0$ ($s_{j\,m} \to 0$) and for $\nu \to \infty$ ($s_{j\,m} \to \infty$). The (j, m) term has a single maximum with respect to ν at $s_{j\,m} = -1$ thus at the point

$$\nu = \omega_0 \left\{ \left[\frac{(2\,m + 1)\,\pi}{2\,h} \right]^2 + \frac{\mu_j^2}{R^2} \right\}^{-1} . \tag{22}$$

The larger j and m, the smaller the value of ν at which the j, m term has its maximum. Thus to order $(I'/I)^2$, at least, $\Delta - \Delta_0$ vanishes for $\nu \to 0$ and for $\nu \to \infty$ as we already observed in the previous sections. It is also clear, however, that $\Delta - \Delta_0$ has a single maximum with respect to ν and it occurs at a slightly lower value of ν than that of equation (22) with $j = 1$, $m = 0$. If we denote by ν_{max} the value of ν where $\Delta - \Delta_0$ is a maximum with respect to ν for fixed R, h and I', then

$$\nu_{max} < \omega_0 \left\{ \frac{\pi^2}{4\,h^2} + \frac{\mu_1^2}{R^2} \right\}^{-1} . \tag{23}$$

This is not only an upper bound on the value of ν_{max}; it is also a fairly close estimate. For $R/h \to 0$, equation (23) implies that $R(\omega_0/\nu_{max})^{1/2} > \mu_1 \sim 3{\cdot}8$ as compared with a correct value of 4·3 computed by PRISS [6]. The broken line of Figure 3 shows, approximately, the curve in the ξ_0, η_0 plane where Δ has a maximum with respect to ν for fixed R, h and I'.

We can also obtain from equation (21c) simple upper and lower bounds on the maximum value of Δ, Δ_{max}. Δ_{max} is larger than the maximum value of the first term alone but smaller than the sum of the terms evaluated at their respective maximum values. This gives

$$\frac{I'}{4\,I} \geqq \Delta_{max} - \Delta_0 \geqq \frac{16}{\pi^2\,\mu_1^2} \cdot \frac{I'}{I} \sim \frac{I'}{9\,I} . \tag{24}$$

An exact calculation of Δ_{max} for $h/R \to 0$ gives $\Delta_{max} - \Delta_0 \sim I'/5{\cdot}81$ [6], which is about midway between the limits of equation (24). Equation (24) holds for arbitrary values of h and R, however.

This is all the information we need to test the suitability of a cup for measurements of viscosity. Equation (24) shows that we can guarantee

$\Delta \lesssim 1/10$ [condition (b) of section I,4.] for arbitrary geometry if only

$$\frac{I'}{I} \lesssim \frac{1}{2} \tag{25}$$

and Δ_0 is sufficiently small. This defines more precisely the range implied by equation (19).

In regard to sensitivity of I' and ν to measurements of ω and Δ, the existence of a maximum of Δ as a function of ν poses new problems. If we should try to calculate ν from measured values of I' and Δ (but not ω), we would find that ν was not only a double valued function of Δ but also rather insensitive to the value of Δ if ν should lie near ν_{max}. One must, therefore, be careful to avoid trying to compute ν from I' and Δ if ν is near ν_{max}. Except for this region of ν, the fractional errors in ν will be at least comparable with (but probably somewhat larger than) the fractional errors in $\Delta - \Delta_0$ and I'.

A calculation of ν from measured values of I' and $1 - \omega$ presents no special problems for the intermediate size cup, in fact, ν has its greatest sensitivity to ω in this range. One should note, however, that fractional errors in ν are comparable with fractional errors in $1 - \omega$, not ω itself.

A calculation of both ν and I' from Δ and ω presents no problems, in principle. In effect, the value of I' is inferred mainly from the value of Δ which is nearly proportional to I'/I and ν from the value of $(1 - \omega)/(\Delta - \Delta_0)$ which is nearly independent of I'/I. In this scheme, the fractional error in I' is comparable with that of $\Delta - \Delta_0$ whereas the fractional error in ν is comparable with that of $\Delta - \Delta_0$ or $1 - \omega$ whichever is the larger.

The final problem of actually calculating ν explicitly from any two of the quantities I', Δ and ω is somewhat more difficult than in the cases of the small or large cup but it is still not beyond reasonable limits of complexity.

If we were to use a method of successive approximations (equivalent to a series of corrections in successive powers of I'/I) the first approximation would be the actual solution of equations (20a, b). If we measure ω and I' (but not Δ), we eliminate Δ by considering only equation (20a) and solving it for ν; if we measure Δ and I' (but not ω) we eliminate ω by using only equation (20b); and if we measure ω and Δ (but not I') we eliminate I', to order $(I'/I)^2$, by dividing equations (20a, b). $D(\pm i)\, I/I'$ depends only upon R, h and ν and for any given cup (fixed R and h) it, therefore, depends only upon ν.

From a graph or tables of Re $D(\pm i)\, I/I'$, Im $D(\pm i)\, I/I'$ and their ratio as a function of ν, or better yet the inverse of these functions, the value of ν can be found immediately to order I'/I.

The tabulation of $D(\pm i)$ can be done using equations (21a, b, c) if R and h are comparable size. These series will converge, in this case, fast enough to

be practical particularly in view of the fact that the various terms of each series all have the same functional form and involve only very simple operations.

If $R/h \gg 1$, it would be easier to compute the real and imaginary parts of $D(\pm i)$ from equation (I,33). The real and imaginary parts of the Bessel functions with arguments proportional to $\sqrt{\pm i}$ can be expressed in terms of the tabulated functions ber and bei whereas the function $\tanh(s_\mu \eta_0)$ in equation (I,33) can be represented by its large argument expansion since $s_\mu \eta_0 \sim \mu_i h/R \gg 1$. If on the other hand $h/R \ll 1$, it would be easier to find the real and imaginary parts of $D(\pm i)$ using equation (I,36) and the asymptotic expansion of the Bessel functions for $s_m \beta_0 \sim (2m+1)\pi R/2h \gg 1$.

Successive corrections of ν to higher orders in I'/I can be obtained from a series expansion in powers of I'/I, $1-\omega$ or $1-\Delta$ depending upon which of these are 'knowns' and which are eliminated from the equations. Additional tables for derivatives of $D(s)$ at $s = \pm i$ might be helpful but not necessary for these corrections.

A detailed treatment of the various mathematical steps particularly for $R/h \ll 1$ is described by Priss [6] although it is possible to organize the calculations somewhat more efficiently than described there.

5. Conclusions

We have described here all the possible situations in which a cup filled with a fluid might be used successfully as a viscometer. Based upon the criteria listed in section I,4., we have found virtually no restrictions on the use of a 'small cup', equation (1). For the large cup we found that equation (16) was a necessary condition for usefulness but that one could not easily determine *both* ν and ϱ from Δ and ω. For the intermediate size cup we found equation (25) was sufficient to satisfy most requirements although one cannot always compute ν accurately from observations of only Δ and I'. Equation (25) is also a necessary condition for the intermediate size cup to be useful because if this condition is violated the transient will be of relatively large amplitude, the decrement will be too large and the theoretical calculations exceptionally tedious, thus it violates virtually all of the conditions for suitability.

Because of the many ways in which one might actually perform the final calculations of ν (and perhaps ϱ) from observations of Δ and/or ω, we have avoided giving details of this. We have, however, in each case indicated some methods which would not involve an unreasonable amount of work.

In view of the great flexibility of design and the potentially high accuracy that can be achieved, it appears that an oscillating cup should compete favorably with other types of viscometers particularly for measurements of the viscosity of liquids. Although some use has already been made of such an instrument, its potentialities far exceed its present applications.

6. Acknowledgements

The authors wish to acknowledge the assistance received from Mr. J. R. MOSZYNSKI who checked the equations and from Mr. H. E. WANG who prepared the drawings for both parts I and II.

REFERENCES

[1] J. KESTIN and J. R. MOSZYNSKI, *On the Measurement of the Viscosity of Steam by the Observation of Small Oscillations*, Fifth International Conference on Steam Properties, London 1956.
[2] P. MARIENS and O. VAN PAEMEL, *Theory and Experimental Verification of the Oscillating Disk Method for Viscosity Measurements in Fluids*, Appl. sci. Res. *5*, 411 (1956).
[3] J. KESTIN and H. E. WANG, *Corrections for the Oscillating Disk Viscometer*, J. appl. Mech. *24*, 197 (1957).
[4] J. E. VERSCHAFFELT, *The Viscosity of Liquefied Gases I, II, III*, Commun. phys. Lab. Univ. Leiden *14*, No. 148 b, c, d.
[5] J. KESTIN and L. N. PERSEN, *Small Oscillations of Bodies of Revolution in a Viscous Fluid*, Brown University – OSR Report AF 891/2 (1954).
[6] *Three Papers on the Theory of the Oscillating Cup Viscometer*, translated and condensed by J. KESTIN, Brown University, OSR Report AF 891/4 (1954). Original papers E. G. SHVIDKOVSKII, Uchenye Zepiski MGU (Moscow University) *74*, 135 (1944); A. M. BUTOV, L. S. PRISS, and E. G. SHVIDKOVSKII, Zhur. Tekh. Fiz. *21*, 1319 (1951); L. S. PRISS, Zhur. Tekh. Fiz. *21*, 1050 (1952).
[7] *On the Determination of Viscosity by the Oscillation of a Vessel Enclosing a Fluid*, Part I by C. DA N. ANDRADE and Y. S. CHIONG, Proc. phys. Soc. *48*, 247 (1936); Part II by C. DA N. ANDRADE and L. ROTHERHAM, Proc. phys. Soc. *48*, 261 (1936).
[8] J. KESTIN and L. N. PERSEN, *Slow Oscillations of an Infinite Plate and an Infinite Disk in a Viscous Fluid*, Brown University, OSR Report AF 891/1 (1954).
[9] G. F. NEWELL, J. KESTIN and D. A. BECKWITH, *Theory of the Oscillating Cup Viscometer*, Brown University, OSR Report AF 891/7 (1956).

Zusammenfassung

Diese Notiz ist eine Fortsetzung des ersten Teiles. Hierin wird insbesondere die Frage behandelt, wie die Frequenz und das Dekrement der Schwingung von der Viskosität und Dichte der Flüssigkeit, bei Verwendung von Bechern verschiedener Gestalt und Grösse, abhängt. Vor allem wurden die Fehler abgeschätzt, die bei der Berechnung der Viskosität und der Dichte aus den beobachteten Frequenz- und Dämpfungswerten auftreten können und wenn letztere mit bekannter experimenteller Ungenauigkeit bestimmt wurde. Weiterhin sind Methoden angegeben, wie diese Berechnung leicht erfüllt werden kann.

(Received: June 17, 1957.)

Stresses in a Plate Under Tension and Containing an Infinite Row of Semi-Circular Notches

By AKIRA ATSUMI, Sendai, Japan[1])

Introduction

The purpose of this paper is to determine the stresses in a semi-infinite plate with a row of an infinite number of semi-circular notches when it receives a uniform tension T. The problem of determining the stresses in the neighbourhood of a single semi-circular notch in a plate was solved experimentally by COKER and FILON [1][2]), and M. M. FROCHT [2]; theoretically by F. G. MAUNSELL [3], T. ISHIBASI [4], E. WEINEL [5], C. B. LING [6], and H. UDOGUCHI [7], using polar or bipolar co-ordinates, while the problem regarding the stresses when an infinite number of semi-circular notches are placed so closely as to exercise an influence on one another was theoretically solved by C. WEBER [8], and M. HETÉNYI and T. D. LIU [9] by methods enabling approximately correct solutions to be obtained.

Applying the method MAUNSELL adopted, this paper gives a theoretical solution which strictly satisfies the various boundary conditions of semi-circular notches, and the numerically determined stresses in the neighbourhood of the notches.

Method of Analysis

Consider a semi-infinite plate containing an infinite number of semi-circular notches and receiving a uniform tension T. The radii of the notches and the distances between them are designated as a and b. Denoting the centre of an arbitrary notch of notches O and the centre at an arbitrary distance of $k\,b$ $(k = \pm 1, \pm 2, \ldots)$ from O, O_k, we take the rectangular co-ordinates (x, y) and (x_k, y_k) designated as origins O, O_k. Polar co-ordinates (r, θ) and (r_k, θ_k) are also used. They are assumed as shown in Figure 1. The following equations are obtained:

$$x = r \sin\theta\,, \quad y = r\cos\theta\,, \tag{1a}$$

and

$$x_k = x + k\,b\,, \quad y_k = y\,, \quad r_k = \left\{(x + k\,b)^2 + y^2\right\}^{1/2}, \quad \tan\theta_k = \frac{x + k\,b}{y}\,. \tag{1b}$$

---

[1]) Department of Mechanical Engineering, Tôhoku University.
[2]) Numbers in brackets refer to References, page 477.

When the plate is in a condition of generalized plane stress, the average stress across its thickness can be derived from a stress function χ which satisfies

$$\nabla^4 \chi = 0 . \tag{2}$$

If no notches are present, the uniform tension in the x-direction is given by

$$\chi = \frac{1}{4} T r^2 (1 + \cos 2\theta) . \tag{3}$$

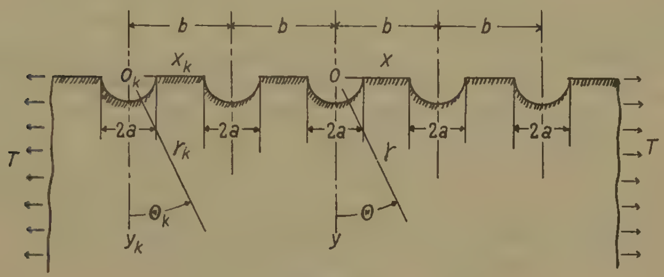

Figure 1
Notched plate under tension.

To complete the solution when the notches are present, we first construct a series of functions which satisfies equation (2) and gives no stresses on the straight boundary and the same traction on each notch. With these functions added to χ and all the boundary conditions at the rims of the notches satisfied, all requirements of the solution are fulfilled. This series of functions is derived by differentiating two fundamental functions which have singularities at the centre of each notch.

As the first fundamental function, we take

$$\chi_0 = -r\,\theta \sin\theta - \sum_k r_k\,\theta_k \sin\theta_k \quad (k = \pm 1, \pm 2, \ldots) , \tag{4}$$

which gives a normal force acting at the centre of each notch.

To express this function in terms of the polar co-ordinates (r, θ), we introduce a complex co-ordinate ϱ referred to the origin O as pole

$$\varrho = x + i\,y = i\,r\,e^{-i\theta} . \tag{5}$$

From equations (1) and (5), we get

$$\log(\varrho + k\,b) = \log r_k + i\left(\frac{\pi}{2} - \theta_k\right) \tag{6a}$$

and

$$\log(\varrho + k\,b) = \log k\,b + \sum_{n=1}^{\infty} \frac{(-)^{n-1}}{n} \left(\frac{\varrho}{k\,b}\right)^n . \tag{6b}$$

From (6a) and (6b) the expansion of θ_k is obtained as follows

$$\theta_k = \sum_{n=0}^{\infty} \frac{(-)^{n+1}}{(2\,n+1)\,(k\,b)^{2n+1}}\, r^{2n+1} \cos(2\,n+1)\,\theta + \sum_{n=1}^{\infty} \frac{(-)^{n+1}}{2\,n\,(k\,b)^{2n}}\, r^{2n} \sin 2\,n\,\theta . \tag{7}$$

In the above expansion, some of the constant terms are omitted as they do not contribute to the stresses.

By substituting equations (1) and (7) for equation (4), it is easy to determine χ_0:

$$\chi_0 = -r\,\theta \sin\theta + \sum_{n=1}^{\infty} \frac{(-)^n\,\sigma_{2n}}{2\,n\,b^{2n}}\, r^{2n+1} \left\{\cos(2\,n-1)\,\theta + \frac{2\,n-1}{2\,n+1} \cos(2\,n+1)\,\theta\right\}, \tag{8}$$

where the trivial terms are omitted and σ_n is defined as follows

$$\sigma_n = \sum_{1}^{\infty} |\,k\,|^{-n} = 1 + 2^{-n} + 3^{-n} + \cdots . \tag{9}$$

Then χ_0 gives stresses

$$\left.\begin{aligned}
\sigma_r &= \frac{1}{r^2} \cdot \frac{\partial^2\chi}{\partial\theta^2} + \frac{1}{r} \cdot \frac{\partial\chi}{\partial r} = -\frac{2}{r} \cos\theta - \sum_{n=1}^{\infty} \frac{(-)^n}{b^{2n}}\, \sigma_{2n}\, r^{2n-1} \\
&\qquad \times \left\{(2\,n-3)\cos(2\,n-1)\,\theta + (2\,n-1)\cos(2\,n+1)\,\theta\right\}, \\
\sigma_\theta &= \frac{\partial^2\chi}{\partial r^2} = \sum_{n=1}^{\infty} \frac{(-)^n}{b^{2n}}\, \sigma_{2n}\, r^{2n-1} \\
&\qquad \times \left\{(2\,n+1)\cos(2\,n-1)\,\theta + (2\,n-1)\cos(2\,n+1)\,\theta\right\}, \\
\tau_{r\theta} &= -\frac{\partial}{\partial r}\left(\frac{1}{r} \cdot \frac{\partial\chi}{\partial\theta}\right) = \sum_{n=1}^{\infty} \frac{(-)^n}{b^{2n}}\, \sigma_{2n}\, r^{2n-1}\,(2\,n-1) \\
&\qquad \times \left\{\sin(2\,n-1)\,\theta + \sin(2\,n+1)\,\theta\right\}.
\end{aligned}\right\} \tag{10}$$

Therefore it indicates no tractions on the straight edge but is analytic in the plane except at the centre of the notch.

Differentiation of χ_0 with respect to x also gives functions with the required properties, but the odd derivatives must be excluded, since they are not even in x and cannot be used in the symmetrical system required. χ_0 itself must also be excluded because it represents an unbalanced force which will have to be

balanced at infinity. The following series of functions is easily found.

$$\left.\begin{aligned}\chi_{2m} = \frac{2\,(-)^m\,\partial^{2m}\,\chi_0}{(2\,m-2)!\,\partial x^{2m}} &= \frac{1}{r^{2m-1}} \\ &\times \{(2\,m+1)\cos(2\,m-1)\,\theta + (2\,m-1)\cos(2\,m+1)\,\theta\} \\ &+ \sum_{n=m+1}^{\infty} \frac{2\,(-)^n\,(2\,n-1)!\,\sigma_{2n}}{(2\,m-2)!\,(2\,n-2\,m+1)!\,b^{2n}}\,r^{2n-2m+1} \\ &\times \{(2\,n-2\,m-1)\cos(2\,n-2\,m+1)\,\theta + (2\,n-2\,m+1) \\ &\times \cos(2\,n-2\,m-1)\,\theta\} \qquad (m \geqq 1)\,.\end{aligned}\right\} \tag{11}$$

As the second fundamental function, we take

$$\chi_0' = -r\,\theta\cos\theta - \sum_k r_k\,\theta_k\cos\theta_k\,, \tag{12}$$

which gives a tangential force acting at the centre of each of the notches. It may be expanded in the same way as mentioned above, into the following form

$$\chi_0' = -r\,\theta\cos\theta + \sum_{n=1}^{\infty} \frac{(-)^n\,\sigma_{2n}}{2\,n\,b^{2n}}\,r^{2n+1}\{\sin(2\,n+1)\,\theta + \sin(2\,n-1)\,\theta\}. \tag{13}$$

Here only the odd derivatives are required and the results are as follows

$$\left.\begin{aligned}\chi_{2m}' = \frac{2\,(-)^{m+1}\,\partial^{2m+1}\,\chi_0'}{(2\,m)!\,\partial x^{2m+1}} &= \frac{1}{r^{2m}}\{\cos 2\,m\,\theta + \cos(2\,m+2)\,\theta\} \\ &+ \sum_{n=m+1}^{\infty} \frac{2\,(-)^{n+1}\,(2\,n-1)!\,\sigma_{2n}}{(2\,m)!\,(2\,n-2\,m-1)!\,b^{2n}}\,r^{2n-2m} \\ &\times \{\cos(2\,n-2\,m)\,\theta + \cos(2\,n-2\,m-2)\,\theta\} \quad (m \geqq 0)\,.\end{aligned}\right\} \tag{14}$$

Now the required function is constructed in the form

$$\chi = T\left\{\frac{1}{4}\,r^2\,(1+\cos 2\,\theta) + \sum_{m=1}^{\infty} A_m\,\chi_{2m} + \sum_{m=0}^{\infty} B_m\,\chi_{2m}'\right\} \tag{15}$$

and then the problem reduced to determining A_m and B_m so that σ_r and $\tau_{r\theta}$ may be zero when r is a.

Since σ_r and $\tau_{r\theta}$ contain terms of cosines and sines of odd multiples of θ respectively, it is necessary to expand these terms into Fourier series between $\theta = -\pi/2$ and $\theta = \pi/2$. The required expansions are

$$\left.\begin{aligned}\cos(2\,m+1)\,\theta &= \frac{4}{\pi}\left\{\frac{(-)^m}{2\,(2\,m+1)} + \sum_{s=1}^{\infty} \frac{(-)^{m+s}\,(2\,m+1)}{(2\,m+1)^2 - 4\,s^2}\cos 2\,s\,\theta\right\}, \\ \sin(2\,m+1)\,\theta &= \frac{4}{\pi}\sum_{s=1}^{\infty} \frac{(-)^{m+s}\,2\,s}{(2\,m+1)^2 - 4\,s^2}\sin 2\,s\,\theta\,.\end{aligned}\right\} \tag{16}$$

Finally, we have the following expressions for the stresses σ_r and $\tau_{r\theta}$:

$$\left.\begin{aligned}
\sigma_r = & \sum_{m=1}^{\infty} \frac{A'_m}{a^{2m+1}} \sum_{s=0}^{\infty} (4 s^2 + 2 m - 1)\, {}^m\alpha_s \cos 2 s \theta \\
& + \sum_{m=1}^{\infty} \sum_{n=m+1}^{\infty} \sum_{s=0}^{\infty} \frac{(-)^n\, 2\, (2 n - 1)!\, a^{2n-2m-1}\, \sigma_{2n}\, A''_m}{(2 m - 2)!\, (2 n - 2 m + 1)!\, b^{2n}} \\
& \times (4 s^2 + 2 m - 2 n - 1)\, {}^{n,m}\alpha_s \cos 2 s \theta \\
& - \sum_{m=0}^{\infty} \frac{2\, (2 m + 1)\, B_m}{a^{2m+2}} \{m \cos 2 m \theta + (m + 2) \cos (2 m + 2) \theta\} \\
& + \sum_{m=0}^{\infty} \sum_{n=m+1}^{\infty} \frac{(-)^n\, 2\, (2 n - 1)!\, a^{2n-2m-2}\, \sigma_{2n}\, B_m}{(2 m)!\, (2 n - 2 m - 2)!\, b^{2n}} \\
& \times \{(2 n - 2 m) \cos (2 n - 2 m) \theta + (2 n - 2 m - 4) \\
& \quad \times \cos (2 n - 2 m - 2) \theta\} + \frac{1}{2} (1 - \cos 2 \theta) = 0\,,
\end{aligned}\right\} \quad (17a)$$

$$\left.\begin{aligned}
\tau_{r\theta} = & \sum_{m=1}^{\infty} \frac{A'_m}{a^{2m+1}} \sum_{s=1}^{\infty} 4\, m\, s\, {}^m\alpha_s \sin 2 s \theta \\
& + \sum_{m=1}^{\infty} \sum_{n=m+1}^{\infty} \sum_{s=1}^{\infty} \frac{(-)^n\, (2 n - 1)!\, a^{2n-2m-1}\, \sigma_{2n}\, A''_m}{(2 m - 2)!\, (2 n - 2 m + 1)!\, b^{2n}} \\
& \times 8\, s\, (m - n)\, {}^{n,m}\alpha_s \sin 2 s \theta \\
& - \sum_{m=0}^{\infty} \frac{2\, (2 m + 1)\, B_m}{a^{2m+2}} \{m \sin 2 m \theta + (m + 1) \sin (2 m + 2) \theta\} \\
& + \sum_{m=0}^{\infty} \sum_{n=m+1}^{\infty} \frac{(-)^{n+1}\, 2\, (2 n - 1)!\, a^{2n-2m-2}\, \sigma_{2n}\, B_m}{(2 m)!\, (2 n - 2 m - 2)!\, b^{2n}} \\
& \times \{(2 n - 2 m) \sin (2 n - 2 m) \theta + (2 n - 2 m - 2) \\
& \quad \times \sin (2 n - 2 m - 2) \theta\} + \frac{1}{2} \sin 2 m \theta = 0\,,
\end{aligned}\right\} \quad (17b)$$

where

$$\left.\begin{aligned}
{}^m\alpha_0 &= \frac{(-)^m}{2\, (2 m - 1)^2\, (2 m + 1)^2}\,, \\
{}^m\alpha_s &= \frac{(-)^{m+s}}{\{(2 m - 1)^2 - 4 s^2\}\, \{(2 m + 1)^2 - 4 s^2\}}\,, \\
A'_m &= \frac{16\, (2 m - 1)\, 2 m\, (2 m + 1)\, A_m}{\pi}\,,
\end{aligned}\right\} \quad (18a)$$

and

$$\left.\begin{aligned} {}^{n,m}\alpha_0 &= \frac{(-)^{n+m}}{2\,(2n-2m-1)^2\,(2n-2m+1)^2}\,, \\ {}^{n,m}\alpha_s &= \frac{(-)^{n+m+s}}{\{(2n-2m-1)^2-4s^2\}\,\{(2n-2m+1)^2-4s^2\}}\,, \\ A''_m &= \frac{16\,(2n-2m-1)\,(2n-2m)\,(2n-2m+1)\,A_m}{\pi}\,. \end{aligned}\right\} \tag{18b}$$

The boundary conditions at the rims of the notches are thus satisfied if the coefficient of each term vanishes identically. After some reductions, we obtain:

$$\left.\begin{aligned} &1+\sum_{m=1}^{\infty}\frac{A'_m}{a^{2m+1}}\,(2m-3)\,{}^m\alpha_1+\frac{2B_0}{a^2} \\ &+\sum_{m=1}^{\infty}\sum_{n=m+1}^{\infty}\frac{(-)^n\,(2n-1)!\,a^{2n-2m-1}\,\sigma_{2n}\,A''_m}{(2n-2m+1)!\,(2m-2)!\,b^{2n}}\,(4m-4n-6)\,{}^{n,m}\alpha_1 \\ &+\sum_{m=0}^{\infty}\frac{(-)^m\,8\,(2m+1)\,\sigma_{2m+2}\,B_m}{b^{2m+2}} \\ &+\sum_{m=0}^{\infty}\frac{(-)^{m+1}\,2\,(2m+3)!\,a^2\,\sigma_{2m+4}\,B_m}{(2m)!\,b^{2m+4}}=0\,, \end{aligned}\right\} \tag{19a}$$

$$\left.\begin{aligned} &\frac{1}{2}+\sum_{m=1}^{\infty}\frac{A'_m}{a^{2m+1}}\,(2m-1)\,{}^m\alpha_1-\frac{2B_1}{a^4} \\ &+\sum_{m=1}^{\infty}\sum_{n=m+1}^{\infty}\frac{(-)^n\,(2n-1)!\,a^{2n-2m-1}\,\sigma_{2n}\,A''_m}{(2n-2m+1)!\,(2m-2)!\,b^{2n}}\,(4m-4n-2)\,{}^{n,m}\alpha_1 \\ &+\sum_{m=0}^{\infty}\frac{(-)^m\,4\,(2m+1)\,\sigma_{2m+2}\,B_m}{b^{2m+2}} \\ &+\sum_{m=0}^{\infty}\frac{(-)^{m+1}\,4\,(2m+3)!\,a^2\,\sigma_{2m+4}\,B_m}{3\,(2m)!\,b^{2m+4}}=0\,, \end{aligned}\right\} \tag{19b}$$

$$\left.\begin{aligned} &\sum_{m=1}^{\infty}\frac{A'_m}{a^{2m+1}}\,(2s-2m+1)\,{}^m\alpha_s-\frac{2B_{s-1}}{a^{2s}} \\ &+\sum_{m=1}^{\infty}\sum_{n=m+1}^{\infty}\frac{(-)^n\,(2n-1)!\,a^{2n-2m-1}\,\sigma_{2n}\,A''_m}{(2n-2m+1)!\,(2m-2)!\,b^{2n}}\,(4n-4m+4s+2)\,{}^{n,m}\alpha_s \\ &+\sum_{m=0}^{\infty}\frac{(-)^{s+m}\,8s\,(2s+2m-1)!\,a^{2s-2}\,\sigma_{2s+2m}\,B_m}{(2m)!\,(2s-1)!\,b^{2s+2m}} \\ &+\sum_{m=0}^{\infty}\frac{(-)^{s+m+1}\,4\,(2s+2m+1)!\,a^{2s}\,\sigma_{2s+2m+2}\,B_m}{(2m)!\,(2s)!\,b^{2s+2m+2}}=0 \qquad (s>1)\,, \end{aligned}\right\} \tag{19c}$$

$$\left.\begin{aligned}
&\sum_{m=1}^{\infty} \frac{A'_m}{a^{2m+1}} (2s - 2m - 1)\ {}^{m}\alpha_s + \frac{2 B_s}{a^{2s+2}} \\
&+ \sum_{m=1}^{\infty} \sum_{n=m+1}^{\infty} \frac{(-)^n (2n-1)!\, a^{2n-2m-1}\, \sigma_{2n}\, A''_m}{(2n-2m+1)!\,(2m-2)!\, b^{2n}} (4n + 4s - 4m - 2)\ {}^{n,m}\alpha_s \\
&+ \sum_{m=0}^{\infty} \frac{(-)^{s+m}\, 4\,(2s+2m-1)!\, a^{2s-2}\, \sigma_{2s+2m}\, B_m}{(2m)!\,(2s-2)!\, b^{2s+2m}} \\
&+ \sum_{m=0}^{\infty} \frac{(-)^{m+s+1}\, 8s\,(2s+2m+1)!\, a^{2s}\, \sigma_{2m+2s+2}\, B_m}{(2m)!\,(2s+1)!\, b^{2m+2s+2}} = 0 \qquad (s > 1)\,.
\end{aligned}\right\} \quad (19\text{d})$$

B_s can now be eliminated, and the following equations are obtained:

$$\left.\begin{aligned}
&\frac{1}{2} + \sum_{m=1}^{\infty} \frac{A'_m}{a^{2m+1}} (2m - 1)\ {}^{m}\alpha_0 \\
&+ \sum_{m=1}^{\infty} \sum_{n=m+1}^{\infty} \frac{(-)^n\, 2\,(2n-1)!\, a^{2n-2m-1}\, \sigma_{2n}\, A''_m}{(2n-2m+1)!\,(2m-2)!\, b^{2n}} (2m - 2n - 1)\ {}^{n,m}\alpha_0 \\
&+ \sum_{m=0}^{\infty} \frac{(-)^m\, 4\,(2m+1)\, \sigma_{2m+2}\, B_m}{b^{2m+2}} = 0\,,
\end{aligned}\right\} \quad (20\text{a})$$

$$\left.\begin{aligned}
&-\frac{1}{2} + \sum_{m=1}^{\infty} \frac{A'_m}{a^{2m+1}} \left\{(1 - 2m)\ {}^{m}\alpha_1 + (5 - 2m)\ {}^{m}\alpha_2\right\} \\
&+ \sum_{m=1}^{\infty} \sum_{n=m+1}^{\infty} \frac{(-)^n (2n-1)!\, a^{2n-2m-1}\, \sigma_{2n}\, A''_m}{(2n-2m+1)!\,(2m-2)!\, b^{2n}} \\
&\times \left\{(4n - 4m + 2)\ {}^{n,m}\alpha_1 + (4n - 4m + 10)\ {}^{n,m}\alpha_2\right\} \\
&+ \sum_{m=0}^{\infty} \frac{(-)^{m+1}\, 4\,(2m+1)\, \sigma_{2m+2}\, B_m}{b^{2m+2}} \\
&+ \sum_{m=0}^{\infty} \frac{(-)^m\, 4\,(4m+3)!\, a^2\, \sigma_{2m+4}\, B_m}{(2m)!\, b^{2m+4}} \\
&+ \sum_{m=0}^{\infty} \frac{(-)^{m+1}\,(2m+5)!\, a^4\, \sigma_{2m+6}\, B_m}{3!\,(2m)!\, b^{2m+6}} = 0\,,
\end{aligned}\right\} \quad (20\text{b})\,.$$

$$\left.\begin{aligned}
&\sum_{m=1}^{\infty} \frac{A'_m}{a^{2m+1}} \left\{(2\,s - 2\,m - 1)\,{}^{m}\alpha_s + (2\,s - 2\,m + 3)\,{}^{m}\alpha_{s+1}\right\} \\
&+ \sum_{m=1}^{\infty} \sum_{n=m+1}^{\infty} \frac{(-)^n\,(2\,n-1)!\,a^{2n-2m-1}\,\sigma_{2n}\,A''_m}{(2\,n-2\,m+1)!\,(2\,m-2)!\,b^{2n}} \\
&\quad \times \left\{(4\,s+4\,n-4\,m-2)\,{}^{n,m}\alpha_s + (4\,s+4\,n-4\,m+6)\,{}^{n,m}\alpha_{s+1}\right\} \\
&+ \sum_{m=0}^{\infty} \frac{(-)^{m+s}\,4\,(2\,m+2\,s-1)!\,a^{2s-2}\,\sigma_{2m+2s}\,B_m}{(2\,m)!\,(2\,s-2)!\,b^{2m+2s}} \\
&+ \sum_{m=0}^{\infty} \frac{(-)^{m+s+1}\,8\,(2\,m+2\,s+1)!\,a^{2s}\,\sigma_{2m+2s+2}\,B_m}{(2\,m)!\,(2\,s)!\,b^{2m+2s+2}} \\
&+ \sum_{m=0}^{\infty} \frac{(-)^{m+s}\,4\,(2\,m+2\,s+3)!\,a^{2s+2}\,\sigma_{2m+2s+4}\,B_m}{(2\,m)!\,(2\,s+2)!\,b^{2m+2s+4}} = 0 \qquad (s > 1)\,.
\end{aligned}\right\} \qquad (20\text{c})$$

A formal solution of the set in equations (19) and (20) can be found in LING's paper [10]: By assuming the terms including σ_n/b^n as zero, the first approximation is obtained. This is thus equivalent to MAUNSELL's solution [3]; except that, in one pair of the corresponding parametric coefficients, the signs differ from each other. Then, with the coefficients determined in the first approximation, the values of the terms including σ_n/b^n are calculated. As the constants of (19) and (20) this values being taken, the second approximation is determined. Such approximations are repeated until the values given are convergent. Thus the values of A_m and B_m are obtained. Therefore, the approximations carried on subsequent to the first one are indeed corrections of the effects of the neighbouring notches.

For brevity, no proof of convergence is pursued here, but it will be illustrated by the numerical examples which follow.

Numerical Examples

The foregoing solution was worked out for the cases $b/a = 4$, 6, and 10, with a as unity. The values of A_m and B_m determined are shown in Table 1. On working out the values of σ_r and $\tau_{r\theta}$ at the rim of the notch, by using the values shown in Table 1, the greatest values found were 0·003 T, 0·013 T, and 0·018 T for $b/a = 4, 6,$ and 10 respectively. These are the values of σ_r for $\theta = \pi/2$. Therefore the values shown in Table 1 are thought to be sufficient to get the stresses with a high degree of approximation.

The values of

σ_θ on the edge of the semi-circular notch (Table 2),

σ_r on the straight edge (Table 3),

Table 1
Coefficients A_m, B_m

m	$b/a = 4$		$b/a = 6$		$b/a = 10$	
	A_m	B_m	A_m	B_m	A_m	B_m
0		-5.0105×10^{-1}		-6.2119×10^{-1}		-7.1882×10^{-1}
1	2.1474×10^{-1}	-1.6958×10^{-1}	2.6131×10^{-1}	-1.8015×10^{-1}	3.0086×10^{-1}	-1.9877×10^{-1}
2	2.5731×10^{-2}	-1.9423×10^{-2}	2.4600×10^{-2}	-1.1747×10^{-2}	2.6041×10^{-2}	-8.851×10^{-3}
3	-4.775×10^{-4}	3.983×10^{-3}	-1.176×10^{-3}	2.905×10^{-3}	-1.674×10^{-3}	3.020×10^{-3}
4	-4.30×10^{-5}	-1.104×10^{-3}	1.780×10^{-4}	-1.160×10^{-3}	2.759×10^{-4}	-1.354×10^{-3}
5	2.34×10^{-5}	5.234×10^{-4}	-3.61×10^{-5}	5.762×10^{-4}	-5.96×10^{-5}	6.888×10^{-4}
6	-1.95×10^{-5}	-2.155×10^{-4}	5.7×10^{-6}	-3.132×10^{-4}	1.28×10^{-5}	-3.794×10^{-4}
7	1.05×10^{-5}	1.154×10^{-4}	1.2×10^{-6}	1.747×10^{-4}	-1.2×10^{-6}	2.205×10^{-4}
8	-6.9×10^{-6}	-5.44×10^{-5}	-2.4×10^{-6}	-1.058×10^{-4}	-1.7×10^{-6}	-1.328×10^{-4}
9	4.2×10^{-6}	2.58×10^{-5}	2.2×10^{-6}	6.29×10^{-5}	2.0×10^{-6}	8.01×10^{-5}
10	-2.6×10^{-6}	-1.84×10^{-5}	-1.8×10^{-6}	-3.95×10^{-5}	-1.8×10^{-6}	-4.98×10^{-5}
11	2.1×10^{-6}	4.7×10^{-6}	1.5×10^{-6}	1.91×10^{-5}	1.6×10^{-6}	2.67×10^{-5}
12	-1.8×10^{-6}		-1.2×10^{-6}		-1.3×10^{-6}	

Table 2
σ_θ/T for $r=a$

$\theta°$	$b/a=4$	$b/a=6$	$b/a=10$
0	2·13	2·46	2·79
15	1·91	2·25	2·56
30	1·34	1·67	1·94
45	0·65	0·94	1·13
60	0·12	0·30	0·39
75	−0·06	−0·02	−0·01
90	0·00	0·00	0·00

Table 3
σ_r/T for $\theta=90°$

r/a	$b/a=4$	$b/a=6$	$b/a=10$
1·0	0	0	0
1·1	−0·02	−0·02	−0·02
1.25	−0·04	−0·03	−0·03
1·5	−0·03	0·05	0·07
1·75	−0·00	0·15	0·21
2·0	+0·01	0·23	0·33

Table 4
σ_r for $\theta=0°$

r/a	$b/a=4$	$b/a=6$	$b/a=10$
1·0	0	0	0
1·1	0·15	0·18	0·20
1·25	0·23	0·29	0·33
1·5	0·24	0·31	0·37
1·75	0·20	0·28	0·35
2·0	0·16	0·24	0·30

Table 5
σ_θ for $\theta=0°$

r/a	$b/a=4$	$b/a=6$	$b/a=10$
1·0	2·13	2·46	2·79
1·1	1·73	2·01	2·28
1·25	1·40	1·61	1·82
1·5	1·14	1·28	1·43
1·75	1·04	1·13	1·25
2·0	1·00	1·05	1·14

σ_r and σ_θ along the symmetrical line Oy (Tables 4, 5), have been calculated, and are here given.

The results of Tables 2–5 for $b/a=4$ are shown in Figure 2, where the corresponding stresses given by MAUNSELL are also plotted for comparison.

The striking features of the results are that the maximum concentration of stress becomes smaller, and the tension on the straight edge changes into compression, though small in amount, as the neighbouring notches are placed more closely together. The reduction of the stress concentration is shown in Figure 3.

It will be noted that the maximum concentration of stress for the case of $b/a=4$ is 2·13 T, which is just coincident with the result given by C. WEBER[8], while that given by M. HETÉNYI [9] is 2·175 T.

Acknowledgement

The author wishes to express his deep gratitude to Professor emeritus SEIICHI HIGUCHI of Tôhoku University for his kind advice and interest throughout the progress of the present investigation.

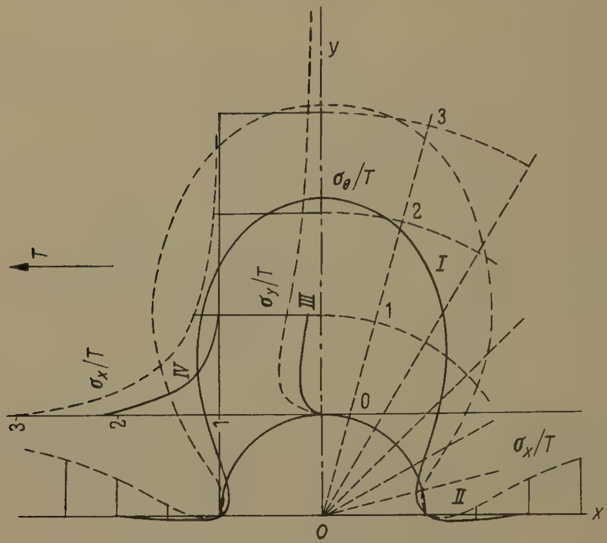

Figure 2

Stresses in the neighbourhood of each of the notches.

I stresses at the rim (Table 2); *II* radial stress on the straight edge (Table 3); *III* radial stress on the symmetrical line (Table 4); *IV* tension across the symmetrical line (Table 5).

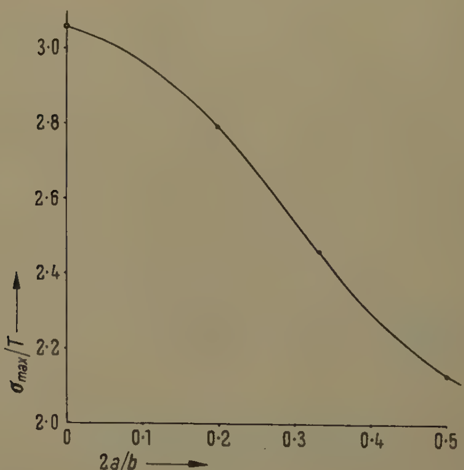

Figure 3

Stress-concentration factor (σ_{max}/T).

REFERENCES

[1] E. G. Coker and L. N. G. Filon, *Photo-Elasticity* (Cambridge University Press, London 1931), p. 560.
[2] M. M. Frocht, *Factors of Stress Concentration Photoelastically Determined*, J. appl. Mech. *57*, A–67 (1935).
[3] F. G. Maunsell, *Stresses in a Notched Plate Under Tension*, Phil. Mag. *21*, 765 (1936).
[4] T. Ishibasi, *Stresses in a Semi-Infinite Plate with a Circular Notch Under Uniform Tension*, Memories, Faculty Engng. Kyushu Imp. Univ. *9*, No. 2, 131 (1940).
[5] E. Weinel, *Die Spannungserhöhung durch Kreisbogenkerben*, Z. angew. Math. Mech. *21*, 228 (1941).
[6] C. B. Ling, *On the Stresses in a Notched Plate Under Tension*, J. Math. Phys. *26*, No. 4, 284 (1947).
[7] H. Udoguchi, Trans. Japan Soc. mech. Engng. *16*, No. 55, 44 (1950) (in Japanese).
[8] C. Weber, *Halbebene mit periodisch gewelltem Rand*, Z. angew. Math. Mech. *22* (February), 29 (1942).
[9] M. Hetényi and T. D. Liu, *A Method for Calculating Stress-Concentration Factors*, J. appl. Mech., Trans. A. S. M. E. *78*, 451 (1956).
[10] C. B. Ling, *Stresses in a Notched Strip Under Tension*, J. appl. Mech., Trans. A. S. M. E. *69*, A–275 (1947).

Zusammenfassung

Es wird hier ein Lösungsverfahren für das Spannungsproblem der Halbebene mit periodischen Halbkreiskerben nach Figur 1 besprochen. Zur Erfüllung der Randbedingungen werden Spannungsfunktionen mit Singularitäten, die periodisch zur x- und symmetrisch zur y-Achse sind, in den Mittelpunkten der Halbkreiskerben angenommen.

Die Spannungserhöhung im Kerbgrunde und auch der Spannungszustand in der Nähe des Randes werden zahlenmässig bestimmt.

(Received: February 16, 1957.)

On a Problem of Heat Conduction with Time-Dependent Boundary Conditions

By Tse-Sun Chow, Warren, Michigan, USA[1])

1. Introduction

In a recent paper [1][2]), Vodička gives general results for heat waves in a homogeneous, isotropic cylinder whose boundaries are subjected to periodic temperature fluctuations. The purpose of this paper is to derive the results for a more general and complete problem: the determination of the distribution of temperature in a homogeneous, isotropic cylinder when its initial temperature distribution is known and its boundaries are subjected to temperature fields which are *arbitrary* functions of time. The method we shall use consists of a substitution which reduces the non-homogeneous time-dependent boundary conditions to homogeneous boundary conditions, and may be considered as an extension of the method used by Mindlin and Goodman in solving vibration problems with time-dependent boundary conditions [2]. The method is, however, quite general, and may be applied to problems of similar types.

2. Statement of the Problem and Removal of Non-Homogeneous Boundary Conditions

Consider a homogeneous isotropic cylinder, $0 \leqq \varrho \leqq r$, $|z| \leqq s$ subjected to time-dependent boundary conditions and an initial temperature distribution at $t = 0$. It is desired to find the temperature distribution in the cylinder at some $t > 0$. Expressed otherwise, we are required to find $u(\varrho, \varphi, z; t)$ from the following equation:

$$\left.\begin{aligned} &\frac{\partial u}{\partial t} = a^2 \left\{ \frac{\partial^2 u}{\partial \varrho^2} + \frac{1}{\varrho} \cdot \frac{\partial u}{\partial \varrho} + \frac{1}{\varrho^2} \cdot \frac{\partial^2 u}{\partial \varphi^2} + \frac{\partial^2 u}{\partial z^2} \right\} \\ &(0 \leqq \varrho < r, \quad 0 \leqq \varphi \leqq 2\pi, \quad |z| < s), \end{aligned}\right\} \tag{2.1}$$

with the following boundary conditions

$$\left.\begin{aligned} &\frac{\partial u}{\partial \varrho} + h_1 u = f_1(\varphi, z)\, \alpha_1(t) \quad (\varrho = r), \qquad \frac{\partial u}{\partial z} + h_2 u = f_2(\varrho, \varphi)\, \alpha_2(t) \quad (z = s), \\ &\frac{\partial u}{\partial z} - h_3 u = f_3(\varrho, \varphi)\, \alpha_3(t) \quad (z = -s), \end{aligned}\right\} \tag{2.2}$$

---

[1]) Research Staff, General Motors Corporation. — The author wishes to thank the Corporation for permission to publish this paper.

[2]) Numbers in brackets refer to References, page 484.

where $h_1, h_2, h_3 > 0$ and the initial condition:

$$u(\varrho, \varphi, z; t) = u_0(\varrho, \varphi, z) \quad (t = 0) . \tag{2.3}$$

By putting

$$u(\varrho, \varphi, z; t) = \psi(\varrho, \varphi, z; t) + \sum_{l=1}^{3} X_l(\varrho, \varphi, z)\, T_l(t) \tag{2.4}$$

and substituting this expression into (2.1), (2.2), (2.3) we find the equations for $\psi(\varrho, \varphi, z; t)$ are

$$\left.\begin{aligned} &\frac{\partial \psi}{\partial t} - a^2 \left\{ \frac{\partial^2 \psi}{\partial \varrho^2} + \frac{1}{\varrho} \cdot \frac{\partial \psi}{\partial \varrho} + \frac{1}{\varrho^2} \cdot \frac{\partial^2 \psi}{\partial \varphi^2} + \frac{\partial^2 \psi}{\partial z^2} \right\} \\ &= a^2 \sum_{l=1}^{3} \left\{ \frac{\partial^2 X_l}{\partial \varrho^2} + \frac{1}{\varrho} \cdot \frac{\partial X_l}{\partial \varrho} + \frac{1}{\varrho^2} \cdot \frac{\partial^2 X_l}{\partial \varphi^2} + \frac{\partial^2 X_l}{\partial z^2} \right\} T_l - \sum_{l=1}^{3} X_l T_l', \end{aligned}\right\} \tag{2.5}$$

$$\left.\begin{aligned} &\frac{\partial \psi}{\partial \varrho} + h_1 \psi = f_1(\varphi, z)\, \alpha_1(t) - \sum_{l=1}^{3} \left\{ \frac{\partial X_l}{\partial \varrho} + h_1 X_l \right\} T_l \quad (\varrho = r) , \\ &\frac{\partial \psi}{\partial z} + h_2 \psi = f_2(\varrho, \varphi)\, \alpha_2(t) - \sum_{l=1}^{3} \left\{ \frac{\partial X_l}{\partial z} + h_2 X_l \right\} T_l \quad (z = s) , \\ &\frac{\partial \psi}{\partial z} - h_3 \psi = f_3(\varrho, \varphi)\, \alpha_3(t) - \sum_{l=1}^{3} \left\{ \frac{\partial X_l}{\partial z} - h_3 X_l \right\} T_l \quad (z = -s) , \end{aligned}\right\} \tag{2.6}$$

$$\psi(\varrho, \varphi, z; 0) = u_0 - \sum_{l=1}^{3} X_l\, T_l(0) . \tag{2.7}$$

We now choose $T_l(t)$ as follows:

$$T_l(t) = \alpha_l(t) , \tag{2.8}$$

while X_l are to be determined by

$$\frac{\partial^2 X_l}{\partial \varrho^2} + \frac{1}{\varrho} \cdot \frac{\partial X_l}{\partial \varrho} + \frac{1}{\varrho^2} \cdot \frac{\partial^2 X_l}{\partial \varphi^2} + \frac{\partial^2 X_l}{\partial z^2} = 0 , \tag{2.9}$$

with the boundary conditions:

$$\left.\begin{aligned} &\frac{\partial X_l}{\partial \varrho} + h_1 X_l = \delta_{l1} f_1(\varphi, z) \quad (\varrho = r) , \\ &\frac{\partial X_l}{\partial z} + h_2 X_l = \delta_{l2} f_2(\varrho, \varphi) \quad (z = s) , \\ &\frac{\partial X_l}{\partial z} - h_3 X_l = \delta_{l3} f_3(\varrho, \varphi) \quad (z = -s) , \end{aligned}\right\} \tag{2.10}$$

where $\delta_{lm} = 1$ for $l = m$ and is otherwise zero.

With this choice of X_l and T_l we find the equations that determine ψ are given by:

$$\frac{\partial\psi}{\partial t} - a^2\left\{\frac{\partial^2\psi}{\partial\varrho^2} + \frac{1}{\varrho}\cdot\frac{\partial\psi}{\partial\varrho} + \frac{1}{\varrho^2}\cdot\frac{\partial^2\psi}{\partial\varphi^2} + \frac{\partial^2\psi}{\partial z^2}\right\} = -\sum_{l=1}^{3} X_l\, T_l', \quad (2.11)$$

$$\left.\begin{array}{l} \dfrac{\partial\psi}{\partial\varrho} + h_1\,\psi = 0 \quad (\varrho = r)\,, \qquad \dfrac{\partial\psi}{\partial z} + h_2\,\psi = 0 \quad (z = s)\,, \\ \qquad\qquad \dfrac{\partial\psi}{\partial z} - h_3\,\psi = 0 \quad (z = -s)\,, \end{array}\right\} \quad (2.12)$$

$$\psi(\varrho, \varphi, z; 0) = u_0 - \sum_{l=1}^{3} X_l\, T_l(0)\,. \quad (2.13)$$

Thus, when X_l and T_l are properly chosen, the problem of determining u is reduced to one of determining X_l satisfying (2.9) and (2.10) and ψ satisfying (2.11) with the homogeneous boundary conditions (2.12) and the initial condition (2.13). We proceed first to find X_l.

3. Determination of $X_l(\varrho, \varphi, z)$

We notice that each X_l satisfies the differential equation (2.9) and two homogeneous boundary conditions and a non-homogeneous one (2.10). Following the classical method of separation of variables we expand each X_l into a doubly infinite sum of the form $R(\varrho)\,\Phi(\varphi)\,Z(z)$. We present the final results here, omitting the necessary details. It is suggested that readers refer to [1] for the proof of the orthogonality property of the characteristic functions and the evaluation of the normalization integrals.

$$X_1(\varrho, \varphi, z) = \sum_{j=1}^{\infty}\sum_{n=-\infty}^{\infty} {}_1A_{nj}\, I_n\left(\frac{\varepsilon_j'}{r}\,\varrho\right) e^{in\varphi}\left\{\cos\frac{\delta_j}{s}\,z + C_j\sin\frac{\delta_j}{s}\,z\right\} \quad (i = \sqrt{-1})\,, \quad (3.1)$$

where δ_j, ε_j', C_j and ${}_1A_{nj}$ are given by

$$\left.\begin{array}{l} (h_2\,h_3\,s^2 - \delta_j^2)\sin 2\,\delta_j + (h_2 + h_3)\,s\,\delta_j\cos 2\,\delta_j = 0\,, \\ \varepsilon_j' = \dfrac{\delta_j\,r}{s}\,, \qquad C_j = \dfrac{\delta_j\sin\delta_j - h_2\,s\cos\delta_j}{\delta_j\cos\delta_j + h_2\,s\sin\delta_j}\,, \\ {}_1A_{nj}\left\{\left(\dfrac{n}{r} + h_1\right) I_n(\varepsilon_j') + \dfrac{\varepsilon_j'}{r}\, I_{n+1}(\varepsilon_j')\right\}\displaystyle\int_{-s}^{+s}\left\{\cos\frac{\delta_j}{s}\,z + C_j\sin\frac{\delta_j}{s}\,z\right\}^2 dz \\ \quad = \dfrac{1}{2\,\pi}\displaystyle\int_{-s}^{+s}\left\{\cos\frac{\delta_j}{s}\,z + C_j\sin\frac{\delta_j}{s}\,z\right\} dz \int_{-\pi}^{+\pi} f_1(\varphi, z)\, e^{-in\varphi}\, d\varphi\,. \end{array}\right\} \quad (3.2)$$

$$X_2(\varrho, \varphi, z) = \sum_{k=1}^{\infty} \sum_{n=-\infty}^{\infty} {}_2A_{n\,k}\, I_n\left(\frac{\varepsilon_{n\,k}}{r}\, \varrho\right) e^{i n \varphi} \left\{\cos \frac{\delta'_{n\,k}}{s}\, z + C'_{n\,k} \sin \frac{\delta'_{n\,k}}{s}\, z\right\}, \quad (3.3)$$

where $\delta'_{n\,k}$, $\varepsilon_{n\,k}$, $C'_{n\,k}$ and ${}_2A_{n\,k}$ are given by

$$\left.\begin{aligned}
&(n + h_1\, r)\, I_n(\varepsilon_{n\,k}) + \varepsilon_{n\,k}\, I_{n+1}(\varepsilon_{n\,k}) = 0\,,\\
&\delta'_{n\,k} = \frac{\varepsilon_{n\,k}\, s}{r}\,, \qquad C'_{n\,k} = \frac{h_3\, s \cos \delta'_{n\,k} - \delta'_{n\,k} \sin \delta'_{n\,k}}{\delta'_{n\,k} \cos \delta'_{n\,k} + h_3\, s \sin \delta'_{n\,k}}\,,\\
&{}_2A_{n\,k}\, \frac{\delta'_{n\,k}\, s\, (h_2 + h_3) \cos 2\, \delta'_{n\,k} + (s^2\, h_2\, h_3 - \delta'^2_{n\,k}) \sin 2\, \delta'_{n\,k}}{s\, (\delta'_{n\,k} \cos \delta'_{n\,k} + h_3\, s \sin \delta'_{n\,k})}\\
&\quad \times \int_0^r \varrho \left\{I_n\left(\frac{\varepsilon_{n\,k}}{r}\, \varrho\right)\right\}^2 d\varrho = \frac{1}{2\,\pi} \int_0^r \varrho\, I_n\left(\frac{\varepsilon_{n\,k}}{r}\, \varrho\right) d\varrho \int_{-\pi}^{+\pi} f_2(\varrho, \varphi)\, e^{-i n \varphi}\, d\varphi\,.
\end{aligned}\right\} \quad (3.4)$$

$$X_3(\varrho, \varphi, z) = \sum_{k=1}^{\infty} \sum_{n=-\infty}^{\infty} {}_3A_{n\,k}\, I_n\left(\frac{\varepsilon_{n\,k}}{r}\, \varrho\right) e^{i n \varphi} \left\{\cos \frac{\delta'_{n\,k}}{s}\, z + C''_{n\,k} \sin \frac{\delta'_{n\,k}}{s}\, z\right\}, \quad (3.5)$$

where $\delta'_{n\,k}$, $\varepsilon_{n\,k}$, $C''_{n\,k}$ and ${}_3A_{n\,k}$ are given by

$$\left.\begin{aligned}
&(n + h_1\, r)\, I_n(\varepsilon_{n\,k}) + \varepsilon_{n\,k}\, I_{n+1}(\varepsilon_{n\,k}) = 0\,,\\
&\delta'_{n\,k} = \frac{\varepsilon_{n\,k}\, s}{r}\,, \qquad C''_{n\,k} = \frac{\delta'_{n\,k} \sin \delta'_{n\,k} - h_2\, s \cos \delta'_{n\,k}}{\delta'_{n\,k} \cos \delta'_{n\,k} + h_2\, s \sin \delta'_{n\,k}}\,,\\
&{}_3A_{n\,k}\, \frac{\delta'_{n\,k}\, s\, (h_2 + h_3) \cos 2\, \delta'_{n\,k} + (s^2\, h_2\, h_3 - \delta'^2_{n\,k}) \sin 2\, \delta'_{n\,k}}{s\, (\delta'_{n\,k} \cos \delta'_{n\,k} + h_2\, s \sin \delta'_{n\,k})}\\
&\quad \times \int_0^r \varrho \left\{I_n\left(\frac{\varepsilon_{n\,k}}{r}\, \varrho\right)\right\}^2 d\varrho = \frac{1}{2\,\pi} \int_0^r \varrho\, I_n\left(\frac{\varepsilon_{n\,k}}{r}\, \varrho\right) \int_{-\pi}^{+\pi} f_3(\varrho, \varphi)\, e^{-i n \varphi}\, d\varphi\,.
\end{aligned}\right\} \quad (3.6)$$

4. Determination of ψ and u

The function ψ satisfies the differential equation (2.11), the homogeneous boundary conditions (2.12) and the initial condition (2.13). This suggests that ψ can be expanded into the triply infinite sum:

$$\psi(\varrho, \varphi, z; t) = \sum_{k=1}^{\infty} \sum_{j=1}^{\infty} \sum_{n=-\infty}^{\infty} F_{n\,k\,j}(t)\, I_n\left(\frac{\varepsilon_{n\,k}}{r}\, \varrho\right) e^{i n \varphi} \left\{\cos \frac{\delta_j}{s}\, z + C_j \sin \frac{\delta_j}{s}\, z\right\}. \quad (4.1)$$

From the boundary conditions (2.12) we see that $\varepsilon_{n\,k}$, δ_j, C_j are determined as follows:

$$\left.\begin{aligned}
&(n + h_1\, r)\, I_n(\varepsilon_{n\,k}) + \varepsilon_{n\,k}\, I_{n+1}(\varepsilon_{n\,k}) = 0\,,\\
&(h_2\, h_3\, s^2 - \delta_j^2) \sin 2\, \delta_j + (h_2 + h_3)\, s\, \delta_j \cos 2\, \delta_j = 0\,,\\
&C_j = \frac{\delta_j \sin \delta_j - h_2\, s \cos \delta_j}{\delta_j \cos \delta_j + h_2\, s \sin \delta_j}\,.
\end{aligned}\right\} \quad (4.2)$$

It remains only to determine the coefficients in (4.1), i. e., $F_{nkj}(t)$. To this end we substitute (4.1) into (2.11). This results

$$\left.\begin{aligned}\sum_{k=1}^{\infty}\sum_{j=1}^{\infty}\sum_{n=-\infty}^{\infty}\left\{F'_{nkj}(t)-a^2\left(\frac{\varepsilon_{nk}^2}{r^2}-\frac{\delta_j^2}{s^2}\right)F_{nkj}(t)\right\}I_n\left(\frac{\varepsilon_{nk}}{r}\varrho\right)e^{in\varphi}&\\ \times\left\{\cos\frac{\delta_j}{s}z+C_j\sin\frac{\delta_j}{s}z\right\}=-\sum_{l=1}^{3}X_l(\varrho,\varphi,z)\,\alpha'_l(t)\,,&\end{aligned}\right\}\quad(4.3)$$

where use has been made of the fact that $I_n(\varepsilon_{nk}\varrho/r)$ satisfies the following equation:

$$\frac{d^2}{d\varrho^2}I_n\left(\frac{\varepsilon_{nk}}{r}\varrho\right)+\frac{1}{\varrho}\cdot\frac{d}{d\varrho}I_n\left(\frac{\varepsilon_{nk}}{r}\varrho\right)-\left(\frac{\varepsilon_{nk}^2}{r^2}+\frac{n^2}{\varrho^2}\right)I_n\left(\frac{\varepsilon_{nk}}{r}\varrho\right)=0\,. \quad (4.4)$$

To solve for $F_{nkj}(t)$ in (4.3) we expand $X_l(\varrho,\varphi,z)$ into the following triply infinite sums:

$$X_l(\varrho,\varphi,z)=\sum_{j=1}^{\infty}\sum_{k=1}^{\infty}\sum_{n=-\infty}^{\infty}{}_lB_{nkj}\,I_n\left(\frac{\varepsilon_{nk}}{r}\varrho\right)e^{in\varphi}\left\{\cos\frac{\delta_j}{s}z+C_j\sin\frac{\delta_j}{s}z\right\}. \quad (4.5)$$

Using the orthogonality property of $I_n(\varepsilon_{nk}\varrho/r)$ and $\left\{\cos(\delta_j/s)\,z+C_j\sin(\delta_j/s)\,z\right\}$, we find the relations between ${}_lB_{nkj}$ and ${}_lA_{nkj}$ to be, from (3.1), (3.3) and (3.5):

$$\left.\begin{aligned}&{}_1B_{nkj}\int_0^r\varrho\left\{I_n\left(\frac{\varepsilon_{nk}}{r}\varrho\right)\right\}^2d\varrho={}_1A_{nkj}\int_0^r\varrho\,I_n\left(\frac{\varepsilon'_j}{r}\varrho\right)I_n\left(\frac{\varepsilon_{nk}}{r}\varrho\right)d\varrho\,,\\ &{}_2B_{nkj}\int_{-s}^{+s}\left\{\cos\frac{\delta_j}{s}z+C_j\sin\frac{\delta_j}{s}z\right\}^2dz\\ &\quad={}_2A_{nkj}\int_{-s}^{+s}\left\{\cos\frac{\delta'_{nk}}{s}z+C'_{nk}\sin\frac{\delta'_{nk}}{s}z\right\}\left\{\cos\frac{\delta_j}{s}z+C_j\sin\frac{\delta_j}{s}z\right\}dz\,,\\ &{}_3B_{nkj}\int_{-s}^{+s}\left\{\cos\frac{\delta_j}{s}z+C_j\sin\frac{\delta_j}{s}z\right\}^2dz\\ &\quad={}_3A_{nkj}\int_{-s}^{+s}\left\{\cos\frac{\delta'_{k}}{s}z+C''_{nk}\sin\frac{\delta'_{nk}}{s}z\right\}\left\{\cos\frac{\delta_j}{s}z+C_j\sin\frac{\delta_j}{s}z\right\}dz\,.\end{aligned}\right\}\quad(4.6)$$

By substituting (4.5) into (4.3) we obtain by equating coefficients:

$$F'_{nkj}(t)-a^2\left(\frac{\varepsilon_{nk}^2}{r^2}-\frac{\delta_j^2}{s^2}\right)F_{nkj}(t)=-\sum_{l=1}^{3}{}_lB_{nkj}\,\alpha'_l(t) \quad (4.7)$$

and upon integration, we have immediately

$$F_{nkj}(t) = F_{nkj}(0) \exp\left\{a^2\left(\frac{\varepsilon_{nk}^2}{r^2} - \frac{\delta_j^2}{s^2}\right)t\right\}$$
$$-\sum_{l=1}^{3} {}_lB_{nkj} \exp\left\{a^2\left(\frac{\varepsilon_{nk}^2}{r^2} - \frac{\delta_j^2}{s^2}\right)t\right\}\int_0^t \alpha_l'(\tau) \exp\left\{-a^2\left(\frac{\varepsilon_{nk}^2}{r^2} - \frac{\delta_j^2}{s^2}\right)\tau\right\} d\tau\,,$$

i. e.,

$$\left.\begin{aligned} F_{nkj}(t) = {} & F_{nkj}(0) \exp\left\{a^2\left(\frac{\varepsilon_{nk}^2}{r^2} - \frac{\delta_j^2}{s^2}\right)t\right\} \\ & - \sum_{l=1}^{3} {}_lB_{nkj}\left\{\alpha_l(t) - \alpha_l(0) \exp\left\{a^2\left(\frac{\varepsilon_{nk}^2}{r^2} - \frac{\delta_j^2}{s^2}\right)t\right\}\right\} \\ & - \sum_{l=1}^{3} a^2\left(\frac{\varepsilon_{nk}^2}{r^2} - \frac{\delta_j^2}{s^2}\right) {}_lB_{nkj} \exp\left\{a^2\left(\frac{\varepsilon_{nk}^2}{r^2} - \frac{\delta_j^2}{s^2}\right)t\right\} \\ & \int_0^t \alpha_l(\tau) \exp\left\{-a^2\left(\frac{\varepsilon_{nk}^2}{r^2} - \frac{\delta_j^2}{s^2}\right)\tau\right\} d\tau\,, \end{aligned}\right\} \quad (4.8)$$

by integration by parts. The coefficients $F_{nkj}(0)$ are determined by the initial condition (2.7). Let $u_0(\varrho, \varphi, z)$ be expanded into the triply infinite sum:

$$u_0(\varrho, \varphi, z) = \sum_{j=1}^{\infty}\sum_{k=1}^{\infty}\sum_{n=-\infty}^{\infty} D_{nkj}\, I_n\left(\frac{\varepsilon_{nk}}{r}\,\varrho\right) e^{in\varphi}\left\{\cos\frac{\delta_j}{s}\,z + C_j \sin\frac{\delta_j}{s}\,z\right\}, \quad (4.9)$$

then from (2.7), (4.1), (4.5) and (4.9) we obtain

$$F_{nkj}(0) = D_{nkj} - \sum_{l=0}^{3} {}_lB_{nkj}\,\alpha_l(0)\,. \quad (4.10)$$

From (4.1), (4.8) and (4.10) we therefore obtain

$$\left.\begin{aligned} & \psi(\varrho, \varphi, z; t) \\ & = \sum_{j=1}^{\infty}\sum_{k=1}^{\infty}\sum_{n=-\infty}^{\infty}\left[D_{nkj} \exp\left\{a^2\left(\frac{\varepsilon_{nk}^2}{r^2} - \frac{\delta_j^2}{s^2}\right)t\right\} - \sum_{l=1}^{3} {}_lB_{nkj}\,\alpha_l(t)\right. \\ & \qquad - a^2 \sum_{l=1}^{3}\left(\frac{\varepsilon_{kn}^2}{r^2} - \frac{\delta_j^2}{s^2}\right) {}_lB_{nkj} \exp\left\{a^2\left(\frac{\varepsilon_{nk}^2}{r^2} - \frac{\delta_j^2}{s^2}\right)t\right\} \\ & \qquad \left.\times \int_0^t \alpha_l(\tau) \exp\left\{-a^2\left(\frac{\varepsilon_{nk}^2}{r^2} - \frac{\delta_j^2}{s^2}\right)\tau\right\} d\tau\right] \\ & \qquad \times I_n\left(\frac{\varepsilon_{nk}}{r}\,\varrho\right) e^{in\varphi}\left\{\cos\frac{\delta_j}{s}\,z + C_j \sin\frac{\delta_j}{s}\,z\right\}. \end{aligned}\right\} \quad (4.11)$$

Remembering that $u(\varrho, \varphi, z; t) = \psi(\varrho, \varphi, z; t) + \sum_{l=1}^{3} X_l(\varrho, \varphi, z)\, \alpha_l(t)$ and using (4.5) we finally obtain from (4.11) the solution in the following form:

$$\left.\begin{aligned} &u(\varrho, \varphi, z; t) \\ &= \sum_{j=1}^{\infty} \sum_{k=1}^{\infty} \sum_{n=-\infty}^{\infty} \Bigg[D_{nkj} \exp\left\{a^2 \left(\frac{\varepsilon_{nk}^2}{\gamma^2} - \frac{\delta_j^2}{s^2}\right) t\right\} \\ &\qquad - a^2 \sum_{l=1}^{3} \left(\frac{\varepsilon_{nk}^2}{\gamma^2} - \frac{\delta_j^2}{s^2}\right) {}_lB_{nkj} \exp\left\{a^2 \left(\frac{\varepsilon_{nk}^2}{\gamma^2} - \frac{\delta_j^2}{s^2}\right) t\right\} \\ &\qquad \times \int_0^t \alpha_l(\tau) \exp\left\{-a^2 \left(\frac{\varepsilon_{nk}^2}{\gamma^2} - \frac{\delta_j^2}{s^2}\right) \tau\right\} d\tau \Bigg] \\ &\qquad \times I_n\left(\frac{\varepsilon_{nk}}{\gamma}\, \varrho\right) e^{in\varphi} \left\{\cos\frac{\delta_j}{s}\, z + C_j \sin\frac{\delta_j}{s}\, z\right\}, \end{aligned}\right\} \quad (4.12)$$

where ${}_lB_{nkj}$, D_{nkj} are given by (4.6), (4.9) respectively, and ε_{nk}, δ_j, C_j are given by (4.2).

REFERENCES

[1] Václav Vodička, *Circular Cylinder Under Periodic Fluctuations of Temperature*, ZAMP *8*, 1, 53 (1957).

[2] R. D. Mindlin and L. E. Goodman, *Beam Vibrations with Time-Dependent Boundary Conditions*, J. appl. Mech. *17*, 377 (1950).

Zusammenfassung

Das folgende Wärmeleitungsproblem wird analytisch behandelt. Auf dem Mantel und den Deckflächen eines Kreiszylinders sei eine *zeitlich veränderliche* Temperaturverteilung und ausserdem die Temperatur einer Kurve zur Zeit $t = 0$ gegeben. Gesucht ist die Innentemperatur für alle Zeiten. Die verwendete Separationsmethode kann auch auf andere Randwertprobleme angewendet werden.

(Received: April 30, 1957.)

Design of Circular Plates for Minimum Weight[1])

EMIN TURAN ONAT[2]), WALTER SCHUMANN[3]) and RICH. THORPE SHIELD[2]),
Providence, R. I., USA

1. Introduction

The minimum weight design of circular plates has been investigated by HOPKINS and PRAGER [1][4]) and FREIBERGER and TEKINALP [2] for the case of a uniformly loaded plate with a simply supported edge. Intuitive arguments were used in [1] to obtain the minimum weight design, and [2] employed the calculus of variations. In this paper the direct design procedures developed by DRUCKER and SHIELD [3, 4] are used. These formal design procedures were derived from the theorems of limit analysis [6]. Both built-in and simply supported edge conditions are considered and the plate is loaded by an arbitrary rotationally symmetric distribution of pressure. The designs obtained are absolute minimum weight designs for the sandwich plate but the minimum is a relative one for the solid or homogeneous plate.

2. Statement of the Problem

The problem under consideration is the design of a circular plate under rotationally symmetric types of loading and edge support. The design is to be such that the plate is just at the point of collapse under the given loads and such that minimum volume of a given elastic-perfectly plastic material is involved. The material is assumed to be homogeneous so that the design for minimum volume coincides with the design for minimum weight. As in work on the load-carrying capacities of circular plates (see [5], for example), the term collapse is used in the sense of limit analysis [6], and membrane stresses are ignored in the analysis.

The plate is assumed to be horizontal and loaded by a distribution of pressure $p(r)$ on its upper surface, r measuring distance from the plate center. The edge $r = R$ of the plate is simply supported or built-in. The radial and circumferential bending moments are denoted by M and N, respectively, with the convention that positive values of these moments stress the lower surface

---

1) The results presented in this paper were obtained in the course of research work sponsored by Watertown Arsenal Laboratory under Contract DA-19-020-ORD-2598-DA-19-020-501-ORD-3984.

2) Brown University.

3) ETH and Brown University.

4) Numbers in brackets refer to References, page 499.

of the plate in tension. For equilibrium the moments satisfy the equation

$$\frac{d^2(r\,M)}{dr^2} - \frac{dN}{dr} + r\,p = 0\,. \tag{1}$$

The shear force Q is given by

$$r\,Q = \frac{d(r\,M)}{dr} - N\,. \tag{2}$$

The curvature rates $\varkappa$, λ in the radial and circumferential directions are given by

$$\varkappa = -\frac{d^2w}{dr^2}\,, \qquad \lambda = -\frac{1}{r} \cdot \frac{dw}{dr}\,, \tag{3}$$

where w is the deflection rate of the middle surface of the plate in the downwards direction.

For simplicity it is assumed that the elastic-perfectly plastic material obeys TRESCA's yield condition and the associated flow rule. In terms of the moments M and N, plastic yielding can occur when one (or both) of the magnitudes of M and N equals the fully plastic moment M_0 or when the magnitude of $M-N$ equals M_0. The condition defines a yield curve in a plane in which the moments M, N are taken to be rectangular cartesian co-ordinates and the yield curve is a hexagon (Figure 1). For a point on a side of the yield hexagon, the flow rule

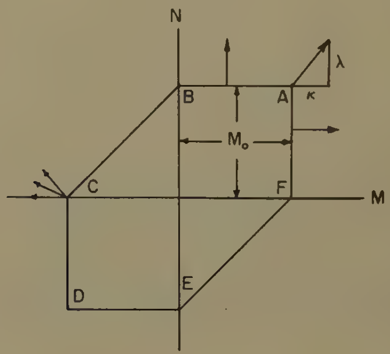

Figure 1

Moment yield condition.

associated with the yield condition requires that during collapse the curvature-rate vector ($\varkappa$, λ) is parallel to the outwards-drawn normal to the sides. At the corner of the hexagon, the vector must lie between the normals to the side which meet at the corner.

The rate of dissipation of energy D_A due to plastic action per unit area of the middle surface of the plate is given by

$$D_A = M\,\varkappa + N\,\lambda\,. \tag{4}$$

Because of the flow rule, the rate of dissipation D_A is uniquely determined by the curvature rates $\varkappa$, λ.

In the problems considered here, replacing the Tresca yield condition by the perhaps more acceptable condition of VON MISES would make an analytic solution impractical and a numerical approach would prove necessary. A similar situation exists in the previously mentioned work on the load-carrying capacities of circular plates. However, when an approximate yield condition is used to estimate load-carrying capacities, bounds to the error committed can be determined [7]. As will be shown, an analogous procedure applies to minimum weight design. For the purposes of illustration we shall assume the von Mises yield condition with yield stress σ_0 in tension to be the true yield condition for the material and the Tresca yield condition to be the approximate condition used to simplify the problem. The extension to any true yield condition and any approximation is obvious. The yield surface defined in principal stress space by the von Mises condition with yield stress σ_0 circumscribes the yield surface defined in the same space by the Tresca condition with yield stress σ_0. It follows that any structure designed to be just at the point of collapse under given loads for the inscribed Tresca condition will be safe or at collapse under the same loads for the von Mises condition. Thus the volume $V_T(\sigma_0)$ of the minimum volume design based on the inscribed Tresca condition with yield stress σ_0 will not be less than the volume $V_M(\sigma_0)$ of the minimum volume design based on the von Mises condition. By the same reasoning, the volume $V_M(\sigma_0)$ of the minimum volume design based on the von Mises condition will not be less than the volume $V_T(2\,\sigma_0/\sqrt{3})$ of the minimum volume design based on the circumscribed Tresca condition with yield stress $2\,\sigma_0/\sqrt{3}$. Thus the true minimum volume $V_M(\sigma_0)$ is bounded from below and above,

$$V_T\left(\frac{2\,\sigma_0}{\sqrt{3}}\right) \leqq V_M(\sigma_0) \leqq V_T(\sigma_0)\,. \tag{5}$$

The accuracy to which $V_M(\sigma_0)$ is determined by (5) depends on the variation of $V_T(\sigma_0)$ with σ_0. In the sandwich plate examples considered in section 3 below, $V_T(\sigma_0)$ is inversely proportional to σ_0 and (5) determines $V_M(\sigma_0)$ to within 7%. In the solid or homogeneous plate examples of section 4 below, the designs obtained are relative minimum volume designs with volume inversely proportional to the square root of σ_0. It seems probable, however, that the designs are in fact absolute minimum volume designs, and with this conjecture (5) determines $V_M(\sigma_0)$ to within 4%.

3. The Sandwich Plate

The sandwich plate has a light-weight core of constant thickness H between two identical face sheets of variable thickness t ($t \ll H$) composed of the given

material. The minimum volume design is just at collapse under the pressure $p(r)$ and involves minimum volume of the face sheets. The core carries no bending stresses and the fully plastic moment M_0 has the value

$$M_0 = \sigma_0 H t, \tag{6}$$

where σ_0 is the yield stress of the cover plate material.

It has been shown [2, 3, 4] that a sandwich plate designed to collapse in a mode such that the rate of dissipation per unit volume in the faces of the plate is constant is an absolute minimum volume design. In terms of the rate of dissipation D_A per unit area of the middle surface, D_A/t is constant for such a design,

$$\frac{D_A}{t} = \frac{M \varkappa + N \lambda}{t} = \text{const}. \tag{7}$$

This condition is independent of the thickness t because of the linear dependence (6) of M_0 and therefore of D_A on t. With the Tresca yield condition (Figure 1), the condition (7) restricts the position of the moment point on the yield hexagon. For example the moment point cannot lie on the side AF for a finite range of r because the flow rule requires $\lambda = 0$ and the condition (7) cannot be satisfied in view of (3). It is readily found that the condition (7) can only be satisfied for a finite range of r when the moment state is represented by one of the points A or D, C or F of the hexagon. The points A and C will be used in the following.

For the point A, condition (7) becomes

$$\frac{d^2 w}{dr^2} + \frac{1}{r} \cdot \frac{dw}{dr} = -\alpha, \tag{8}$$

where α is a positive constant. It follows that

$$w = \beta - \frac{1}{4} \alpha r^2 + \frac{1}{2} \alpha b^2 \log \frac{b}{r}, \tag{9}$$

where b and β are constants. In addition $\varkappa$ and λ are non-negative at the point A and this enforces $r \geqq b$.

For the point C, the condition becomes

$$\frac{d^2 w}{dr^2} = \alpha, \tag{10}$$

so that

$$w = \frac{1}{2} \alpha r (r - 2c) + \gamma, \tag{11}$$

where c and γ are constants. The requirements $-\varkappa \geqq \lambda \geqq 0$ restrict the range of r to $c \geqq r \geqq c/2$.

When the plate is *simply supported* at the edge $r = R$ and loaded by a downwards-acting pressure $p(r)$, the assumption that the curvature rates $\varkappa, \lambda$ are both non-negative leads to the minimum volume design. The moment state through the plate is then represented by the point A in Figure 1. At the edge $r = R$ the deflection rate w is zero and at the center dw/dr is zero since λ is finite there. The appropriate form of (9) is therefore

$$w = \frac{1}{4} \alpha (R^2 - r^2) . \tag{12}$$

For the point A, $M = N = M_0$ and substitution in the equilibrium equation (1) yields

$$\frac{r d^2 M_0}{dr^2} + \frac{dM_0}{dr} = -r p(r) . \tag{13}$$

At the edge of the plate $M = 0$ and the shearing force Q given by (2) is zero at $r = 0$, assuming that there is no concentrated load at the center. With these conditions, integration of (13) gives

$$M_0 = \sigma_0 H t = \int_r^R \frac{1}{\xi} d\xi \int_0^\xi \varrho p(\varrho) d\varrho , \tag{14}$$

and the thickness t given by (14) is the minimum volume design [since $p(r)$ is non-negative, t is non-negative]. A ring of uniform force per unit length on the circle $r = a$ can be included by suitable interpretation of the integral with respect to ϱ in (14). The particular case of a concentrated force P at the center adds a term

$$\frac{P}{2\pi} \log \frac{R}{r} \tag{15}$$

to the right-hand side of (14), producing an infinite value of t at the center but the face sheets have finite volume. The result for uniform pressure has been obtained previously [1]. Further examples of simple types of loading are studied in more detail below.

For the plate with a *built-in* edge and non-negative $p(r)$, near the edge of the plate where $\varkappa \leqq 0$, $\lambda \geqq 0$, the point C of Figure 1 will apply. Near the center of the plate $\varkappa$ and λ are non-negative and the point A applies. Assuming that regime A applies for $0 \leqq r < a$ and regime C for $a < r \leqq R$, equations (9) and (11) govern the deflection rate in these regions respectively. At the built-in edge w and dw/dr are zero and at the center dw/dr is zero. Also w and dw/dr are continuous at the junction $r = a$ of the two regions[5]. In order to satisfy the

[5]) It will be seen that the thickness t of the face sheets in the minimum volume design is zero at the junction $r = a$ and collapse modes exist for which dw/dr is not continuous across $r = a$. As we require a collapse mode in which the rate of dissipation per unit volume is constant in order to show that the design is a minimum volume design, discontinuities in dw/dr are not permissible in this type of collapse mode.

conditions it is found that we must have $a = 2\,R/3$, and we obtain finally

$$w = \begin{cases} \frac{1}{12}\,\alpha\,(2\,R^2 - 3\,r^2) & \left(0 \leqq r \leqq \frac{2}{3}\,R\right), \\ \frac{1}{2}\,\alpha\,(r - R)^2 & \left(\frac{2}{3}\,R \leqq r \leqq R\right). \end{cases} \tag{16}$$

For $0 \leqq r \leqq 2\,R/3$, $M = N = M_0$ and M_0 satisfies equation (13). In the outer annulus $2\,R/3 \leqq r \leqq R$, $M = -M_0$ and $N = 0$ so that for equilibrium

$$\frac{d^2}{dr^2}\,(r\,M_0) = r\,p(r)\,. \tag{17}$$

At $r - 2\,R/3$, M is continuous and therefore zero and the shearing force Q is continuous. As before Q is zero at $r = 0$ in the absence of a concentrated load at the center. With these conditions, equations (13) and (17) give on integration

$$M_0 = \sigma_0\,H\,t = \begin{cases} \int\limits_r^{2R/3} \frac{1}{\xi}\,d\xi \int\limits_0^{\xi} \varrho\,p(\varrho)\,d\varrho & \left(0 \leqq r \leqq \frac{2}{3}\,R\right), \\ \frac{1}{r} \int\limits_{2R/3}^{r} d\xi \int\limits_0^{\xi} \varrho\,p(\varrho)\,d\varrho & \left(\frac{2}{3}\,R \leqq r \leqq R\right). \end{cases} \tag{18}$$

Rings of force per unit length can be included as for the simply supported plate. The case of a concentrated load at the center and other simple types of loading are examined below.

The case when part of the plate is loaded by pressure on the lower surface, that is when $p(r)$ is negative for a range of r, will not be considered here. In addition to the points A and C, moment states represented by the points F and D of the hexagon may have to be used, depending on the pressure distribution $p(r)$.

(i) *Circular Loading, Simply Supported Edge*

In this case $p(r)$ has the constant value p for $0 \leqq r \leqq r_0$ and is zero for $r_0 < r \leqq R$. Direct substitution in equation (14) gives the thickness t of the minimum volume design,

$$\sigma_0\,H\,t = \begin{cases} \frac{1}{4}\,p\,(r_0^2 - r^2) + \frac{1}{2}\,p\,r_0^2 \log\frac{R}{r_0} & (0 \leqq r \leqq r_0)\,, \\ \frac{1}{2}\,p\,r_0^2 \log\frac{R}{r} & (r_0 \leqq r \leqq R)\,. \end{cases} \tag{19}$$

The volume V of the face sheets is found to be

$$V = \frac{1}{4}\left(2 - \frac{r_0^2}{R^2}\right)\frac{\pi\,p\,r_0^2\,R^2}{\sigma_0\,H}\,. \tag{20}$$

As might be expected, the volume V for a given total load $\pi p r_0^2$ decreases as the area over which the load is spread increases. It can be seen from (20) that the average thickness depends linearly on the total load $\pi p r_0^2$ and otherwise only on the ratio r_0/R, for given σ_0 and H.

The thickness t_c for a plate with face sheets of constant thickness which is just at the point of collapse under the same loading and support conditions can be deduced from the results of HOPKINS and PRAGER [5]. The volume V_c of the plate with constant face thickness is found to be

$$V_c = \left(1 - \frac{2}{3} \cdot \frac{r_0}{R}\right) \frac{\pi p r_0^2 R^2}{\sigma_0 H}. \tag{21}$$

Comparison of (20) and (21) shows that the saving effected by the minimum volume design over the constant thickness design increases from 25% to 50% as r_0/R decreases from unity to zero.

The case of a concentrated force P at the center of the plate can be obtained as a limiting case by letting $\pi p r_0^2$ tend to P as r_0 tends to zero. The thickness distribution is given by

$$\sigma_0 H t = \frac{P}{2\pi} \log \frac{R}{r}, \tag{22}$$

and the volume of the face sheets is

$$V = \frac{1}{2} \cdot \frac{PR^2}{\sigma_0 H}. \tag{23}$$

(ii) *Circular Loading, Built-in Edge*

The form of the thickness distribution depends on whether the radius r_0 of the loaded area is less than or greater than $2R/3$, the radius of the junction between the regimes A and C.

For $r_0 < 2R/3$, equation (18) gives

$$\sigma_0 H t = \left\{ \begin{array}{ll} \frac{1}{4} p (r_0^2 - r^2) + \frac{1}{2} p r_0^2 \log \frac{2R}{3r_0} & (0 \leqq r \leqq r_0), \\ \frac{1}{2} p r_0^2 \log \frac{2R}{3r} & \left(r_0 \leqq r \leqq \frac{2}{3} R\right), \\ \frac{1}{2} p r_0^2 \frac{r - 2R/3}{r} & \left(\frac{2}{3} R \leqq r \leqq R\right). \end{array} \right\} \tag{24}$$

For $r_0 > 2R/3$, the corresponding result is

$$\sigma_0 H t = \left\{ \begin{array}{ll} \frac{1}{4} p \left(\frac{4}{9} R^2 - r^2\right) & \left(0 \leqq r \leqq \frac{2}{3} R\right), \\ \frac{1}{6} p \frac{r^3 - 8R^3/27}{r} & \left(\frac{2}{3} R \leqq r \leqq r_0\right), \\ \frac{1}{6} p \frac{3 r_0^2 r - 8R^3/27 - 2 r_0^3}{r} & (r_0 \leqq r \leqq R). \end{array} \right\} \tag{25}$$

The concentrated load P at the center is a particular case of (24) and the thickness is given by

$$\sigma_0 H t = \begin{cases} \dfrac{P}{2\pi} \log \dfrac{2R}{3r} & \left(0 \leq r \leq \dfrac{2}{3} R\right), \\ \dfrac{P}{2\pi} \cdot \dfrac{r - 2R/3}{r} & \left(\dfrac{2}{3} R \leq r \leq R\right). \end{cases} \tag{26}$$

The volume V of the face sheets has the value

$$V = \frac{1}{3} \cdot \frac{P R^2}{\sigma_0 H}. \tag{27}$$

As has been shown by HOPKINS and PRAGER, the limit value of a concentrated central load P is $2\pi M_0$ for a circular plate with constant fully plastic bending moment M_0 for both the simply supported and the built-in plates. Thus the face sheets of the constant thickness plate which is just at collapse under the central load P have the volume

$$V_c = \frac{P R^2}{\sigma_0 H}, \tag{28}$$

irrespective of the support conditions. The saving effected by the minimum volume design over the constant thickness design is 67% for the built-in plate compared with 50% for the simply supported plate.

The thickness distribution for the built-in, uniformly loaded plate follows from (25) by giving r_0 the value R. The minimum weight design for this case is shown diagrammatically in Figure 2(a). The volume of the face sheets has the value

$$V = 0{\cdot}117 \frac{\pi p R^4}{\sigma_0 H}. \tag{29}$$

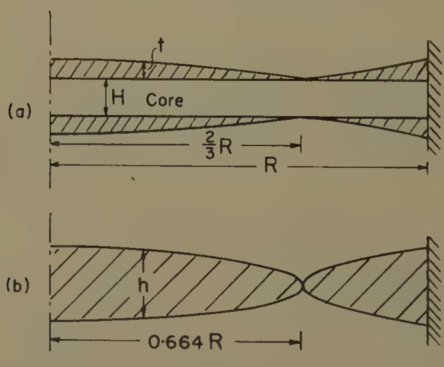

Figure 2
Minimum weight designs for built-in circular plate under uniform pressure: (a) sandwich plate, (b) solid plate.

With the results of [5], the volume V_c of the face sheets of the constant thickness plate is found to be

$$V_c = 0{\cdot}178 \; \frac{\pi \, p \, R^4}{\sigma_0 \, H} \tag{30}$$

so that the minimum volume design effects a saving of 34% over the constant thickness plate.

(iii) *Annular Loading*

The results for annular loading, that is $p(r)$ has the constant value p in the annulus $r_0 \leq r \leq r_1$ and zero elsewhere, can be obtained from the general formulae (14) and (18). For both the simply supported and built-in plates, the thickness t is constant in the central region $0 \leq r \leq r_0$. In particular, the thickness t is zero in the unloaded central region for the built-in plate when r_0 is greater than $2\,R/3$.

4. The Solid Plate

For the solid or homogeneous plate, the fully plastic moment M_0 is given by

$$M_0 = \frac{1}{4} \, \sigma_0 \, h^2 \,, \tag{31}$$

where h is the (variable) thickness of the plate. The results are less definite and the analysis is less tractable for the solid plate than for the sandwich plate. As has been shown [2, 3, 4], a solid plate designed to collapse in a mode such that the rate of dissipation per unit volume is constant on the surfaces of the plate is a relative minimum volume design. Here 'relative minimum' is used in the following sense. If h_m is the thickness distribution of the relative minimum volume design, then any neighboring plate with thickness $h = h_m + \delta h$, where $|\,\delta h\,| \ll h_m$, which is safe or just at collapse under the given loads will involve a greater volume of material. In terms of the rate of dissipation D_A per unit area of the middle surface, the condition for a relative minimum volume design is

$$\frac{D_A}{h} = \frac{M \, \varkappa + N \, \lambda}{h} = \text{const} \, . \tag{32}$$

Since D_A is proportional to h^2, this condition involves the design thickness h, a circumstance which complicates the analysis. Thus in contrast to the sandwich plate, it is not immediately apparent that points A and D, C and F of the yield hexagon in Figure 1 are the only moment states involved in a relative minimum design. In the following, moment states represented by the points A and C will be used to obtain solutions.

Considering first the *simply supported* circular plate, loaded by a non-negative pressure $p(r)$, the use of moment states represented by the point A

provide the relative minimum volume design. The assumption $M = N = M_0$ and the equilibrium equation together with the conditions at the center and edge of the plate lead to

$$M_0 = \frac{1}{4}\,\sigma_0\,h^2 = \int\limits_r^R \frac{1}{\xi}\,d\xi \int\limits_0^\xi \varrho\,p(\varrho)\,d\varrho\,, \tag{33}$$

as in the previous section. For non-negative $p(r)$, h^2 and therefore h is a monotonic decreasing function of r. In order to show that the design thickness h given by (33) is a relative minimum volume design, it is necessary to show that an associated collapse mode exists satisfying (32). For the point A, (32) becomes

$$\frac{d^2w}{dr^2} + \frac{1}{r}\cdot\frac{dw}{dr} = -\frac{\alpha}{h}\,, \tag{34}$$

where α is a positive constant. As dw/dr is zero at $r = 0$, it follows that

$$\frac{dw}{dr} = -\frac{\alpha}{r}\int\limits_0^r \frac{\varrho}{h(\varrho)}\,d\varrho\,, \tag{35}$$

and therefore since w is zero at the edge $r = R$,

$$w = \alpha\int\limits_r^R \frac{1}{\xi}\,d\xi \int\limits_0^\xi \frac{\varrho}{h(\varrho)}\,d\varrho\,. \tag{36}$$

In order that the collapse mode be associated with the point A, dw/dr and d^2w/dr^2 must be non-positive. It follows immediately from (35),

$$\frac{d^2w}{dr^2} = \frac{\alpha}{r^2}\int\limits_0^r \frac{\varrho}{h(\varrho)}\,d\varrho - \frac{\alpha}{h(r)}\,,$$

and since $h(r)$ is monotonic decreasing

$$\frac{d^2w}{dr^2} \leqq \frac{\alpha}{r^2\,h(r)}\int\limits_0^r \varrho\,d\varrho - \frac{\alpha}{h(r)} = -\frac{1}{2}\cdot\frac{\alpha}{h(r)} \leqq 0\,. \tag{37}$$

Hence the thickness h given by (33) provides a relative minimum design.

For the *built-in* plate under pressure $p(r)$, we assume as in the previous section that regime A applies for $0 \leqq r < a$ and regime C for $a < r \leqq R$. In

the same way that equation (18) was derived we obtain

$$M_0 = \frac{1}{4}\,\sigma_0\,h^2 - \begin{cases} \displaystyle\int_r^a \frac{1}{\xi}\,d\xi \int_0^\xi \varrho\,p(\varrho)\,d\varrho & (0 \leqq r \leqq a)\,, \\ \displaystyle\frac{1}{r}\int_a^r d\xi \int_0^\xi \varrho\,p(\varrho)\,d\varrho & (a \leqq r \leqq R)\,. \end{cases} \tag{38}$$

The thickness h is zero at $r = a$ and for non-negative $p(r)$ is monotonic decreasing for $0 \leqq r \leqq a$ and is monotonic increasing for $a \leqq r \leqq R$. It remains to determine a and the associated collapse mode w satisfying (32). For $0 \leqq r \leqq a$, w satisfies equation (34), where h is now given by (38), and as before it can be shown that dw/dr and d^2w/dr^2 are non-positive in this region. For $a \leqq r \leqq R$, condition (32) requires

$$\frac{d^2w}{dr^2} = \frac{\alpha}{h}\,. \tag{39}$$

Since dw/dr is zero at the built-in edge it follows that

$$\frac{dw}{dr} = -\alpha \int_r^R \frac{d\varrho}{h(\varrho)} \qquad (a \leqq r \leqq R)\,. \tag{40}$$

At the point C, $-\varkappa \geqq \lambda \geqq 0$ and with (3), (39) and (40) this requires

$$\frac{1}{h(r)} \geqq \frac{1}{r}\int_r^R \frac{d\varrho}{h(\varrho)} \qquad (a \leqq r \leqq R)\,. \tag{41}$$

The radius a is determined by the condition that dw/dr is continuous at $r = a$. For $0 \leqq r \leqq a$, dw/dr is given by (35) and with (40) the condition becomes

$$\int_0^a \frac{\varrho}{h(\varrho)}\,d\varrho = a \int_a^R \frac{d\varrho}{h(\varrho)}\,. \tag{42}$$

When a has been determined from this equation for a given $p(r)$, the inequality (41) must be checked. Inequality (41) is always satisfied if a $\geqq R/2$. In the range $a \leqq r \leqq R$, $h(r)$ is a monotonic increasing function of r and it follows that in this range

$$\frac{1}{r}\int_r^R \frac{d\varrho}{h(\varrho)} \leqq \left(\frac{R}{r} - 1\right)\frac{1}{h(r)}\,. \tag{43}$$

Comparison of (41) and (43) shows that (41) is satisfied if $a \geqq R/2$.

(i) *Circular Loading, Simply Supported Edge*

When the plate is loaded by a constant pressure p over the area $0 \leqq r \leqq r_0$, the thickness distribution for a simply supported plate is obtained by direct substitution in (33),

$$h = \begin{cases} \left(\dfrac{p}{\sigma_0}\right)^{1/2} \left\{r_0^2 - r^2 + 2\, r_0^2 \log \dfrac{R}{r_0}\right\}^{1/2} & (0 \leqq r \leqq r_0)\,, \\ \left(\dfrac{p}{\sigma_0}\right)^{1/2} r_0 \left(2 \log \dfrac{R}{r}\right)^{1/2} & (r_0 \leqq r \leqq R)\,. \end{cases} \tag{44}$$

The result for uniform loading, $r_0 = R$, has been obtained previously by Hopkins and Prager [1]. The volume of the plate is proportional to the square root of the total load $\pi\, p\, r_0^2$ and inversely proportional to the square root of σ_0. As the ratio r_0/R decreases from unity to zero the saving in volume effected by the design (44) over the constant thickness design increases from 18% to 37%.

For a plate with a concentrated load P at the center, the relative minimum volume design is

$$h = \left(\frac{P}{\pi\, \sigma_0}\right)^{1/2} \left(2 \log \frac{R}{r}\right)^{1/2} \tag{45}$$

with volume

$$V = \frac{1}{2} \left(\frac{P}{\sigma_0}\right)^{1/2} \pi\, R^2\,. \tag{46}$$

(ii) *Circular Loading, Built-in Edge*

As for the sandwich plate, the form of the thickness distribution depends on whether the radius r_0 of the loaded area is less than or greater than the radius a of the junction between the regimes A and C.

For $r_0 < a$, equation (38) gives directly

$$\frac{1}{4}\, \sigma_0\, h^2 = \begin{cases} \dfrac{1}{4}\, p\, (r_0^2 - r^2) + \dfrac{1}{2}\, p\, r_0^2 \log \dfrac{a}{r_0} & (0 \leqq r \leqq r_0)\,, \\ \dfrac{1}{2}\, p\, r_0^2 \log \dfrac{a}{r} & (r_0 \leqq r \leqq a)\,, \\ \dfrac{1}{2}\, p\, r_0^2\, \dfrac{r-a}{r} & (a \leqq r \leqq R)\,. \end{cases} \tag{47}$$

For $r_0 > a$, the corresponding result is

$$\frac{1}{4}\, \sigma_0\, h^2 = \begin{cases} \dfrac{1}{4}\, p\, (a^2 - r^2) & (0 \leqq r \leqq a)\,, \\ \dfrac{1}{6}\, p\, \dfrac{r^3 - a^3}{r} & (a \leqq r \leqq r_0)\,, \\ \dfrac{1}{6}\, p\, \dfrac{3\, r_0^2\, r - a^3 - 2\, r_0^3}{r} & (r_0 \leqq r \leqq R)\,. \end{cases} \tag{48}$$

In each case the junction radius a must be such that equation (42) is satisfied. The substitution of either form (47) or (48) for h into (42) gives a transcendental equation for a. The values of a/R were determined by graphical methods for the values 0, 0·2, 0·4, 0·6, 0·7, 0·8, 0·9 and 1·0 of r_0/R. The results are shown graphically in Figure 3. The distances a and r_0 are equal when r_0/R is equal to 0·695 approximately. It can be seen from the figure that $a > R/2$ and it follows from the discussion of inequality (41) that an associated collapse mode exists satisfying the condition (32) for a relative minimum volume design.

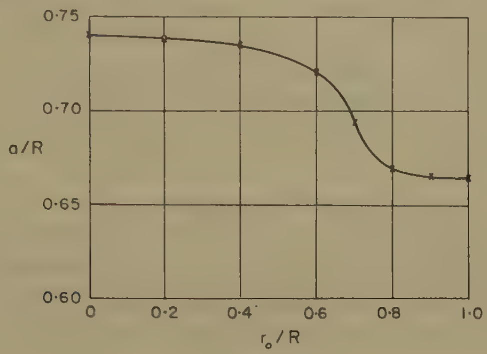

Figure 3

Variation of a/R with r_0/R for the solid built-in plate under circular loading.

The minimum weight design for the case of uniform loading ($r_0/R = 1$) is shown diagrammatically in Figure 2 (b) and may be contrasted with the sandwich plate design [Figure 2 (a)] for the same conditions of loading and support.

For a concentrated load P at the center, $r_0 = 0$ and the thickness is given by

$$\frac{1}{4}\,\sigma_0\,h^2 = \begin{cases} \dfrac{P}{2\,\pi}\log\dfrac{a}{r} & (0 \leqq r \leqq a)\,, \\[2ex] \dfrac{P}{2\,\pi}\cdot\dfrac{r-a}{r} & (a \leqq r \leqq R)\,. \end{cases} \tag{49}$$

Here a has the value 0·74 R in order to satisfy equation (42). The volume of the plate is found to be

$$V = 0{\cdot}407\left(\frac{P}{\sigma_0}\right)^{1/2}\pi\,R^2\,. \tag{50}$$

A solid plate of uniform thickness which is just at collapse under a central load P has the volume

$$V_c = 0{\cdot}798\left(\frac{P}{\sigma_0}\right)^{1/2}\pi\,R^2 \tag{51}$$

for both the built-in and simply supported edge conditions. Comparison of (46) and (50) with (51) shows that the savings effected by designs (45) and (49) over the constant thickness design are 37% and 49% respectively.

5. Built-in Sandwich Plate with Weight

In [4], it was shown that, in principle, body forces may be taken into account in the optimum design of a structure. The design of a simply supported circular sandwich plate loaded by uniform pressure and its own weight was obtained as an illustration. Here as a further illustration we obtain the corresponding design for a built-in plate.

The plate is assumed to be horizontal and loaded by a uniform pressure p on its upper surface. As in section 3, the core thickness H is constant and it can be supposed that the weight of the core is included in the pressure p. A minimum volume design is obtained if the plate is designed to collapse in a mode such that the rate of dissipation of energy due to plastic action less the rate at which the body force does work is constant in the face sheets (4). This condition can be written

$$\frac{M\,\varkappa + N\,\lambda}{2\,t} - \gamma\,w = \text{const}\,, \tag{52}$$

where γ is the weight per unit volume of the material of the face sheets.

We assume that regime A of Figure 1 applies for $0 \leqq r < a$ and regime C applies for $a < r \leqq R$, where R is the radius of the plate. Condition (52) then becomes

$$\left.\begin{aligned} &\frac{d^2 w}{d r^2} + \frac{1}{r}\cdot\frac{d w}{d r} + \beta^2\,w = -\alpha \quad && (0 \leqq r < a)\,,\\ &\frac{d^2 w}{d r^2} - \beta^2\,w = \alpha && (a < r \leqq R)\,, \end{aligned}\right\} \tag{53}$$

where $\beta^2 = 2\,\gamma/\sigma_0\,H$ and α is a positive constant. Equations (53) are subject to the conditions $w = dw/dr = 0$ at the edge $r = R$ of the plate and dw/dr is zero at the center of the plate. Also w and dw/dr are continuous at $r = a$. It is found that

$$w = \left\{\begin{aligned} &\alpha\,[J_0(\beta\,r) - J_0(\beta\,a)\,\operatorname{sech}\beta\,(R-a)] && (0 \leqq r \leqq a)\,,\\ &\alpha\,J_0\,(\beta\,a)\,[\cosh\beta\,(R-r)\,\operatorname{sech}\beta\,(R-a) - \operatorname{sech}\beta\,(R-a)] \\ & && (a \leqq r \leqq R)\,, \end{aligned}\right\} \tag{54}$$

and the radius a is given by

$$\tanh\beta\,(R-a) = \frac{J_1(\beta\,a)}{J_0(\beta\,a)}\,. \tag{55}$$

Equation (55) has a unique solution for a for given values of β and R, and the collapse mode (54) satisfies the appropriate inequalities on $\varkappa$ and λ in the inner and outer regions.

For equilibrium the moments satisfy the equation

$$\frac{d^2}{dr^2}(r\,M) - \frac{dN}{dr} + r\,p + 2\,\gamma\,t\,r = 0\,. \tag{56}$$

In the region $0 \leqq r < a$, $M = N = M_0$ and in the region $a < r \leqq R$, $M = -M_0$, $N = 0$, where M_0 is given by (6). At the junction $r = a$, M is continuous and therefore zero and the shearing force Q is continuous. At the center Q is zero. It is found that

$$\sigma_0\,H\,t = \left\{ \begin{array}{ll} \dfrac{p}{\beta^2}\left\{\dfrac{J_0(\beta\,r)}{J_0(\beta\,a)} - 1\right\} & (0 \leqq r \leqq a)\,, \\ \dfrac{p}{\beta^2}\left\{\dfrac{a}{r}\cosh\beta\,(r-a) - 1 \right. & \\ \qquad \left. + \left[\dfrac{1}{\beta\,r} + \dfrac{a}{r}\tanh\beta\,(R-a)\right]\sinh\beta\,(r-a)\right\} & \\ & (a \leqq r \leqq R)\,. \end{array} \right\} \tag{57}$$

As the parameter β increases, that is as the ratio of the weight of the material to its yield stress increases, the ratio a/R decreases, and the section $r = a$ where the face sheets have zero thickness moves nearer to the center of the plate.

REFERENCES

[1] H. G. Hopkins and W. Prager, *Limits of Economy of Material in Plates*, J. appl. Mech. *22*, 372–374 (1955).

[2] W. Freiberger and B. Tekinalp, *Minimum Weight Design of Circular Plates*, J. Mech. Phys. Solids *4*, 294–299 (1956).

[3] D. C. Drucker and R. T. Shield, *Design for Minimum Weight*, to appear in Proc. 9th Int. Congr. appl. Mech., Brussels (1956).

[4] D. C. Drucker and R. T. Shield, *Bounds on Minimum Weight Designs*, to appear in Quart. appl. Math.

[5] H. G. Hopkins and W. Prager, *The Load-Carrying Capacities of Circular Plates*, J. Mech. Phys. Solids *2*, 1–13 (1953).

[6] D. C. Drucker, W. Prager, and H. J. Greenberg, *Extended Limit Design Theorems for Continuous Media*, Quart. appl. Math. *9*, 381–389 (1952).

[7] R. Hill, *A Note on Estimating Yield-Point Loads in a Plastic-Rigid Body*, Phil. Mag. *43*, 353–355 (1952).

Zusammenfassung

Diese Arbeit befasst sich mit dem Problem der Bemessung einer elastisch-plastischen Kreisplatte veränderlicher Dicke von minimalem Gewicht. Die Platte ist am Rand frei drehbar gelagert oder eingespannt und trägt eine rotationssymmetrische, sonst beliebig verteilte Last. Es wird das von Drucker und Shield entwickelte Verfahren zur Dimensionierung verwendet, welches ein absolutes Minimum für das Gewicht einer Sandwichplatte und ein relatives Minimum für dasjenige einer homogenen Platte liefert.

(Received: April 16, 1957.)

Buchbesprechungen – Book Reviews – Notices bibliographiques

Engineering Analysis. A Survey of Numerical Procedures. Von STEPHEN H. CRANDALL (McGraw-Hill Book Company, New York, Toronto, London 1956). 417 S., 170 Fig.; £3.11s.6d.

Die Aufgabe des vorliegenden Buches besteht darin, dem Ingenieur zu helfen, seine Probleme numerisch zu lösen. Die Fachrichtung spielt eine sekundäre Rolle, da überall im Grunde genommen die gleichen mathematischen Betrachtungen anzustellen sind, wie Schaffung eines mathematischen Modells für eine physikalische Sachlage und die Reduktion des mathematischen Problems zu einem numerischen Verfahren. Vorwiegend wird der zweite Teil im Buch behandelt, doch gibt der Autor manche Beispiele für den ersten Schritt, in der Meinung, dass die Struktur der mathematischen Formulierung diskutiert werden muss zum Verständnis der numerischen Behandlung. Drei Hauptprobleme sind es, die sich im allgemeinen dem Ingenieur darbieten: Gleichgewicht (eingeschwungener Zustand von Temperaturverteilungen, laminare Strömungen, elastische Spannungszustände); Bestimmung von Eigenwerten (kritische Werte von bestimmten Parametern im Gleichgewichtszustand, kritische Frequenzen und Resonanzprobleme) und Ausbreitungsvorgänge (Wärme, Druckwellen in Flüssigkeiten und mechanische Spannungen und Verformungen in elastischen Systemen). Alle Probleme werden in Systemen mit beschränktem Freiheitsgrad (konzentrierte Parameter) sowie in kontinuierlichen behandelt. Auch nichtlineare Probleme, mit Ausnahme der Eigenwertbestimmung, kommen zur Sprache. Zahlreiche Übungsaufgaben dienen der Festigung des Gebotenen.

Dem rechnenden Ingenieur kann das Buch eine wertvolle Hilfe sein.

H. Weber

Wahrscheinlichkeitstheorie. Von H. RICHTER (Springer-Verlag, Berlin 1956 [Grundlehren der Mathematischen Wissenschaften, Band 86]). 435 S., 14 Abb.; DM 66.—, Ganzleinen DM 69.60.

Das hier vorliegende Lehrbuch ist das erste ausführliche Werk in deutscher Sprache, das die neue Entwicklung der Wahrscheinlichkeitsrechnung berücksichtigt, und sein Erscheinen ist schon aus diesem Grunde sehr zu begrüssen.

Der Inhalt gliedert sich in die folgenden Abschnitte: Mathematische Grundlagen, der Wahrscheinlichkeitsbegriff, die Elemente der Wahrscheinlichkeitstheorie, Elemente der Integrationstheorie, zufällige Grössen auf Wahrscheinlichkeitsfeldern, spezielle Wahrscheinlichkeitsverteilungen, die Konvergenz zufälliger Grössen. Besonders ausführlich werden die Grundlagen der Wahrscheinlichkeitstheorie behandelt, und zwar werden die Axiome ungefähr im Sinne von früheren Ausführungen des Verfassers (Math. Ann. 1953–1954) aufgestellt. Das vorgeschlagene Axiomensystem scheint besonders von Anwendungen in physikalischen Problemen beeinflusst zu sein. Die modernen Teilgebiete der Wahrscheinlichkeitsrechnung, die stochastischen Prozesse, die Spieltheorie und die Theorie der statistischen Entscheidungsverfahren werden nicht behandelt.

Vom Leser wird verlangt, dass er mit der mathematischen Denkweise gut vertraut ist, hingegen wird sehr wenig konkretes Wissen vorausgesetzt; insbesondere enthält das Buch die notwendigen mengentheoretischen Voraussetzungen selbst.

P. Schmid

Waffe und Wirkung bei der Fliegerabwehr. Von H. Brändli (Birkhäuser Verlag, Basel und Stuttgart 1956). 91 S., 24 Abb.; Fr. 26.– / DM 26.–.

Bei der vergleichenden Beurteilung verschiedener Flabgeschütze ist es zufolge der grossen Zahl der auftretenden Parameter sehr schwierig, einen Gesamtüberblick zu erlangen. Der Verfasser des vorliegenden Buches versucht für den Fall des Folgeschiessens die theoretischen Grundlagen für einen solchen Vergleich herauszuarbeiten. In einem ersten Teil wird das sogenannte Präzisionsmass unter Berücksichtigung der Geschossflugzeitstreuung untersucht und explizit dargestellt. Daraus kann dann der Abschusskoeffizient, der bei Vernachlässigung wirtschaftlicher Überlegungen taktisch allein massgebend ist, abgeleitet werden und zu einem Vergleich der Wirksamkeit verschiedener Waffen führen. Im zweiten Teil wird auf Grund gewisser Annahmen die Abhängigkeit der Treffwahrscheinlichkeit von der Geschossflugzeit untersucht und ein gelegentlich verwendeter Potenzansatz einer Kritik unterzogen. Schliesslich wird noch die benützte Zielfehlerdefinition gerechtfertigt. – Auch wenn jedenfalls noch verschiedene Hypothesen näher zu untersuchen bleiben, dürfte doch das Buch einen bedeutsamen Beitrag zur Klärung dieser ausserordentlich komplizierten Zusammenhänge liefern. Die übersichtliche und klare Darstellung wird alle Fachleute interessieren, die mit schiesstechnischen Problemen zu tun haben.

E. Roth-Desmeules

Die Transformatoren. Von Milan Vidmar, dritte, vollständig neu bearbeitete Auflage (Birkhäuser Verlag, Basel und Stuttgart 1956). 630 S., 321 Abb.; geb. Fr./DM 68.–, brosch. Fr./DM 64.–.

Der Leser wird in acht Hauptabschnitten in lebendiger und klarer Weise gründlich mit den modernen Transformatoren bekannt gemacht. Es stellt ein in sich abgeschlossenes Werk dar, das sowohl Grundlagen und Eigenschaften wie Probleme beim Bau und Betrieb behandelt. Speziell ausführlich werden die Hauptvertreter, die Drehstromtransformatoren, beschrieben, während weniger ausgesprochene Transformatorenprobleme, wie Regulierapparate usw., nur erwähnt bleiben. Hauptprobleme, die auch andere Elektromaschinenbauer interessieren, sind sehr breit behandelt, so die Wärmeabfuhr aus dem arbeitenden Transformator, der Eisenkern, Leerlauf, Kurzschluss, Einschaltstromstoss und die Wicklung. Losgelöst von allen Landes- und Firmennormen, wird vom physikalischen und wirtschaftlichen Standpunkt alles Vorhandene kritisch gegeneinander abgewogen und diskutiert sowie am Schlusse die Wege des Entwurfes anhand von ausgeführten Transformatoren illustriert. Das Buch wird sowohl dem Praktiker als dem Wissenschaftler und den Studenten gute Dienste leisten.

G. Gubelmann und *R. Weller*

Statistical Analysis of Stationary Time Series. Von U. Grenander und M. Rosenblatt (John Wiley and Sons, New York 1957). 300 S., 8 Fig.; $11.–.

Dieses bemerkenswerte Buch kann nur von solchen Lesern verstanden werden, welche gute Kenntnisse in der Wahrscheinlichkeitsrechnung, der mathematischen Statistik und der Masstheorie besitzen. Die Verfasser setzten sich das hohe Ziel, die statistische Analysis von Zeit-Reihen gemäss modernen, exakten, mathematischen Methoden mit Hilfe der Masstheorie, Fourier-Analyse und Theorie der Matrizen darzustellen. Angesichts der grossen Bedeutung solcher Methoden in der modernen physikalischen und technischen Forschung sollten darin Tätige sich mit Hilfe dieses Buches über den betreffenden Problemkreis und seine mathematisch-statistische Behandlung orientieren.

W. Saxer

Nonparametric Methods in Statistics. Von D. A. S. FRASER (John Wiley and Sons, New York 1957). 300 S., 17 Fig.; $8.50.

In der modernen mathematischen Statistik werden neben klassischen Verteilungen, wie der Normalverteilung, definiert durch bestimmte Parameter, allgemeinere Verteilungen ohne Parameter betrachtet. Ebenso wurden in der statistischen Schätzungstheorie entsprechende Methoden geschaffen, die sich neben wahrscheinlichkeitstheoretischen Begriffen auf die Masstheorie stützen. Dieses Buch gibt einen guten Überblick über den heutigen Stand dieser Theorie, zu welcher der Verfasser wichtige Beiträge beisteuerte. *W. Saxer*

Handbuch der Physik - Encyclopedia of Physics. Herausgegeben von S. FLÜGGE. Bd. 20: *Elektrische Leitungsphänomene II* (Springer-Verlag, Berlin 1957). 491 S., 272 Fig.; DM 112.–.

Band 20 des Handbuchs behandelt elektrische Leitungsphänomene in Nichtmetallen und enthält die vier Beiträge: O. MADELUNG, *Halbleiter*; A. B. LIDIARD, *Ionic Conductivity*; J. M. STEVELS, *The Electrical Properties of Glass*; und E. DARMOIS, *Electrochimie*.

Der Artikel von MADELUNG, der die Hälfte des Bandes einnimmt, gehört zu den besten unter den neueren zusammenfassenden Arbeiten auf dem Gebiet der Halbleiterphysik. In einer bester Handbuchtradition entsprechenden Darstellung – es sei hier nur auf die Zusammenstellung der Koeffizienten der elektrischen, magnetischen und thermischen Effekte in Abschnitt C hingewiesen – wird ein Überblick über das weitschichtige Gebiet gegeben. Dass dabei die Diskussion spezieller Halbleiter etwas zu kurz kommt, dürfte zum Teil auf Platzmangel, zum Teil aber auch auf die gegenwärtig noch sehr lückenhaften experimentellen Ergebnisse zurückzuführen sein.

Auch die zweite, von LIDIARD stammende Arbeit erfüllt in vollem Umfang die Ansprüche, welche an einen Handbuchartikel gestellt werden. In kurzer und übersichtlicher Form werden auf 100 Seiten alle wesentlichen Gebiete der Ionenleitung behandelt. Besondere Erwähnung verdient eine Zusammenstellung neuer und neuester Literatur, die, nach Substanzen getrennt, vom Fachmann sehr begrüsst werden dürfte.

Entsprechend dem heutigen Stand der Forschung enthält der Beitrag von STEVELS über die elektrischen Eigenschaften von Glas vorwiegend experimentelle Ergebnisse.

Man frägt sich, ob die Arbeit von DARMOIS über Elektrochemie im 20. Band des Handbuches an der richtigen Stelle steht. (Der Artikel von GARLICK, Bd. 19, über Photoleitung hätte unseres Erachtens besser in diesen Zusammenhang gepasst.) Im übrigen lässt diese Arbeit in bezug auf Übersichtlichkeit sowohl als auch in der Berücksichtigung neuester Ergebnisse zu wünschen übrig. *E. Mooser*

Handbuch der Physik - Encyclopedia of Physics. Herausgegeben von S. FLÜGGE. Band 32: *Strukturforschung* (Springer-Verlag, Berlin 1957). 663 S., 373 Fig.; DM 144.–.

Es ist erstmalig, dass alle Arten von Strukturuntersuchungen mit Röntgen-, Elektronen- und Neutronenstrahlen in einem einzigen Bande dargestellt werden. Nicht nur das Bestimmen von Kristallstrukturen, sondern auch Untersuchungen von Flüssigkeiten, amorphen und makromolekularen Stoffen werden darin behandelt. Der schön ausgestattete und reich illustrierte Band enthält wertvolle Literaturhinweise auf neueste Arbeiten und ist als Hand- und Lehrbuch deshalb sehr willkommen.

Der einführende Artikel von A. GUINIER und G. v. ELLER, *Les méthodes expérimentales des déterminations de structures cristallines par rayons X*, beschreibt ausser den experimentellen Methoden die einzelnen Arbeitsschritte einer vollständigen Kristallanalyse besonders klar. Die theoretische Begründung dazu, insbesondere die Theorie der Röntgenstreuung und -reflexion, wird im Artikel von J. BOUMAN, *Theoretical Principles of Structural Research by X-Rays*, gegeben. G. FOURNET zeigt in *Etude de la structure des fluides et des substances amorphes au moyen de la diffraction des rayons X* durch genaue theoretische Untersuchung, dass die älteren Deutungen von Flüssigkeitsinterferenzen nur teilweise richtig sind. Die Kleinwinkel-Röntgenstreuung findet interessante Anwendungen in der Virus- und Eiweissforschung, wie aus der Arbeit von W. W. BEEMAN, P. KAESBERG, J. W. ANDEREGG und M. B. WEBB, *Size of Particles and Lattice Defects*, hervorgeht. Im zweiten Teil wird gezeigt, welche Aussagen über Gitterfehler durch röntgenographische Untersuchungen gewonnen werden können. In den Beiträgen von H. RAETHER über *Elektroneninterferenzen* und von G. R. RINGO über *Neutron Diffraction and Interference* werden besonders die Unterschiede und die Vorzüge gegenüber den Röntgenverfahren für bestimmte Strukturprobleme hervorgehoben. *H. Gränicher*

Physikalisch-statistische Regeln als Grundlagen für Wetter- und Witterungsvorhersagen. Von FRANZ BAUR. 1. Band (Akademische Verlagsgesellschaft mbH., Frankfurt am Main 1956). 139 S., 30 Abb., 2 farbige Tafeln; geb. DM 46.–.

In diesem Werk, dessen erster Band jetzt vorliegt, unternimmt es der Verfasser, auf Grund jahrzehntelanger Forschungen und anhand eines umfangreichen Materials nachzuweisen, «dass die physikalisch durchdachte, wahrscheinlichkeitstheoretisch kontrollierte Statistik ganz allgemein die den Wettervorgängen am besten angepasste Form der Erfahrungsforschung ist und dass mit ihr auch für die kurz- und mittelfristige Wettervoraussage bessere und überzeugendere Erfahrungsgrundlagen gewonnen werden können als mit den bisher fast ausschliesslich gebrauchten Beispielen vereinzelter Wetterlagen». Dieser Nachweis ist dem Verfasser bis zu einem hohen Grade tatsächlich auch gelungen. Es konnte eine ganze Reihe zutreffender Regeln über Zusammenhänge zeitlich sich folgender Witterungserscheinungen abgeleitet werden, die auch für weitere theoretische und empirische Untersuchungen auf dem Gebiet der Witterungsvorhersage als Ausgangspunkt dienen können.

Im ersten Abschnitt werden die statistischen Grundlagen für die *Voraussagen im täglichen Wetterdienst* auf das sogenannte Azorenproblem angewandt, das heisst auf die Beziehung zwischen Luftdruckänderungen auf den Azoren und nachfolgenden Druckänderungen in Mitteleuropa mit den sie begleitenden Wettererscheinungen. Vorhersagen, die nicht nur für *lange Zeitabschnitte*, sondern auch für *Grosswetterlagen* gelten sollen, können nur bei sehr genauer Kenntnis der Verhältnisse der allgemeinen atmosphärischen Zirkulation gemacht werden. Der zweite Abschnitt befasst sich daher mit theoretischen Betrachtungen über die Schwankungen der allgemeinen Zirkulation als Richtschnur für die statistische Grosswetterforschung, während im dritten Abschnitt die Beobachtungstatsachen der täglichen atmosphärischen Zirkulation auf der Nordhalbkugel in den Jahren 1949–1951 dargestellt und gedeutet werden. Schliesslich wird im vierten Abschnitt das ebenso weitschichtige wie schwierige Problem der Zusammenhänge des Grosswetters mit solaren Vorgängen behandelt, indem Regeln über die Zuordnung des Grosswetters zum Sonnenfleckenzyklus gegeben werden.

Der Synoptiker, dessen Voraussagen auf sorgfältigen Untersuchungen *einzelner Wetterlagen*, auf einem guten Gedächtnis und nicht zuletzt auf dem Fingerspitzengefühl aufgebaut sind, kann von den statistischen Methoden der Vorhersage nur profitieren. Das aus reicher Erfahrung entstandene Werk von F. BAUR gehört ohne Zweifel zu den bemerkenswerten Erscheinungen der meteorologischen Literatur. *J. C. Thams*

Fortschritte in der meteorologischen Forschung seit 1900. Von BERNHARD NEIS (Akademische Verlagsgesellschaft mbH, Frankfurt am Main 1956). 238 S., 21 Abb., 1 Titelbild und 3 Porträttafeln; geb. DM 28.–.

Dieses Werk ist aus Vorlesungen an der Freien Universität Berlin hervorgegangen. Es ist weder ein Lehrbuch noch ein Geschichtswerk. Aus dem vorwiegend deutschsprachigen Schrifttum wählt es die Arbeiten aus, die wesentlich dazu beigetragen haben, die Meteorologie zu einer exakten Naturwissenschaft auszugestalten.

Das Werk gliedert sich in vier Abschnitte. Im ersten wird auf die Leitideen der meteorologischen Forschung eingegangen; im zweiten wird das aerologische Beobachtungsgut gedeutet. Der dritte Abschnitt behandelt das Wetter als eine Folge der Energieumsätze in der Atmosphäre, während der vierte Abschnitt der praktischen Meteorologie gewidmet ist. Als Ausgangspunkt wird der Anfang des 20. Jahrhunderts genommen, den der Verfasser als einen Wendepunkt in physikalischer und meteorologischer Hinsicht betrachtet, da erst von 1900 an die Arbeiten geleistet worden seien, welche die Aufstellung einer Theorie des Wetters ermöglichten.

Ohne Zweifel entspricht eine solche kritisch-genetische Schau einem Bedürfnis, und es ist gewiss verdienstvoll, wenn der Verfasser versucht, die treibenden Motive in der Entwicklung der wissenschaftlichen Meteorologie aufzuzeigen. Insofern kann das Werk wirklich ein Helfer beim Meteorologiestudium sein. Es hätte jedoch erheblich gewonnen durch Berücksichtigung der gesamten einschlägigen Literatur. *J. C. Thams*

Acht- und neunstellige Tabellen zu den elliptischen Funktionen. Von M. SCHULER und H. GEBELEIN (Springer-Verlag, Berlin 1955). 296 S., 11 Abb.; DM 58.–.

Fünfstellige Tabellen zu den elliptischen Funktionen. Von M. SCHULER und H. GEBELEIN (Springer-Verlag, Berlin 1955). 114 S., 11 Abb.; DM 29.60.

Beide Werke sind mit vollständigem deutschem und englischem Text versehen und vor allem auf die Möglichkeit einer bequemen Interpolation ausgerichtet. Inhalt:

Jacobische elliptische Funktionen, laufend nach z und q.
Hilfsfunktionen für eine einfache Berechnung der ϑ-Funktionen.
Tafeln für die Umrechnung zwischen dem Legendreschen Modul θ und dem Jacobischen Parameter q.
Im fünfstelligen Werk ferner: Koeffizienten für die Everett-Interpolation.

Tables of Weber Parabolic Cylinder Functions. Von J. C. P. MILLER (Her Majesty's Stationery Office, London 1955). 233 S.; 63 s.

Tabelliert sind die Lösungen $W(a, x)$ und $W(a, -x)$ der Differentialgleichung $y'' + (x^2/4 - a)\, y = 0$ mit reduzierten Ableitungen, für $a = -10\,(1)\,10$ und $x = 0\,(0{,}1)\,10$, sowie verschiedene Hilfsfunktionen. Ausführliche mathematische Einleitung, welche unter anderem die Querverbindung zu anderen Funktionen herstellt. *P. Läuchli*